

**NON-LINEAR LOAD-DEFLECTION MODELS FOR  
SEAFLOOR INTERACTION WITH STEEL CATENARY RISERS**

A Thesis

by

YAGUANG JIAO

Submitted to the Office of Graduate Studies of  
Texas A&M University  
in partial fulfillment of the requirements for the degree of

MASTER OF SCIENCE

May 2007

Major Subject: Civil Engineering

**NON-LINEAR LOAD-DEFLECTION MODELS FOR  
SEAFLOOR INTERACTION WITH STEEL CATENARY RISERS**

A Thesis

by

YAGUANG JIAO

Submitted to the Office of Graduate Studies of  
Texas A&M University  
in partial fulfillment of the requirements for the degree of

MASTER OF SCIENCE

Approved by:

|                         |                                      |
|-------------------------|--------------------------------------|
| Co-Chairs of Committee, | Charles Aubeny<br>Giovanna Biscontin |
| Committee Members,      | Don Murff<br>Jerome J. Schubert      |
| Head of Department,     | David V. Rosowsky                    |

May 2007

Major Subject: Civil Engineering

**ABSTRACT**

Non-linear Load-Deflection Models  
for Seafloor Interaction with Steel Catenary Risers.

(May 2007)

Yaguang Jiao, B.E., Jilin University

Co-Chairs of Advisory Committee: Dr. Charles Aubeny  
Dr. Giovanna Biscontin

The simulation of seafloor-steel catenary interaction and prediction of riser fatigue life required an accurate characterization of seafloor stiffness as well as realistic description of riser load-deflection ( $P$ - $y$ ) response. This thesis presents two load-deflection ( $P$ - $y$ ) models (non-degradating and degradating models) to simulate seafloor-riser interaction. These two models considered the seafloor-riser system in terms of an elastic steel pipe supported on non-linear soil springs with vertical motions. These two models were formulated in terms of a backbone curve describing self-embedment of the riser, bounding curves describing  $P$ - $y$  behavior under extremely large deflections, and a series of rules for describing  $P$ - $y$  behavior within the bounding loop.

The non-degradating  $P$ - $y$  model was capable of simulating the riser behavior under very complex loading conditions, including unloading (uplift) and re-loading (downwards) cycles under conditions of partial and full separation of soils and riser. In the non-degradating model, there was a series of model parameters which included three

riser properties, two trench geometry parameters and one trench roughness parameter, two backbone curve model parameters, and four bounding loop model parameters.

To capture the seafloor stiffness degradation effect due to cyclic loading, a degrading  $P$ - $y$  model was also developed. The degrading model proposes three degradation control parameters, which consider the effects of the number of cycles and cyclic unloading-reloading paths. Accumulated deflections serve as a measure of energy dissipation. The degrading model was also made up of three components. The first one was the backbone curve, same as the non-degrading model. The bounding loops define the  $P$ - $y$  behavior of extreme loading deflections. The elastic rebound curve and partial separation stage were in the same formation as the non-degrading model. However, for the re-contact and re-loading curve, degradation effects were taken into the calculation.

These two models were verified through comparisons with laboratory basin tests. Computer codes were also developed to implement these models for seafloor-riser interaction response.

## **DEDICATION**

To my family and Yue Feng

## ACKNOWLEDGEMENTS

I would like to express my deepest appreciation for the guidance, encouragement, and support of my advisors, Dr. Charles Aubeny and Dr. Giovanna Biscontin. This thesis would not have reached its goal without their strong support and valuable suggestions. I wish to express my deep and sincere gratitude to Dr. Charles Aubeny for his support, advice and encouragement. In particular, I must express my deepest appreciation for the guidance, patience, and time of Dr. Giovanna Biscontin who provided critical ideas and constant support of this work. I also deeply appreciate my committee members, Dr. Don Murff and Dr. Jerome Schubert, for their advice and time.

I wish to thank fellow graduate student Jung Hwan You for his help on this research. I would also thank my friends Ming Yang, Jun Kyung Park and Anand V Govindasamy for their encouragement.

I deeply appreciate the support and encouragement of my family. The love from my family is the source of my strength. I give special thanks to Yue Feng for her help and dedication.

## TABLE OF CONTENTS

|   | Page |
|---|------|
| ABSTRACT .....  | iii  |
| DEDICATION .....  | v    |
| ACKNOWLEDGEMENTS .....  | vi   |
| TABLE OF CONTENTS .....   | vii  |
| LIST OF FIGURES.....  | ix   |
| LIST OF TABLES .....  | xii  |
| <br>CHAPTER   |      |
| I INTRODUCTION.....   | 1    |
| 1.1. General Description of SCR.....  | 1    |
| 1.2. Objective of This Thesis .....   | 3    |
| 1.3. Organization of This Thesis .....  | 4    |
| II BACKGROUND.....  | 6    |
| 2.1. Seafloor-Riser Interaction Mechanisms .....                                      | 6    |
| 2.1.1 Seafloor Resistance on Riser.....   | 7    |
| 2.1.2 The Influences on Seafloor Soil .....   | 8    |
| 2.1.3 Trench Effect.....  | 9    |
| 2.1.4 Model Tests of Steel Catenary Riser.....  | 10   |
| 2.2. Soil-Riser Interaction Models .....  | 12   |
| 2.2.1 Load-Deflection Model for Seafloor-SCR Interaction.....                         | 12   |
| 2.2.2 Model Tests to Simulate Soil-Riser/Pipe Interaction.....                        | 20   |
| 2.2.3 Beam Equations for Soil-Riser/Pipe Interaction Model.....                       | 24   |
| III NON-DEGRADATING <i>P</i> - <i>y</i> MODEL FOR SEAFLOOR-RISER<br>INTERACTION ..... | 30   |
| 3.1. Introduction .....   | 30   |
| 3.2. Non-Degradating <i>P</i> - <i>y</i> Model.....                                   | 32   |
| 3.2.1 Model of Backbone Curve .....   | 33   |

## TABLE OF CONTENTS (Continued)

| CHAPTER  | Page |
|--|------|
| 3.2.2 Formulation of Bounding Loop.....  | 36   |
| 3.2.3 Model of Reversal Curves from and within Bounding Loop.....                | 41   |
| 3.3. Non-Degradating <i>P</i> - <i>y</i> Model Programming.....                  | 44   |
| 3.4. Parametric Study and Verification .....                                     | 47   |
| 3.4.1 Parametric Study on Soil Strength and Trench Formulation .....             | 47   |
| 3.4.2 Parametric Study on Bounding Loop Parameters .....                         | 51   |
| 3.4.3 Validation of the Model .....  | 54   |
| IV DEGRADATING <i>P</i> - <i>y</i> MODEL FOR SEAFLOOR-RISER<br>INTERACTION ..... | 56   |
| 4.1. Introduction .....  | 56   |
| 4.2. Degradating <i>P</i> - <i>y</i> Model .....                                 | 58   |
| 4.2.1 Backbone Curve of Degradating Model.....                                   | 60   |
| 4.2.2 Bounding Loop of Degradating Model .....                                   | 61   |
| 4.2.3 Degradating Reversal Cycles from or within the Bounding<br>Loop .....      | 64   |
| 4.3. Degradating <i>P</i> - <i>y</i> Model Programming .....                     | 68   |
| 4.4. Parametric Study and Verification .....                                     | 71   |
| 4.4.1 Parametric Study on Degradating Effect.....                                | 71   |
| 4.4.2 Validation of the Model .....  | 73   |
| V SUMMARY, CONCLUSIONS AND RECOMMENDATION .....                                  | 76   |
| 5.1. Summary and Conclusions.....  | 76   |
| 5.2. Recommendations for Future Research .....                                   | 78   |
| REFERENCES.....  | 80   |
| APPENDIX A .....   | 83   |
| APPENDIX B .....   | 90   |
| APPENDIX C .....   | 94   |
| APPENDIX D .....   | 105  |
| VITA .....   | 109  |



## LIST OF FIGURES

| FIGURE  | Page |
|---|------|
| 1.1 General Configuration of SCR.....   | 2    |
| 2.1 Example of Variation of Fatigue Life with Seafloor Stiffness.....         | 8    |
| 2.2 Test and Analytical Bending Moment Data.....                              | 11   |
| 2.3 Backbone Curve and Soil-Riser Response Curve.....                         | 13   |
| 2.4 Soil Suction Model with Comparison of Test Data.....                      | 14   |
| 2.5 Soil-Riser Interaction Model.....   | 16   |
| 2.6 Penetration and Re-penetration Curves with Breakout.....                  | 17   |
| 2.7 Static and Small Deflection Stiffness and Large Deflection Stiffness..... | 19   |
| 2.8 Results of Displacement Controlled Test.....                              | 22   |
| 2.9 Backbone Curve with Effects of Loading Cycles.....                        | 23   |
| 2.10 Spring-Risers Model.....   | 26   |
| 2.11 Example of Riser Deflection in Tough Down Zone.....                      | 28   |
| 3.1 Seafloor Spring Model.....  | 30   |
| 3.2 Rise Pipe Motion Model.....   | 31   |
| 3.3 Non-degradating $P$ - $y$ Model.....                                      | 32   |
| 3.4 Example of Backbone Curve.....  | 35   |
| 3.5 Hyperbolic Boundary Curve.....  | 38   |
| 3.6 Lower Boundary Curve.....   | 39   |
| 3.7 Example of Boundary Loop.....   | 40   |

## LIST OF FIGURES (Continued)

| Figure   | Page |
|--|------|
| 3.8 Example of Reversal Curve from Hyperbolic Unloading Boundary ..... | 41   |
| 3.9 Example of Reversal Curve from Cubic Reloading Boundary .....      | 42   |
| 3.10 Reversal Curves inside Boundary Loops .....                       | 43   |
| 3.11 Cubic Reversal Curve from Cubic Unloading Boundary.....           | 44   |
| 3.12 Flow Chart of Non-Degradating $P$ - $y$ Curve Code.....           | 46   |
| 3.13 Effects of $S_{u0}$ .....   | 47   |
| 3.14 Effects of $S_g$ .....  | 48   |
| 3.15 Comparison of the Influence of $S_{u0}$ and $S_g$ .....           | 49   |
| 3.16 Effects of Trench Width.....                                      | 50   |
| 3.17 Effects of Roughness.....   | 50   |
| 3.18 Effects of $k_0$ .....  | 51   |
| 3.19 Effects of $\omega$ .....   | 52   |
| 3.20 Effects of $\phi$ .....   | 53   |
| 3.21 Effects of $\psi$ .....   | 53   |
| 3.22 Comparison of Model Simulation with Measured Data.....            | 54   |
| 4.1 Cyclic Modulus Degradating Curves .....                            | 56   |
| 4.2 Typical Degradating $P$ - $y$ Curves .....                         | 59   |
| 4.3 Backbone Curve of Degradating Model.....                           | 60   |

## LIST OF FIGURES (Continued)

| Figure  | Page |
|---|------|
| 4.4 Illustration of Bounding Loops of Degrading $P$ - $y$ Model<br>under Extremely Large Condition..... | 61   |
| 4.5 Example Bounding Loop for Degrading Model.....  | 64   |
| 4.6 Illustration of Hyperbolic Reversal Curves<br>from Elastic Rebound Bounding Curve .....             | 65   |
| 4.7 Illustration of Cubic Reversal Curve.....   | 66   |
| 4.8 Illustration of Hyperbolic Reversal Curves<br>from Re-contact Reloading Bounding Curve.....         | 66   |
| 4.9 Illustration of Reversal Curves within Bounding Curve .....   | 67   |
| 4.10 Flow Chart of Degrading $P$ - $y$ Curve Code .....   | 70   |
| 4.11 Effects of $\lambda_n$ and $\alpha$ on Riser Deflection .....                                      | 71   |
| 4.12 Effects of Cycle Number $n$ and $\alpha$ on Riser Deflection .....                                 | 72   |
| 4.13 Effects of $\alpha$ on Riser Deflection .....  | 73   |
| 4.14 Comparison of the Degrading Model with Experiment .....  | 74   |
| 4.15 Degrading $P$ - $y$ curve for $P_{\max} = 16.7$ lb and $n=100$ .....                               | 74   |

**LIST OF TABLES**

| TABLE   | Page |
|---|------|
| 2.1 Coefficients for Power Law Function ..... | 34   |
| 3.1 Soil and Riser Properties .....           | 55   |
| 3.2 Model Parameters.....                     | 55   |

## CHAPTER I

### INTRODUCTION

#### 1.1 GENERAL DESCRIPTION OF SCR

As hydrocarbon production has been moving into deep and ultra-deep waters, compliant systems comprised of large floating production systems, tethered to the seafloor by mooring lines, are progressively replacing conventional gravity systems. Steel catenary riser (SCR) is a single steel pipe suspended freely from the surface support facilities in a catenary shape and lying down to the seabed for transmitting of oil and gas. As more and more compliant floating facilities are deployed into deep waters, steel catenary risers for these compliant systems have become a viable option for oil and gas export from floating production facilities to shore, shallow water platforms, or to subsea pipeline hubs.

Steel catenary risers are a good choice for compliant floating systems due to their technical and economic advantages. Steel catenary risers have been less expensive than other types of risers such as flexible risers, which has a complex set of layers and not as strong as rigid steel in resisting hydrostatic pressure (Mekha, 2001). Large external pressures in these great depths cause flexible risers run into weight and cost problems. However, the steel pipe configurations to maintain curvatures that cause little bending make the SCRs suitable for these environment. Due to these advantages, more and more steel catenary risers are installed in the Gulf of Mexico, Brazil and West Africa.

---

The thesis follows the style of the *Journal of Geotechnical and Geoenvironmental Engineering*.

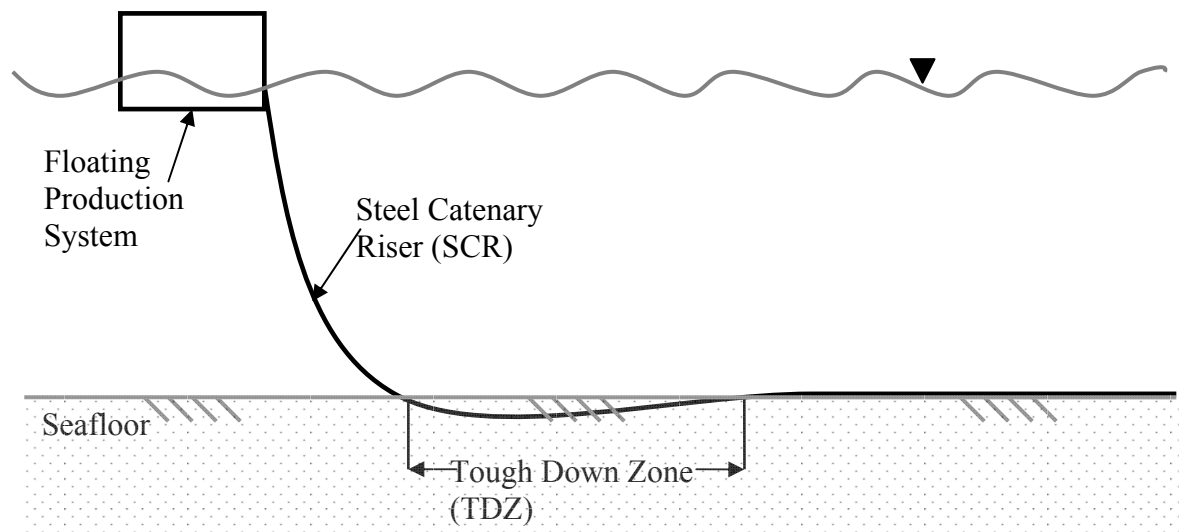


Figure 1.1 General Configuration of SCR

The most critical issue in the design of SCR systems is fatigue damage which is highly dependent on the riser-seafloor interaction in the touchdown zone (TDZ), as shown in Figure. 1.1. The bending stresses are largest as the catenary shape of SCR imposes high stresses in this area. Fatigue stress is mainly associated with vessel movements, vortex-induced vibrations, currents and sea waves (Hale et al., 1992). The shape variation of the riser due to floating vessel motions and direct effects of waves, fatigue damage and high stresses caused by dynamic motions become important aspect of SCR design. Analysis typically shows that fatigue damage also involves complex non-linear processes including non-linear soil stiffness, trench formation, soil suction and broken path of the riser from the seafloor (Bridge et al., 2003). Particularly, recent research indicates that fatigue damage is sensitive to seafloor stiffness, which is characterized by non-linear  $P$ - $y$  relationship of seafloor-riser interaction.

## 1.2 OBJECTIVE OF THIS THESIS

The purpose of this thesis is to develop and verify a non-linear load-deflection ( $P$ - $y$ ) model to characterize the complex interaction between the soil and the riser. The non-linear  $P$ - $y$  curve for a laterally loaded pile or pipe clearly describes the relationship between the unit length force and the lateral displacement of the pile/pipe through:  $P = ky$  (Eq.1.1), where  $k$  is nonlinear. Thus, from the  $P$ - $y$  curve of seafloor-riser interaction, we could successfully characterize the seafloor stiffness ( $k$ ), which is a critical factor for further simulation of seafloor-riser interaction. The load-deflection ( $P$ - $y$ ) relationship is based on a soil-riser interaction model comprising a linearly elastic pipe supported by non-linear springs (Aubeny et al., 2006). Only vertical riser motions are considered in this study, though lateral motions can also affect the riser response as the compliance of floating structures usually causes the SCRs to move back and forth by stretching and kneeling (Mekha, 2001).

This  $P$ - $y$  model is capable of realistically describing complex pattern of behavior of seafloor-riser interaction, including initial penetration into seafloor due to riser's self-weight (riser's self-embedment), load-deflection behavior under extreme deflection (bounding loops), seafloor-riser separations due to large magnitude of deflection and load-deflection relationship within the bounding loops under cyclic loading (reversal of deflection directions). This model is a non-degradating one as it does not involve in the cyclic degradation effects.

Model tests of riser pipes supported on soft soils (Dunlap et al., 1990; Clukey et al., 2005) indicate that soil stiffness degradation effects can be significant. Considering these

degradation effects on seafloor stiffness, a degrading  $P$ - $y$  model is proposed to simulate the cyclic degradation behavior based on the non-degrading model.

In addition, these  $P$ - $y$  models must be calibrated and verified through comparison with experimental measurement (e.g., Dunlap et al., 1990; Clukey et al., 2005). Furthermore, parametric study is carried out to refine and implement the  $P$ - $y$  model to various soil and trench conditions, as well as complex loading paths.

### **1.3 ORGANIZATION OF THIS THESIS**

This thesis focuses on the development, calibration and verification of the numerical model for the load-deflection relationship of seafloor-riser interactions. It consists of five chapters:

Chapter I briefly describes the concept of steel catenary riser and introduces the fatigue damage problem of SCR, the objective and scope of research.

Chapter II contains a selected literature view of previous work on seafloor-steel catenary riser interaction. The first section briefly describes recent works in soil-steel catenary riser interaction effects, as well as model tests to simulate riser-soil interaction. The second section summarizes load-deflection ( $P$ - $y$ ) models for seafloor-riser or soil-pile interaction. The goal is to provide a framework on load-deflection ( $P$ - $y$ ) models for seafloor-catenary riser interaction on which the experimental and numerical modeling presented in is based.

Chapter III describes the formulation of the non-degrading  $P$ - $y$  model and a documentation of how the  $P$ - $y$  model functions under various load conditions and load



reversals is presented in detail. A programming code in Matlab is developed to simulate the  $P$ - $y$  response when the riser is under complex displacement loading condition. Refinements for various soil and trench conditions as well as parametric studies of this model are also included in this chapter. The validation of the implemented model with selected laboratory test data is described.

Chapter IV proposes the degradation component of the  $P$ - $y$  model considering cyclic degradation effects. The concept and mechanism of degradation effects are described and illustrated. A Matlab code is formulated to simulate this effect. Degradation parameters are studied and also calibrated using model tests data. The coupled model formulation is applied to the data of laterally loaded pile cyclic test data for validation.

Chapter V presents a summary of results obtained by this work. It includes the findings of this study, and recommendations for future research.

## **CHAPTER II**

### **BACKGROUND**

A number of research studies have been conducted to investigate riser-seafloor interaction mechanisms. In recent years, various soil stiffness models have been developing as well as a series of model tests to simulating soil-riser interaction were carried out (e.g., Aubeny et al., 2006; Willis and West, 2001; Bridge and Willis, 2002; Bridge et al., 2003; Bridge et al., 2004) .

In this chapter, a series of previous work associated with seafloor-riser interaction mechanism and simulation models, as well as load-deflection models, will be described and discussed. Several model tests related to this area will be presented and described.

#### **2.1 SEAFLOOR-RISER INTERACTION MECHANISMS**

Seafloor-riser interaction involves in very complex responses among riser pipe, seafloor and water. The interaction mechanisms (Thethi and Moros, 2001) include the effect of seafloor resistance on the riser, the effect of riser motions on seafloor and the effect of water on seafloor.

Full-scale model tests (Bridge and Willis, 2002; Bridge et al., 2004) also show that the seafloor-riser interaction problem involves complex non-linear processes including trench formation, non-linear soil stiffness, finite soil suction, and breakaway of the riser from the seafloor.

### **2.1.1 Seafloor Resistance on Riser**

The seafloor has a complex resistance to riser movements in lateral and vertical directions.

Lateral resistance consists of friction between seafloor and the riser, and the passive resistance of the soil as the riser moves sideways out of a depression or into a trench wall. Corresponding to large lateral vessel motions, the touch down zone will be moved sideways, initially mobilizing the friction resistance of the seafloor combined with its passive resistance. As it shears out of the depression, the riser experiences only frictional resistance of the trench bed until it impacts the side of the trench.

There are two kinds of vertical seafloor resistance: downward resistance (soil stiffness) and upward resistance (soil suction) (Willis and West, 2001). For riser downward movements, the seafloor exhibits some degree of elasticity (small deflections) or plasticity (large deflections), which is good for the riser fatigue life in the touch down zone. While for upward movements, the riser would experience suction forces from seafloor soils adhering to the riser. This suction force is caused by reduction in compression. This suction force would resist the upward movement of the riser to prevent the separation of the seafloor and the riser.

The effect of seafloor on the riser is very critical for riser's fatigue damage. Case studies on generic steel catenary risers show that the predicted fatigue damage is dependant on the soil stiffness (Bridge et al., 2004). If the level of soil stiffness used in SCR analysis is high then the predicted fatigue life would be low, and conversely if the soil stiffness is low then the predicted fatigue life may be high. If the soil stiffness is

reduced from 10,000 kPa to 1,000 kPa, the fatigue damage reduces by approximately 30%, an increase in fatigue life of 43%. Figure.2.1 shows fatigue life in the critical tough down zone increasing with seafloor soil stiffness for a 28 in riser under long-term loading conditions.

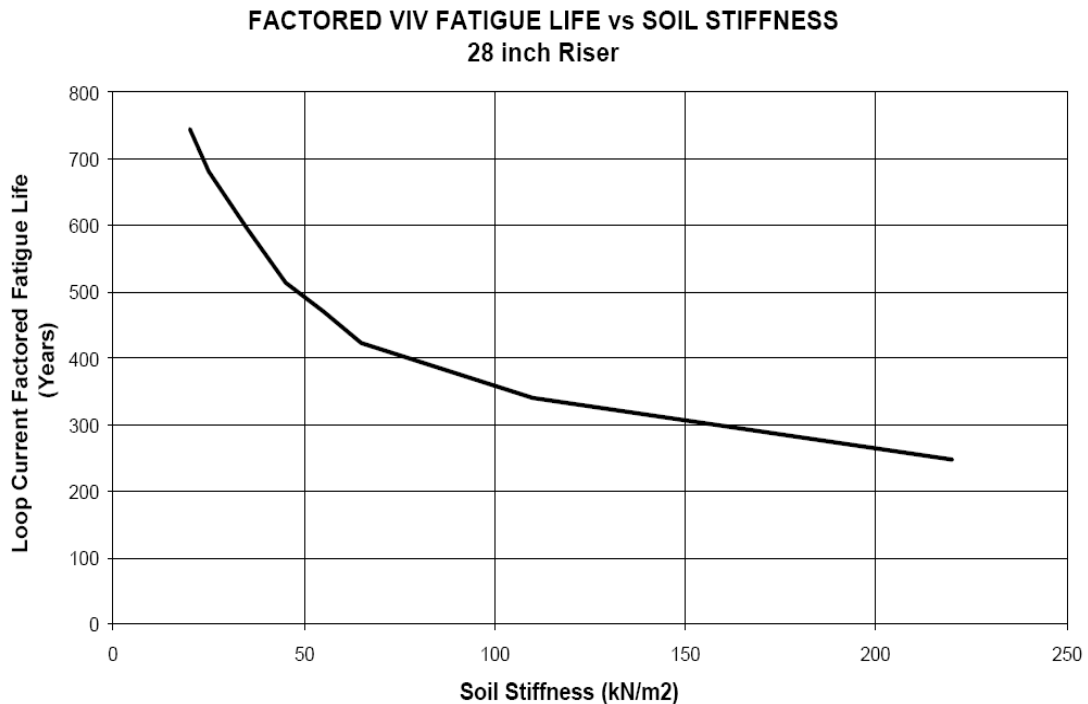


Figure.2.1 Example of Variation of Fatigue Life with Seafloor Stiffness  
(Thethi and Moros, 2001)

### 2.1.2 The Influences on Seafloor Soil

The movements of riser would degrade the seafloor soil stiffness through self-embedment and plastic deformation. Especially under cyclic loading conditions, the degradation effects become much more significant as the seafloor stiffness would decrease very much.

According to the riser movements into and out of the seafloor, the water in the seafloor soil would accelerate out as the riser moves downward, and accelerate in as the riser uplifts. This “pumping” mechanism helps to dislodge already degraded soil from riser impact which would make the soil become much weaker. This action also helps the formation of the trench.

### **2.1.3 Trench Effect**

Trench formation also has significant effect on seafloor-riser response. Aubeny et al. (2006) indicate that the trench depth, trench width and roughness at soil-riser surface could affect soil resistance. Soil resistance would increase with trench increasing and it would decrease as trench becomes wider. Seafloor soil with a rough interface would have a larger resistance than smooth case.

Mechanisms involved in trench formation are a combination of soil plastic deformation and the pumping action of water around the riser (Thethi and Moros, 2001). Based on the observation of riser trenches, Bridge et al. (2003) concluded that: 1) the dynamic motions applied by the vessel motions, may have dug the trench. In addition any vertical motion in the touch down zone would cause the water beneath the riser to be pumped out of the trench, carrying sediment with it. 2) The flow of tides may have scoured and washed away the sediment around the riser. 3) The flow of the seawater across the riser can cause high frequency vortex induced vibration (VIV). This motion could act like a saw, slowly cutting into the seabed. 4) When the harbor test riser is submerged the buoyancy force causes the riser to lift away from the seabed. Any loose sediment in the trench or attached to the riser would be washed away.

#### **2.1.4 Model Tests of Steel Catenary Riser**

A full scale mode test of a steel catenary riser was conducted as part of the STRIDE III JIP, by 2H Offshore Engineering Ltd to investigate the effects of fluid/riser/soil interaction on catenary riser response and wall stresses. A 110m (360ft) long 0.1683m (6-5/8inch) diameter SCR was hung from an actuator on the harbor wall to an anchor point at the Watchet Harbour in the west of England. The harbor seabed soils have properties similar to deepwater Gulf of Mexico seafloor soils. The seafloor is characterized by soft clay, with the undrained shear strength of 3 to 5 kPa, a sensitivity of 3, a plasticity index of 39%, and a naturally consolidated shear strength gradient below the mudline.

The top end of the pipe was programmed to simulate the wave and vessel drift motions of a spar platform in 1,000 m (3,300 ft) water depth. The pipe was fully instrumented with 13 sets of strain gauges measuring vertical and horizontal bending strain and load cells measuring the tensions and shear forces at the actuator and the tension at the anchor. The objectives of this test were to assess the effects of seafloor-riser interaction and to identify key soil modeling parameters for simulation of this interaction.

The results from the harbor test are presented as bending moment versus actuator position at strain gauge locations. In addition, each test measurement from a strain gauge location was compared to a similar point on the analytical model. Computed bending moments were bracketed by analytical predictions considering the effect of suction force. The results of this comparison showed good agreement as illustrated in Figure 2.2.

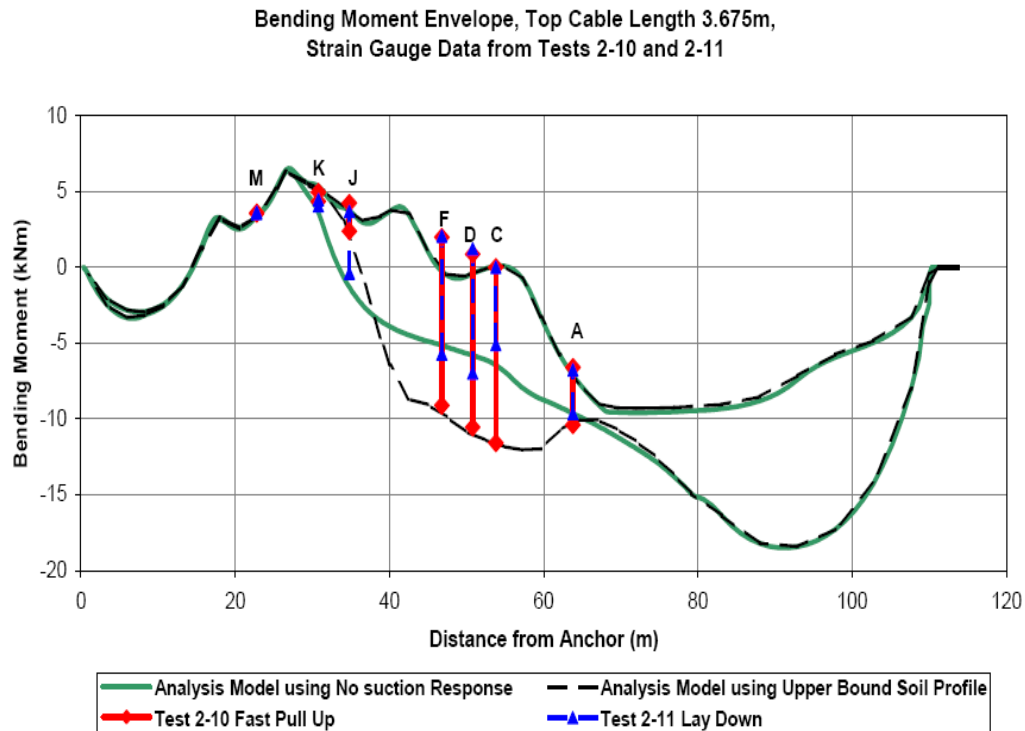


Figure.2.2 Test and Analytical Bending Moment Data (Bridge and Willis, 2002)

The authors also compared pull up and lay down response to investigate the difference in bending moments between the two responses due to soil suction. The results of these comparisons are as follows:

- 1) A sudden vertical displacement of a catenary riser at its touchdown point (TDP) after a period at rest can cause a peak in the bending stress.
- 2) Soil suction forces are subject to hysteresis effects.
- 3) The soil suction force is related to the consolidation time.
- 4) Pull up velocity does not strongly correlate with the bending moment response on a remolded seabed.

Bridge et al. (2003) reviewed the results of full-scale riser test by 2H Offshore Engineering Ltd. The authors concluded that the soil suction force, repeated loading, pull up velocity and the length of the consolidation time can affect the fluid, riser and soil interaction from the test data.

## **2.2 SOIL-RISER INTERACTION MODELS**

### **2.2.1 Load-Deflection Model for Seafloor-SCR Interaction**

Thethi and Moros (2001) recommended that seafloor-riser response curves should be modeled as structural or “soil support” springs in a structural analysis model. However, the soil response at a riser element is unsuitable to be described by a single soil support spring because of repeated loading and gross plastic deformation of soils. Instead, the shape of the spring response should change with time, varying from a virgin soil response curve to a degraded response. A riser element may have zero contact over a large displacement range as the pipe is separated from the seafloor.

The virgin response curve is often termed as a ‘backbone curve’ for the initial penetration due to self-weight. It serves as the bounding limit curves for soil stiffness and suction response. Conversely, the soil-riser interaction curve can be considered as a load path bounded by the backbone curve. Figure.2.3 illustrated these concepts, which presents penetration and suction backbone curves, and examples load-displacement paths of subsequent and successive load reversals.

Aside from the dependence on soil properties and riser diameter and thickness, the seafloor-riser  $P$ - $y$  deflection characteristics are also dependent upon the burial depth,



which vary along the riser in the tough down zone. Hence, it is necessary to incorporate the response characteristics for different burial depth.

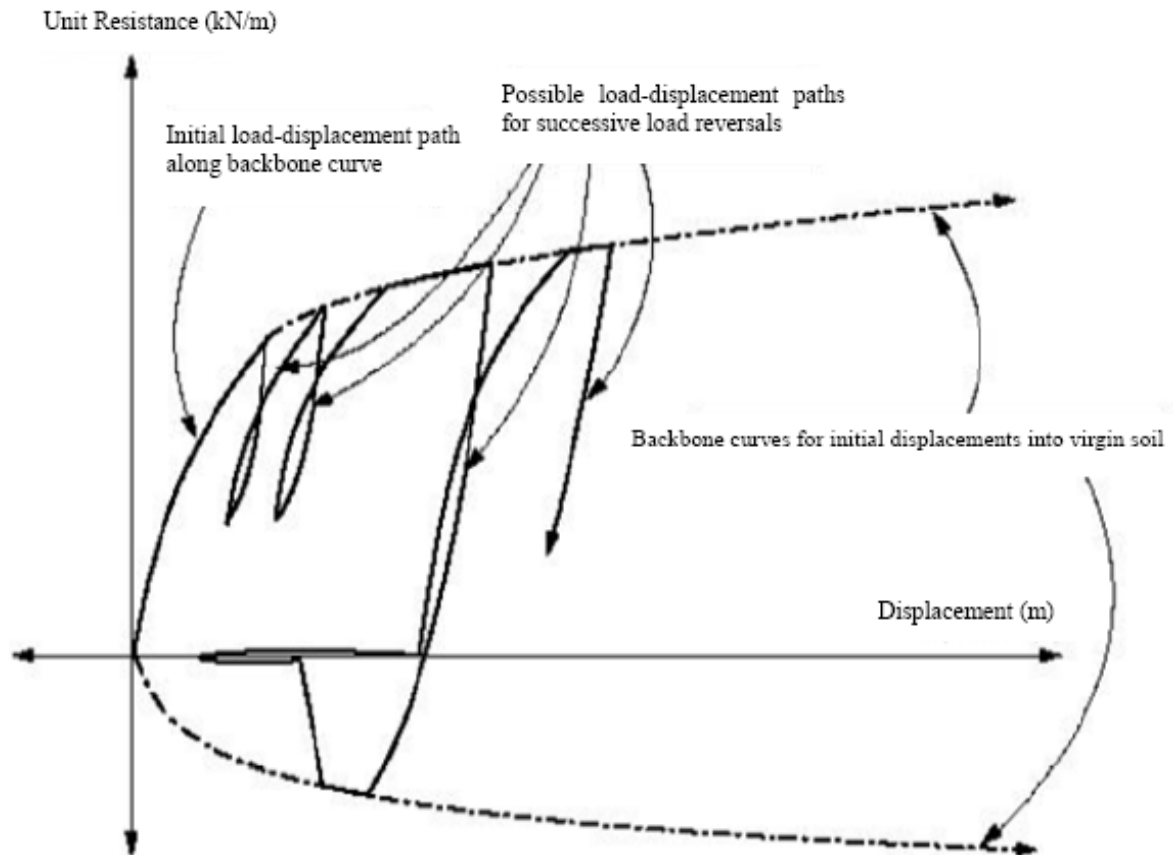


Figure.2.3 Backbone Curve and Soil-Riser Response Curve (Thethi and Moros, 2001)

Bridge and Willis (2002) proposed a soil suction model (Figure.2.4) based on the previous STRIDE 2D pipe/soil interaction work. The soil curve consists of 3 sections: suction mobilization, the suction plateau and suction release. Suction mobilization describes the resistance force increasing from zero to the maximum value as the riser initially moves upwards. The suction plateau is defined as range of displacement in

which the suction force remains constant while the riser is still moving. The suction release stage is the reduction in resistance back to zero as the riser continues its upward movements.

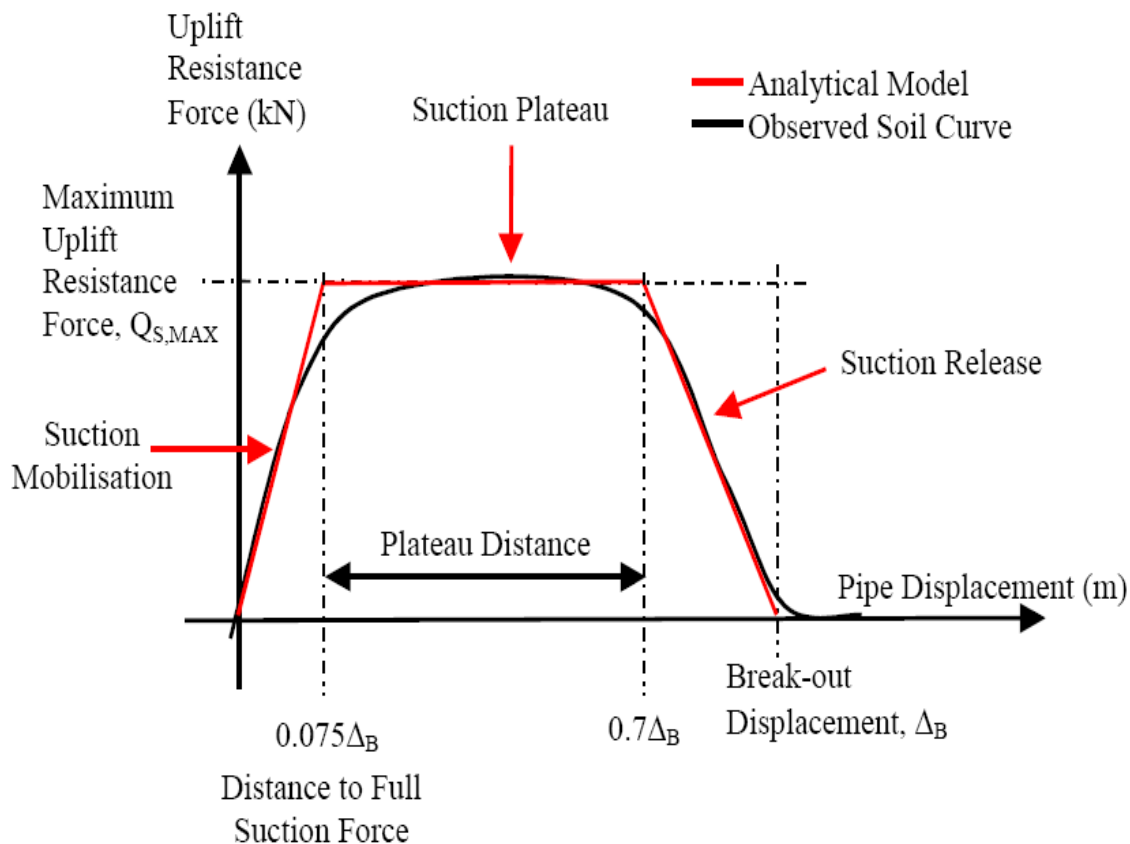


Figure.2.4 Soil Suction Model with Comparison of Test Data (Bridge and Willis, 2004)

Based on previous work, Bridge et al. (2004) developed advanced soil stiffness and soil suction models using STRIDE and CARISIMA JIP test data and other published literature data. This newer model describes the load-deflection response of the soil-pipe interaction associated with the riser vertical movement. The model is illustrated in Figure.2.5, in which the right hand column show soil-riser interaction curves associated with the vertical movement of the riser pipe illustrated in the left hand column.

The mechanism of soil-riser interaction includes the following components:

- (1) The riser is initially in contact with a virgin soil.
- (2) The riser penetrates into the soil due to self-weight, and plastically deforms the seafloor. The soil-riser interaction curve follows the backbone curve. A backbone curve shows how the maximum compressive soil resistance force per unit length varies with depth below the seabed surface as a pipe is continuously pushed into the soil for the first time. Typically, backbone curves are constructed using concepts from the bearing capacity theory for strip foundations.
- (3) The riser moves up and the soil responds elastically. The riser and soil interaction curve should move apart from the backbone curve, and the interaction force decreases caused by unloading.
- (4) The riser resumes penetrating into the soil, deforming it elastically. The riser and soil interaction curve follows an elastic loading curve. And it used hyperbolic equations to simulate vertical downward and upward soil-riser interaction curves.
- (5) The riser keeps penetrating into the soil beyond its original depth, plastically deforming it. The pipe and soil interaction curve follows again with the backbone curve and tracks it.

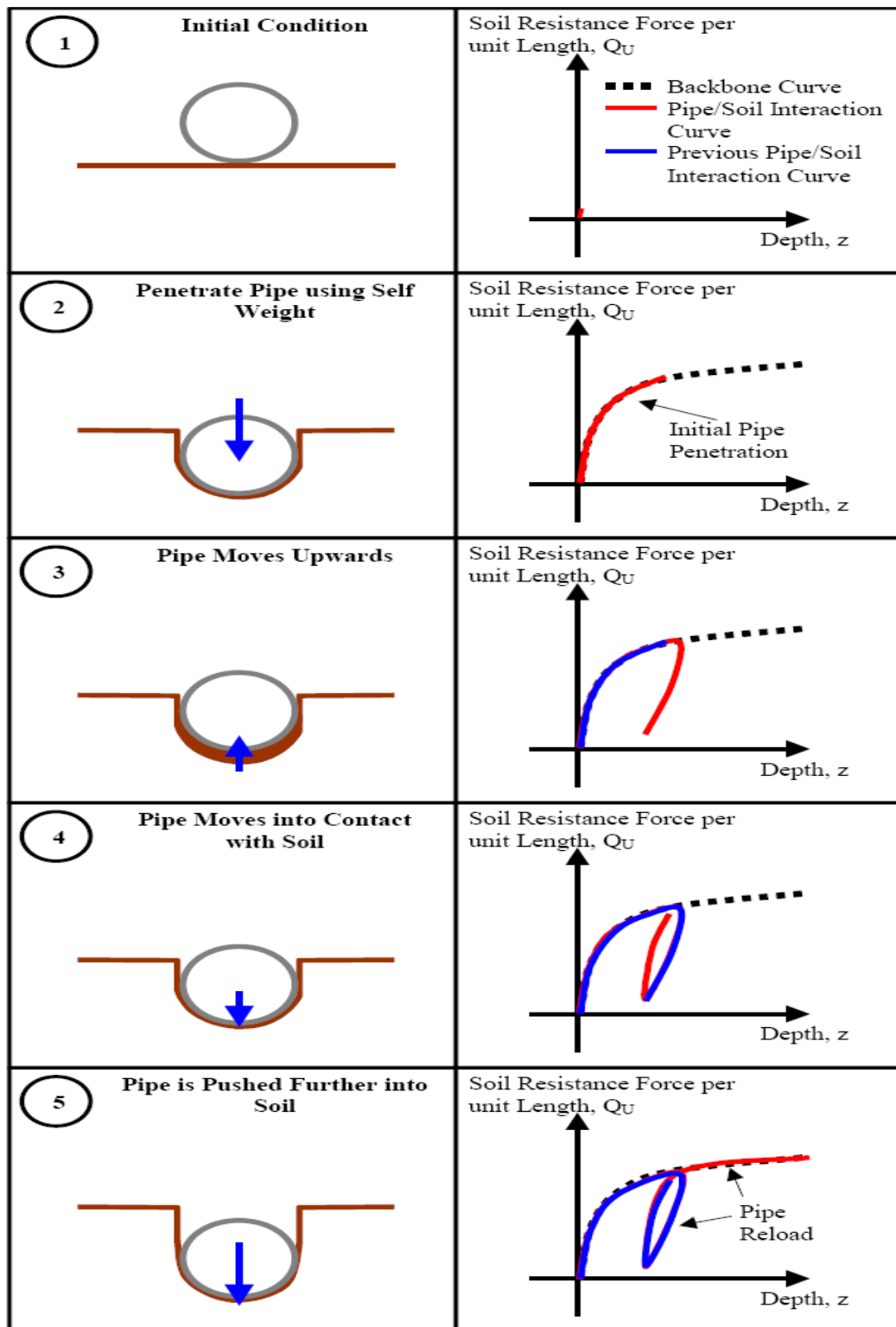


Figure.2.5 Soil-Riser Interaction Model (Bridge et al., 2004)

Furthermore, Bridge et al. (2004) developed a load-deflection model for soil-riser interaction within an extremely load cycle. This  $P$ - $y$  curve model is shown in Figure.2.6 and described below.

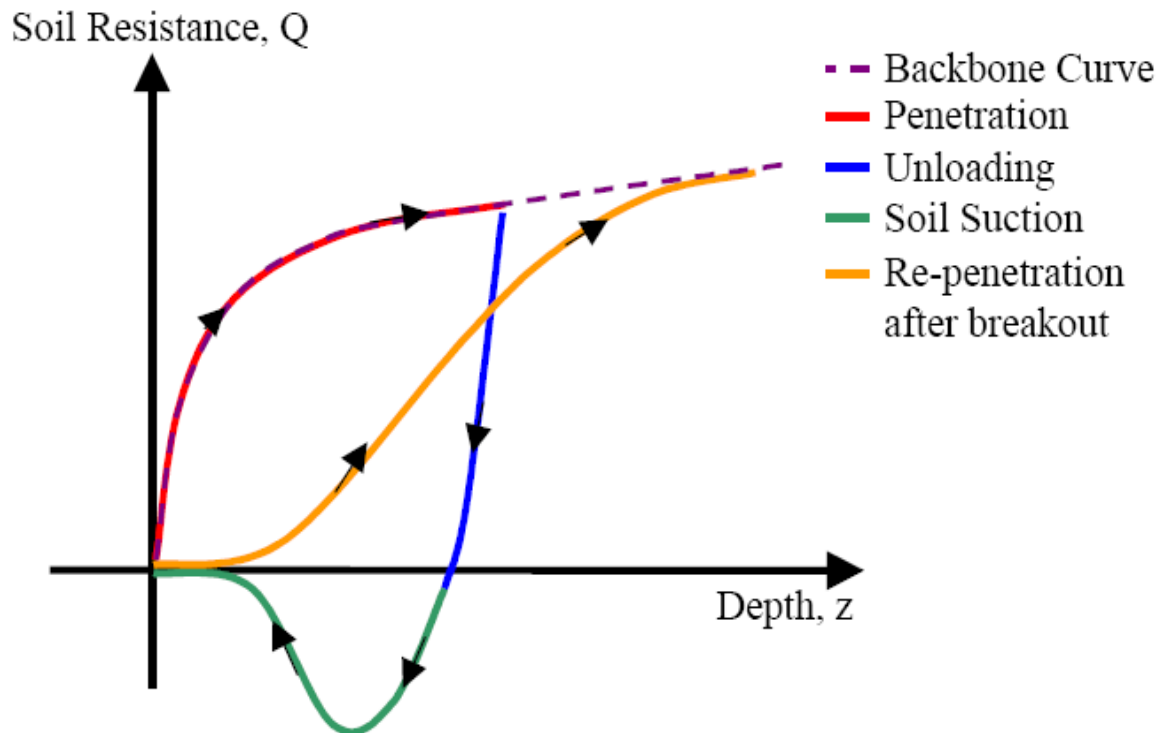


Figure.2.6 Penetration and Re-penetration Curves with Breakout (Bridge et al., 2004)

- (1) Penetration – the riser penetrates into the soil to a depth where the soil force equals the penetration force (weight of the riser pipe). The  $P$ - $y$  curve should follow the backbone curve which demonstrates plastic behavior.
- (2) Unloading – the penetration force reduces to zero allowing the soil to swell as the riser moves up.
- (3) Soil suction – as the riser continues to uplift the adhesion between the soil and the riser causes a tensile force resisting the riser motion. The adhesion force

quickly increases to a maximum and then decreases to zero as the riser breaks up with the seafloor and finally pulls out of the trench.

- (4) Re-penetration –Before the riser and the seafloor re-contacting, there would be no force existing until the riser returns into the trench. The riser and soil interaction force then increases until it rejoins the backbone curve at a lower depth than the previous penetration. Any further penetration should follow the backbone curve.

Bridge et al. (2004) proposed three types of soil stiffness to be used in modeling soil-riser interaction: static stiffness, large deflection dynamic stiffness, and small deflection dynamic stiffness.

Static stiffness is used to estimate the initial penetration of SCR into virgin seafloor, and it equals to the secant stiffness on the backbone curve. Small deflection dynamic stiffness is used to model any soil-riser interaction under unloading (moving upwards) and reloading (moving downwards) conditions. While the riser is still in contact with the soil, large deflection dynamic stiffness is typically a modified secant stiffness which accounts for the plastic deformation when soil-riser separation occurs. Figure.2.7 (a) illustrates static stiffness and small deflection dynamic stiffness and Figure. 2.7 (b) describes the large deflection stiffness.

Pesce et al. (1998) researched soil rigidity effect in the touch down boundary layer of riser on static problem. Their work developed previous analysis performed on the catenary riser TDP static boundary-layer problem by considering a linearly elastic soil. A non-dimensional soil rigidity parameter was defined as follows:

$$K = \frac{k\lambda^4}{EI} = \frac{k\lambda^2}{T_0} \quad (\text{Eq. 2.1})$$

where  $k$  = the rigidity per unit area

$EI$  = the bending stiffness

$T_0$  = the static tension at TDP, defined as  $T_0 = \frac{EI}{\lambda^2}$

$\lambda$  = the flexural-length parameter representing the TDP boundary later length scale.

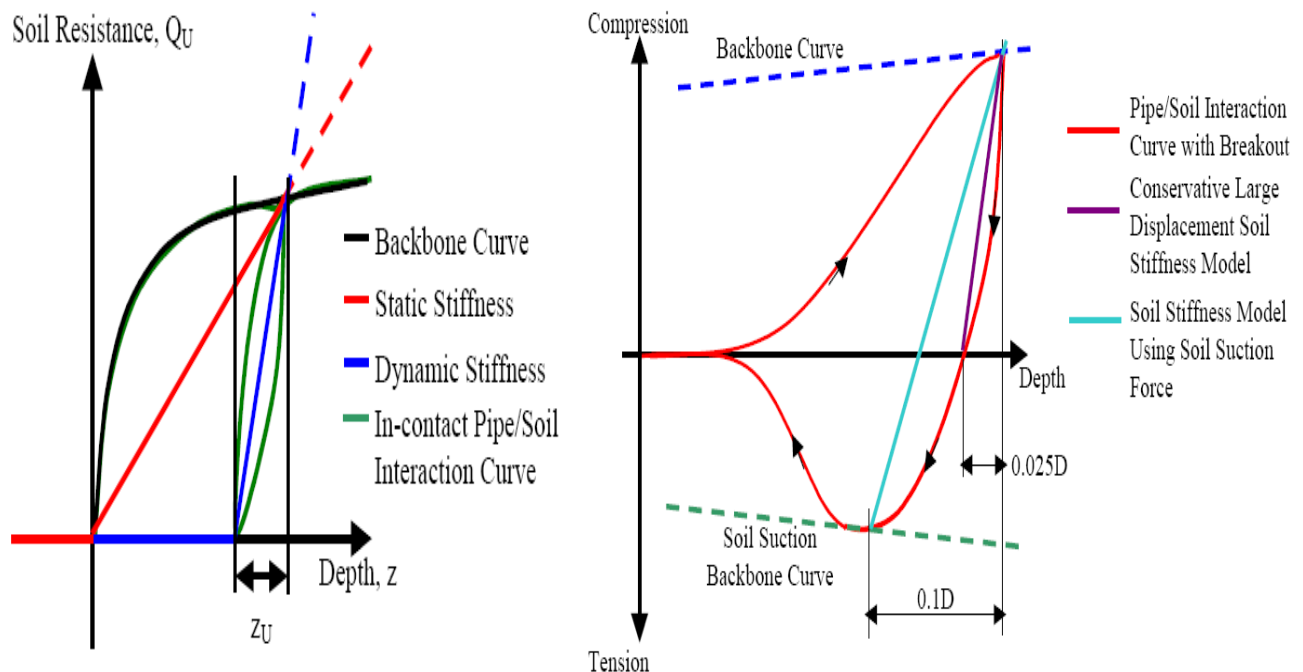


Figure.2.7 (a) Static and Small Deflection Stiffness and (b) Large Deflection Stiffness (Bridge et al., 2004)

A typical oscillatory behavior for the elasticity on the supported part of the pipe line was showed by the constructed solution. Also, it indicated how this behavior matched smoothly the catenary solution along the suspended part, removing the discontinuity in the shear effort, attained in the infinitely rigid soil case. In that previous case, the

flexural length parameter  $\lambda = \sqrt{EI/T_0}$  had been shown to be a measure for the position of the actual TDP, with regard to the ideal cable configuration.

Unlike the previous case, in the linearly elastic soil problem, the parameter  $\lambda$  has been shown to measure the displacement of the point of horizontal tangency about corresponding TDP attained in the ideal cable solution, in rigid soil. Having  $K$  as parameter some non-dimensional diagrams have been presented, showing, for  $K \geq 10$ , the local elastic line, the horizontal angle, the shear effort, and the curvature, as functions of the local non-dimensional arc-length parameter  $\varepsilon = s/\lambda$ . Also, another non-dimensional curve was presented, enabling the determination of the actual TDP position as a function of soil rigidity  $K$ .

### **2.2.2 Model Tests to Simulate Soil-Riser/Pipe Interaction**

Laboratory model tests of vertically loaded horizontal pipes in sediment provide valuable information for the understanding of soil-riser interaction (Dunlap et al., 1990; Clukey et al., 2005). These tests data produce the general load-deflection pattern for soil-riser interaction and necessary information for the validation of the  $P$ - $y$  models and the determination of parameters used in the model.

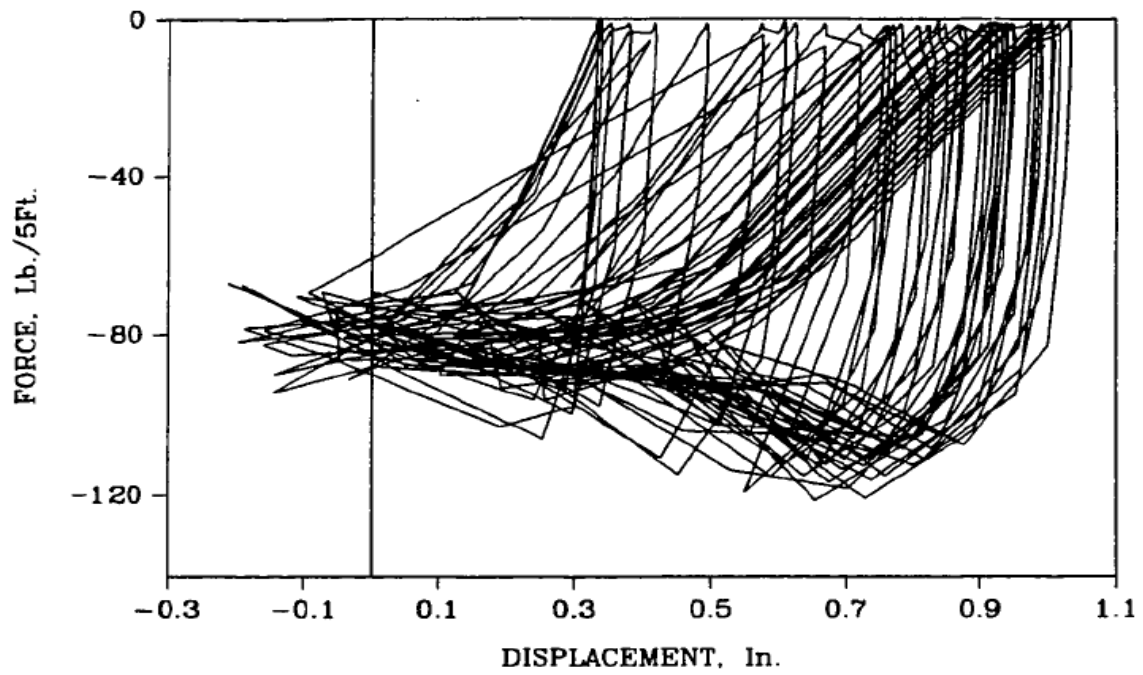
Dunlap et al. (1990) carried out laboratory tests to simulate pipeline-sediment interaction under cyclic load conditions. The model pipe was a 0.5ft diameter, 5ft long aluminum tube with 3/8 in. thick wall. The test basin was 6ft by 6ft in cross section and 4ft deep. The sediment was a green-gray calcium bentonite mixture. The liquid limit of



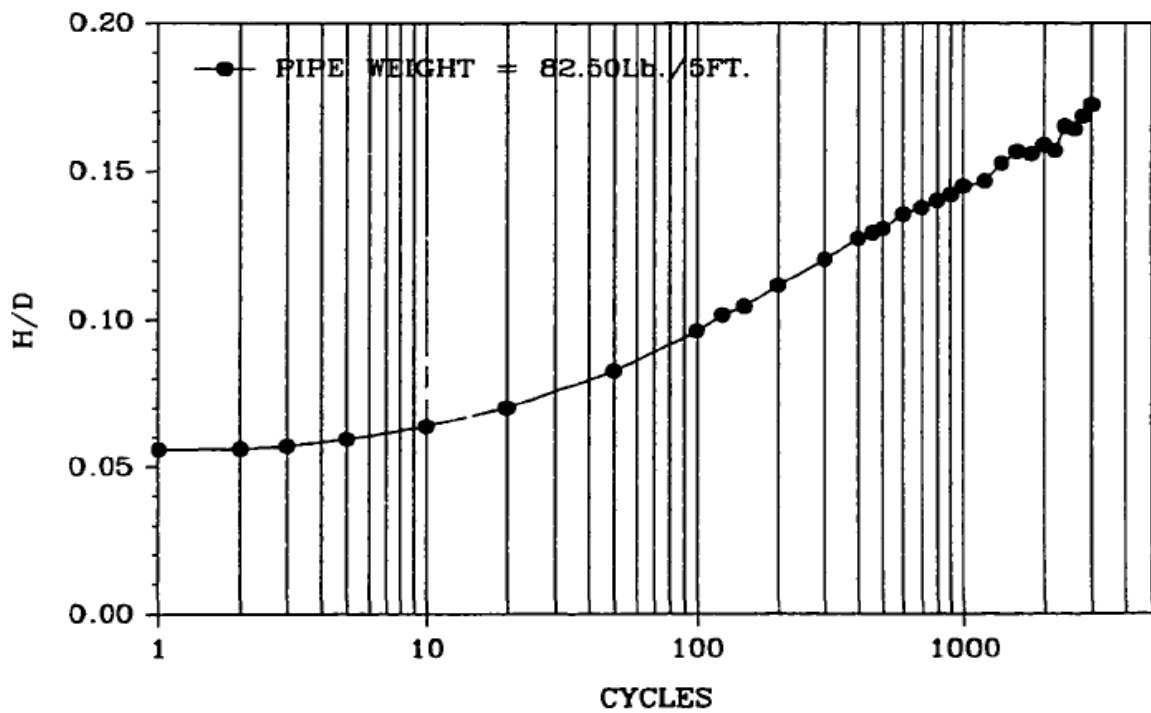
the sediment was 101 and the plasticity index was 62, which classified it as a highly plastic clay.

The test program includes two series: force controlled cyclic tests and displacement controlled cyclic tests. Force controlled tests were performed by applying cyclic loads with constant maximum and minimum force levels about a median load. While displacement controlled test represents a “force down-displacement up” test, as the pipe was loaded with reinforcing bars to a predetermined weight and allowed to settle freely under its own weight during the downward stroke of the lever arm and on the upward stroke of the arm, the pipe was pulled free of the sediment under constant cyclic displacement loads. Thus, displacement controlled tests closely reproduced the actual behavior of pipes which may be alternately be pulled completely free of the sediment and then pushed into the sediment. Figure.2.8 shows the result of displacement controlled tests where (a) gives the  $P$ - $y$  plot and (b) shows the relationship between riser embedment and loading cycles.

After two hours cyclic loading, the backbone curve was developed as the embedment of the pipe due to 1, 10, 100, 1000, and 3000 cycles were plotted versus soil forces. The comparison of 1st and 3000th cycles also revealed the degradation effects of the sediment strength under the influence of cyclic loading. Figure.2.9 shows the backbone curve model as well as the degradation effects due to cyclic loading with the comparison with 1st and 3000th load cycles.



(a) Load-Deflection Curve for Displacement Controlled test



(b) Load-Deflection Curve for Displacement Controlled test

Figure.2.8 Results of Displacement Controlled Test (Dunlap et al., 1990)

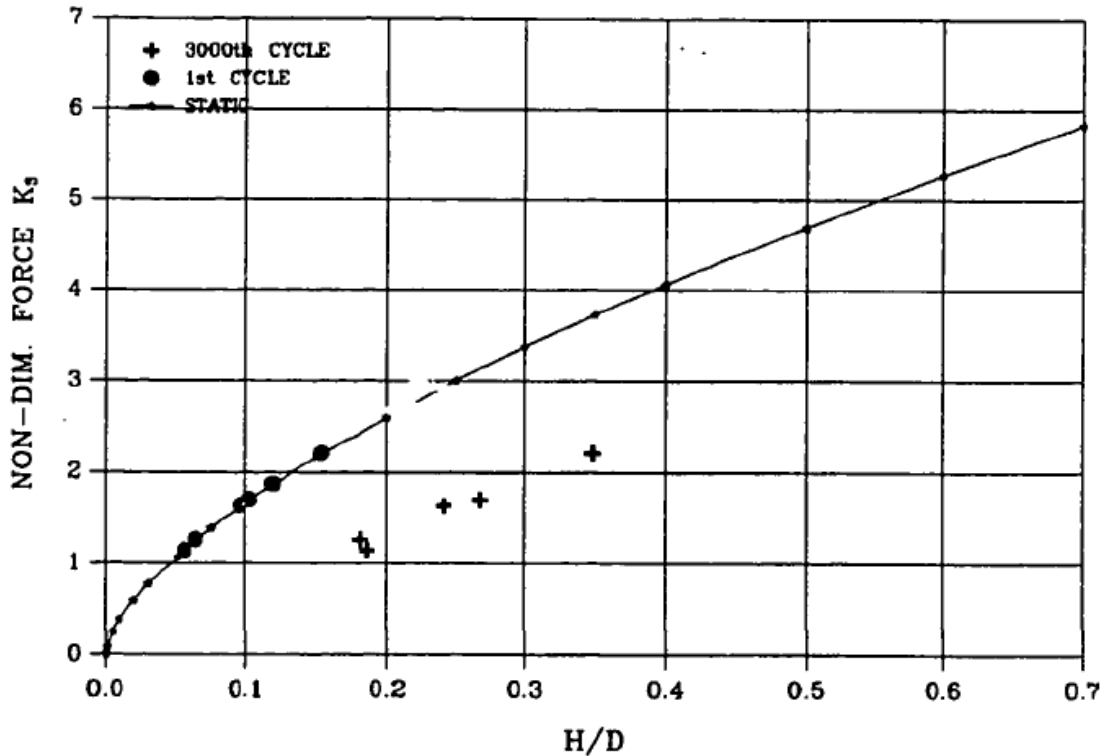


Figure.2.9 Backbone Curve with Effects of Loading Cycles (Dunlap et al., 1990)

A series of vertically loaded tests were performed by Clukey et al. (2005) to investigate the soil interaction with a steel catenary riser. Tests were performed in both load and displacement controlled conditions to investigate the soil response under small, intermediate and large displacements, with emphasis on understanding soil response under cyclic loading and under soil-riser separation conditions.

Clukey et al. (2005) concluded that as the riser was subjected to downward vertical forces with relatively small uplift forces, the  $P$ - $y$  curves were reasonably modeled by an unload-reload hyperbolic model. With additional sustained loading, the soil stiffness degraded to values closely following those predicted hyperbolic models. If soil-riser separation occurred, the hyperbolic models are no longer suitable for modeling  $P$ - $y$

curves as first the stiffness became softer as separation happened and then got stiffer as the pipe re-penetrated further into the soil. A reduction in the soil stiffness was observed to be related to soil-water mixing and pumping action created when soil-riser separation occurred, rather than soil sensitivity in its remolded state.

### 2.2.3 Beam Equations for Soil-Riser/Pipe Interaction Model

For beams on elastic foundations and laterally loaded piles, the relationship between deflection  $y$  and the internal moment  $M$ , internal shear stress, and intensity of applied load  $q$  can be formulated as:

$$M = (EI) \frac{d^2 y}{dx^2} \quad (\text{Eq.2.2})$$

$$V = -\frac{dM}{dx} = -(EI) \frac{d^3 y}{dx^3} \quad (\text{Eq.2.3})$$

$$q = -\frac{dV}{dx} = (EI) \frac{d^4 y}{dx^4} \quad (\text{Eq.2.4})$$

For linear springs, the applied load  $q$  is a function of deflection, which could be expressed as:  $q = -ky$  (Eq.2.5), finally the governing equation for beam resting on springs is:

$$(EI) \frac{d^4 y}{dx^4} = -ky \quad (\text{Eq.2.5})$$

Aubeny et al. (2006) considered the seafloor-riser interaction problem in terms of a steel elastic pipe resting on a bed of soil springs (Figure.2.10). The stiffness should be determined by non-linear load-deflection curves. The load term  $P$  designates the soil resistance in units of force per unit length in the horizontal ( $x$ ) direction, and  $y$  refers to

the vertical deflection of the riser pipe. This interaction model is governed by a non-linear, fourth-order ordinary differential equation:

$$EI \frac{d^4 y}{dx^4} = W - P \quad (\text{Eq. 2.6})$$

where E= modulus of elasticity of the riser pipe

I = moment of inertia of the riser pipe

W=weight per unit length of the riser pipe

Here W is the weight of riser with oil/gas and it should get rid of the influence of buoyancy of sea water. The terms P and y are the soil resistance and deflection in the current calculation step. Due to the non-linearity of the P-y relationship, the analysis procedure must iterate until the value of y assumed at the beginning of an iteration lies sufficiently close to that computed from updated P and y values at the end of the iteration calculation. A first-order central finite difference method was applied to solve soil-riser interaction model, as the fourth order could be expressed by:

$$\frac{d^4 y}{dx^4} = \frac{y_{i+2} - 4y_{i+1} + 6y_i - 4y_{i-1} + y_{i-2}}{dx^4} \quad (\text{Eq. 2.7})$$

Thus Eq.2.6 can be written as:

$$EI \frac{y_{i+2} - 4y_{i+1} + 6y_i - 4y_{i-1} + y_{i-2}}{dx^4} = W - P \quad (\text{Eq. 2.8})$$

It is noted that the lateral deflection of the riser in the touch down zone is relatively small when compared to the horizontal length of the riser. Hence, it is reasonable to use of small-strain, small-deflection beam theory implicit in Eq.2.6 when evaluating riser interaction effects within the touchdown zone.

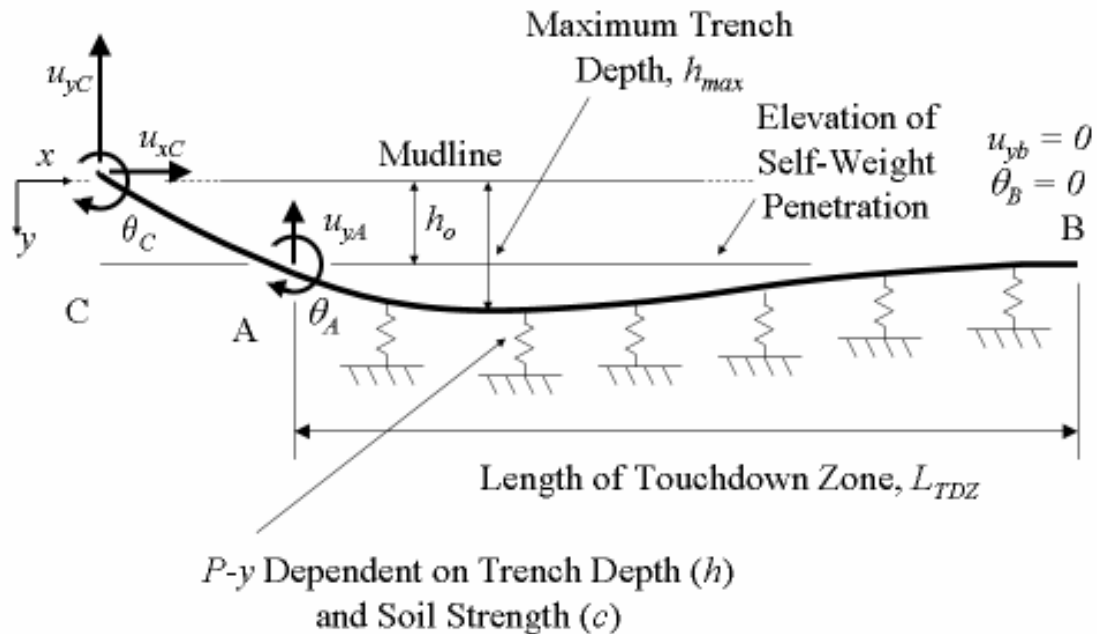


Figure.2.10 Spring-Riser Model (Aubeny et al., 2006)

The boundary conditions for this model are illustrated in Figure.2.10. For an arbitrary point (Point C, Figure.2.10) on the riser pipe, there are total three freedoms of planar motions: two displacement freedoms at horizontal and vertical direction ( $u_{xC}$ ,  $u_{yC}$ ) and one rotational degree of freedom ( $\theta_C$ ). As the touchdown point (Point A, Fig.2.10) is approached, the horizontal stiffness of the system is governed by the axial stiffness of an infinitely long pipe; for all practical purposes the system has infinite stiffness to the right of Point A and no horizontal deformations occur within the touchdown zone. Hence, conditions within the touchdown zone are modeled as a horizontal beam subjected to a time history of vertical displacements ( $u_{yA}$ ) and rotations ( $\theta_A$ ) at the touchdown point. For the far end of the riser (Point B, Fig.2.10), the displacement restrains are:  $u_{yB} = 0$ ;  $\theta_B = 0$ . This requires the shear and bending moment approach

zero at Point B, which could be satisfied by ensuring the length of the tough down zone sufficiently large. It is noted that the boundary conditions are referenced to the self-embedment depth. While the vertical displacement is calculated from the mudline:  $y = h_0 - u_y$ .

The analysis of soil-riser interaction proceeds through the following sequence to solve Eq.2.8: 1) computation of self-weight penetration of an undeformed pipe; 2) establishing an initial deformed configuration of the pipe; 3) Applying a time history of successive motions  $(u_{yA}, \theta_A)$  to the pipe at the touchdown point.

The initial self-weight penetration calculation is solved by simply equating pipe weight  $W$  to collapse load of a pipe embedded in a trench. The initial riser configuration could be established based on observation data. Solution of Eq.2.8 with an imposed contact angle  $\theta_A$  at the touchdown point to achieve a target  $h_{\max}$  appears to provide a reasonable basis for establishing an initial riser configuration. For the example simulation in question (Fig.2.11), a rotation  $\theta_A = 0.15$  radians produced a maximum pipe embedment of about 3 pipe diameters below the mudline, or about 2 diameters below the depth of self-weight penetration. Notice that both the self-weight penetration and the initial pipe configuration calculations are based on a purely plastic model of soil resistance. In the third step, subsequent motions are imposed to the initial configuration to simulate further configuration of the riser. In this example, a single uplift motion of two pipe diameters,  $u_{yA} = 2D$ , is imposed. The resulting computed pipe configuration (Figure.2.11) shows a region extending about  $x = 45D$  from the touchdown point in

which uplifting of the pipe occurs. The seafloor-riser interaction in this region will be characterized by elastic rebound of the soil and, throughout much of this region, separation of the pipe from the seafloor. Beyond  $x = 45D$  the direction of deflections reverses and continued plastic penetration into the seafloor occurs.

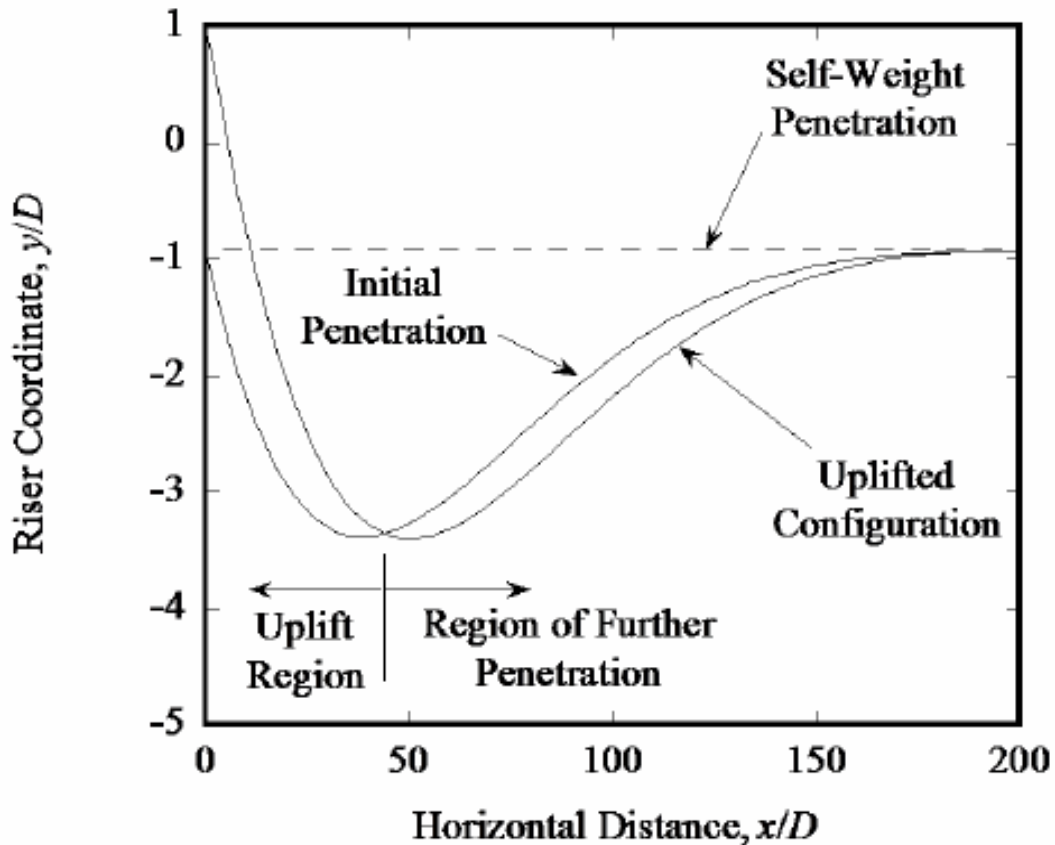


Figure.2.11 Example of Riser Deflection in Tough Down Zone  
(Aubeny and Biscontin, 2006)

Aubeny et al. (2006) indicate that the simulation of the riser's response using this model requires a non-linear P-y model which is capable of describing a relatively complete pattern of behavior involving elastic rebound, seafloor-riser separation, highly variable magnitudes of deflection, reversal of deflection direction, and plastic



penetration. The following chapters will focus on the development and verification of the  $P$ - $y$  model which satisfies these requirements.

## CHAPTER III

### NON-DEGRADATING $P$ - $y$ MODEL FOR SEAFLOOR-RISER INTERACTION

#### 3.1 INTRODUCTION

The seafloor stiffness, characterized by load-deflection curve, is one key factor for the analysis of soil-riser interaction. Thus, developing  $P$ - $y$  curves to accurately and realistically reflect the soil-riser response is very critical to the seafloor-steel catenary riser interaction analysis.

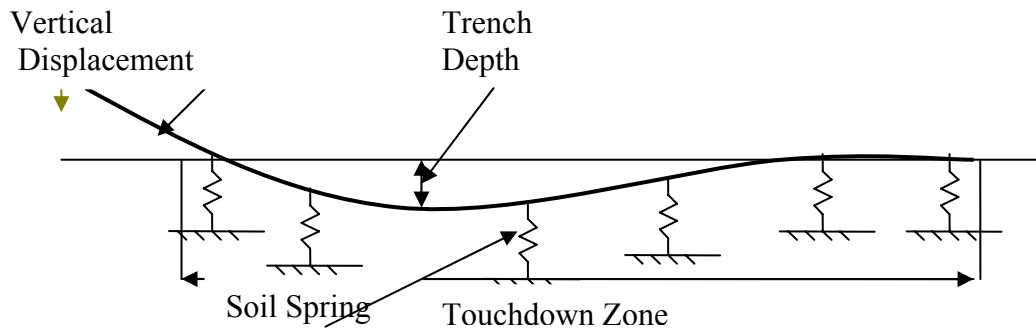


Figure 3.1 Seafloor Spring Model

In this thesis, the seafloor-steel catenary riser system is modeled as an elastic steel pipe lying on non-linear soil springs (Figure.3.1), the stiffness of which is characterized by non-linear load-deflection ( $P$ - $y$ ) curves. For an arbitrary soil spring element, the load-deflection ( $P$ - $y$ ) curves define the relationship between soil-riser interaction force and the movement of the spring (also the riser pipe) as well as describe the response behavior of seafloor-riser interactions.

After the steel catenary riser initially touching the seafloor, deflections occurred along the riser pipe due to vessel movements, vortex-introduced vibrations and extreme

storms (Morris et al. 1988). Base on previous work (Bridge et al., 2003, Aubeny et al., 2006), the motion of the steel catenary riser can be generally divided into: 1) Initial penetration into seafloor due to self-weight, as the soil-riser interaction forces finally equal to riser pipe's self-weight and all riser elements have the same trench depth. 2) As the movements of the floating system are transmitted to all the length of the riser pipe, an arbitrary riser element would be subjected to alternating uplift or downward motions alternatively (as under cyclic loading). The configuration of these processes is shown in Figure.3.2.

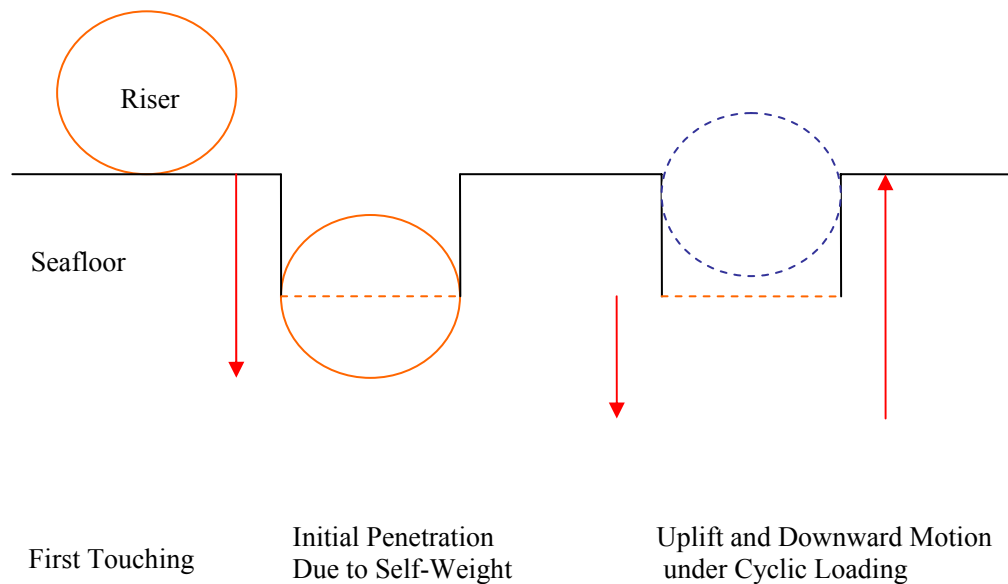


Figure 3.2 Rise Pipe Motion Model

In the following study, numerical models are proposed to model the actual  $P$ - $y$  curves of soil-riser response based on previous research work (Bridge et al., 2004 and Aubeny et al., 2006) and a Matlab code is developed to simulate  $P$ - $y$  curves under complex displacement loading condition. This  $P$ - $y$  model only considers vertical

displacement though lateral and axial displacements also have some influence on soil-riser behavior. The stiffness degradation effects are not considered in this model but will be studied in Chapter IV.

### 3.2 NON-DEGRADATING $P$ - $y$ MODEL

Generally, there are four deflection stages for the motion of an arbitrary riser node:

- 1) Penetration stage which includes initial penetration due to self-weight and further penetration as the riser deflection becomes greater than the initial penetration depth in the downward movement.
- 2) Uplift and downward reversal loading stage before the separation of the riser and the seafloor occurs.
- 3) Uplift and downward movement stage after the riser being partially detached from the seafloor or being re-contacted with the seafloor.
- 4) Fully separation stage in uplift or downward movement.

Figure.3.3 shows the general components of this model.

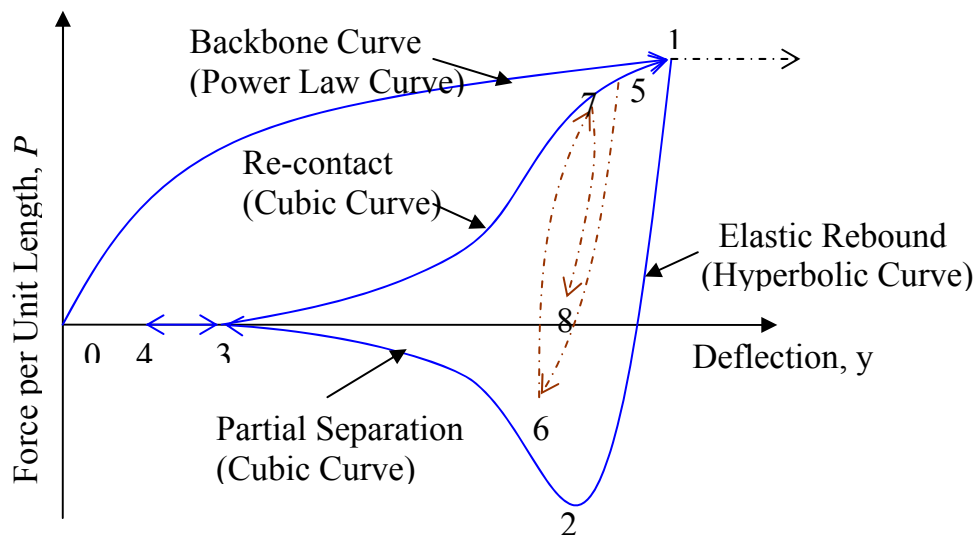


Figure.3.3 Non-degradating  $P$ - $y$  Model

Correspondingly, four sections of the  $P$ - $y$  formulation are developed to define and describe these stages. In this model, three bounding envelope which consist of one backbone curve, two suction force limiting curves (lower boundary) and one re-contact boundary curve (upper boundary), are defined and serve as the bounding surface for subsequent soil-riser response curve. Thus all displacement load cases can be considered as load path from the bounding envelop.

### 3.2.1 Model of Backbone Curve

Penetration occurs as the riser pipe is pushed into the virgin seafloor to a depth where the soil force equals to the penetration fore. This stage includes the initial penetration due to riser's self-weight, and further penetration when riser downward movement reaches the previous trench depth. In this stage, the seafloor springs deform plastically and the  $P$ - $y$  curve follows what is commonly called a backbone curve.

The backbone curve defines how the maximum compressive resistance force of the seafloor varies with the deflection of the riser pipe. Typically, the backbone curve is constructed using bearing capacity theory (Bridge et al., 2004; Aubeny et al., 2006).

The equation for calculating the resistance force per length  $P$  is given as:

$$P = qd \quad (\text{Eq.3.1})$$

$$q = N_p S_u \quad (\text{Eq.3.2})$$

where  $q$  = ultimate bearing pressure

$d$  = the diameter of the riser pipe

$N_p$  = dimensionless bearing factor

$S_u$  = undrained shear strength of soil

For non-uniform undrained shear strength soil profiles:

$$S_u = S_{u0} + S_g z \quad (\text{Eq.3.3})$$

where  $S_{u0}$  is the shear strength at the mudline and  $S_g$  is strength gradient with respect to riser trench depth  $z$ .

Table.2.1 Coefficients for Power Law Function

| Pipe Roughness | Coefficients $a$ and $b$ |             |                  |                             |              |             |
|----------------|--------------------------|-------------|------------------|-----------------------------|--------------|-------------|
|                | $w/d=1$                  |             | $1 < w/d < 2$    |                             | $w/d > 2$    |             |
| Smooth         | $h/d < 0.5$              | $h/d > 0.5$ | $h/d < 0.5$      | $h/d > 0.5$                 | $h/d < 0.5$  | $h/d > 0.5$ |
|                | $a=4.97$                 | $a=4.88$    | $a=4.97$         | $a = 4.88 - 0.48(w/d - 1)$  | $a=4.97$     | $a=4.40$    |
|                | $b=0.23$                 | $b=0.21$    | $b=0.23$         | $b = 0.21 - 0.21(w/d - 1)$  | $b=0.23$     | $b=0$       |
|                |                          |             |                  |                             |              |             |
| Rough          | $w/d=1$                  |             | $1 < w/d < 2.75$ |                             | $w/d > 2.75$ |             |
|                | $h/d < 0.5$              | $h/d > 0.5$ | $h/d < 0.5$      | $h/d > 0.5$                 | $h/d < 0.5$  | $h/d > 0.5$ |
|                | $a=6.73$                 | $a=6.15$    | $a=6.73$         | $a = 6.15 - 0.31(w/d - 1)$  | $a=6.73$     | $a=5.60$    |
|                | $b=0.29$                 | $b=0.15$    | $b=0.29$         | $b = 0.15 - 0.086(w/d - 1)$ | $b=0.29$     | $b=0$       |

Aubeny et al. (2006) found that the bearing factor  $N_p$  is sensitive to trench geometry, including riser pipe trench depth and trench width, and the roughness of the soil-pipe interface. Based on finite element calculations, they proposed an empirical power law function as:

$$N_p = a\left(\frac{y}{d}\right)^b \quad (\text{Eq.3.4})$$

where  $a$  and  $b$  are curve coefficients which vary with trench conditions and pipe roughness, and  $y$  is the trench depth (also equals to the deflection of the riser element in the penetration stage).

Based on the finite element simulation data of Aubeny and Shi (2006), Table.2.1 presents the values of  $a$  and  $b$  for various conditions.

The final functional form of the backbone curve in power law equation is:

$$P = a\left(\frac{y}{d}\right)^b (S_{u0} + S_g y) d \quad (\text{Eq.3.5})$$

and the value of  $a$  and  $b$  could be selected depending on the condition of trench depth and width from Table.1.

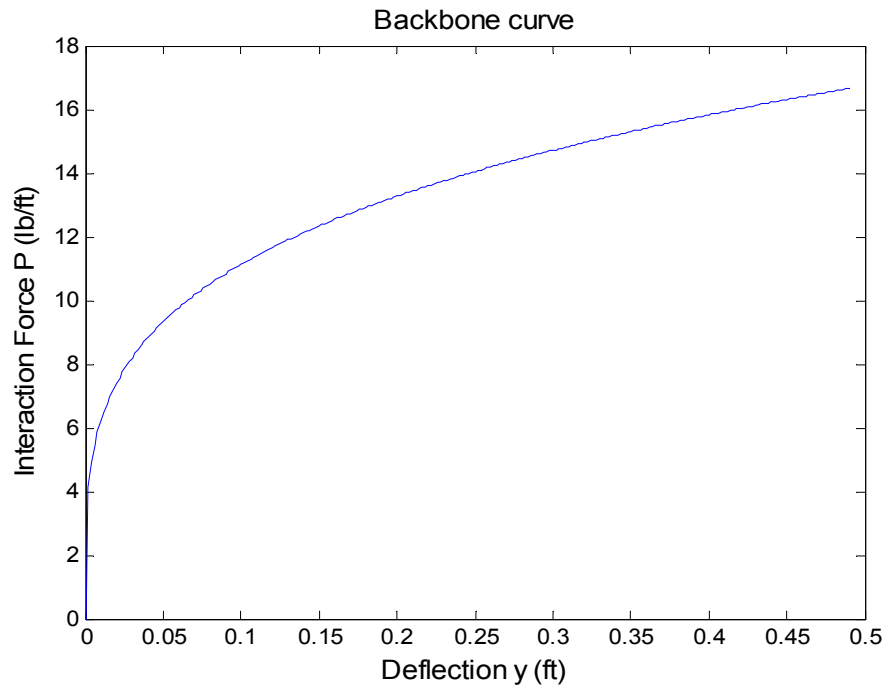


Figure 3.4 Example of Backbone Curve

An example backbone curve for the initial penetration process is shown in Figure.3.4, with pipe and soil parameters: diameter  $d=0.5$  ft; self-weight per unit length  $w=16.61$  lb/ft; soil strength  $S_{u0}=5$ ,  $S_g=0$ ; trench width  $w/d=1$ .

### 3.2.2 Formulation of Bounding Loop

When a riser element experiences extremely large up-lift displacement, the riser would move uplift and tension forces can develop due to the adhesion between the riser pipe and the soil. This tensile force is often referred to as a suction force. The suction force would increase to its maximum value as the uplift deflection increases. As the riser starts to be partially detached from the soil the suction force gradually decreases and finally reaches zero when the riser pipe is fully separated from the seafloor soil. There would be no interaction force exists if the riser keeps moving up after full separation. Hence, the behavior of riser under extremely large displacement is an important component in seafloor-riser response. It needs to be accurately described in the proposed model.

Researchers usually use bounding loop to define and describe the behavior under large displacement. This thesis will utilize the model proposed by Aubeny et al. (2006) to define the bounding loop. The geometry of the bounding loop is defined by three critical points. Point 1 ( $y_1, P_1$ ) is defined as the initial point of the cyclic loading curves which is at the end of the backbone curve. Point 2 ( $y_2, P_2$ ) is defined as the point of maximum tension of the soil spring reached. Point 3 ( $y_3, P_3$ ) is the point at which the riser pipe totally broken-up from the seafloor.



Point 1 ( $y_1, P_1$ ) as the previous maximum compression force, equals to the soil force at the greatest plastic penetration deflection  $y_1$  as:

$$P_1 = a\left(\frac{y_1}{d}\right)^b (S_{u0} + S_g y_1) d \quad (\text{Eq.3.6})$$

The maximum tension during uplift is related to the maximum compression as:

$$P_2 = -\phi P_1 \quad (\text{Eq.3.7})$$

where  $\phi$  is the defined as tension limit parameter, which is determined by laboratory model tests or field data.

The point of full separation, ( $y_3, P_3$ ), is defined using the relationship between the deflection interval over the detaching stage and the deflection interval over fully contacting stage:

$$(y_2 - y_3) = \psi (y_1 - y_2) \quad (\text{Eq.3.8})$$

$$P_3 = 0 \quad (\text{Eq.3.9})$$

and  $\psi$  is defined as soil-riser separation parameter. It is used to determine the deflection of the riser when full separation occurred. Its value is also determined by model test results.

The elastic rebound curve between Points 1 and 2, as the seafloor soil and the riser pipe are in full contact is described as a hyperbolic relationship:

$$P = P_1 + \frac{y - y_1}{\frac{1}{k_0} - \frac{y - y_1}{(1 + \omega)P_1}} \quad (\text{Eq.3.10})$$

The parameter  $\omega$  is the parameter which controls the asymptote of the hyperbolic curve and also controls the deflection  $y_2$  at which the separation starts in corporation of parameter  $\phi$  as:

$$y_2 = y_1 - \frac{(1 + \omega)P_1}{k_0} \frac{1 + \phi}{\omega - \phi} \quad (\text{Eq.3.11})$$

Figure.3.5 shows the hyperbolic function which describes the elastic rebound curve (Point 1-Point 2).

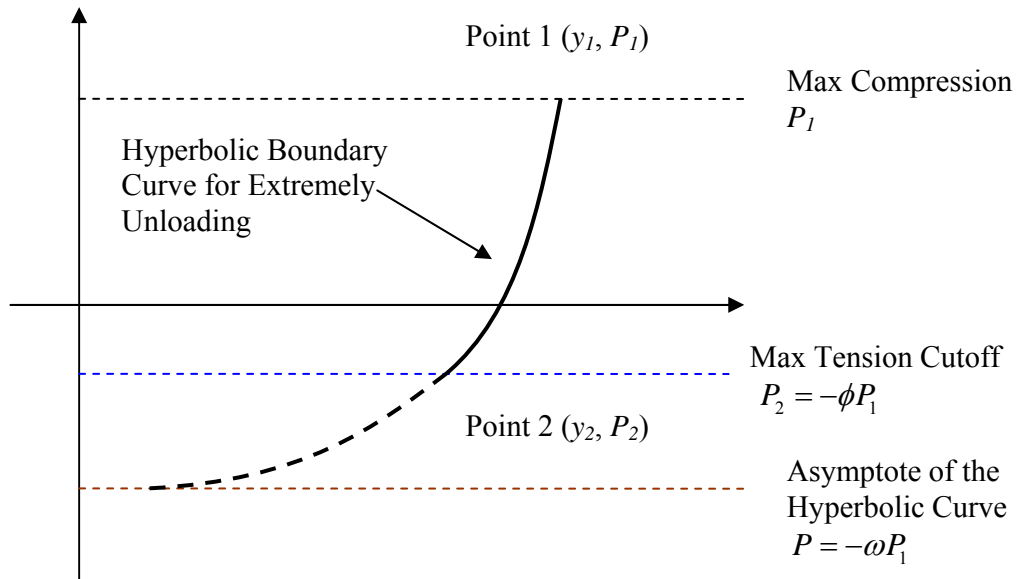


Figure 3.5 Hyperbolic Boundary Curve

$k_0$  is the initial slope of the hyperbolic curve, which maybe related to the soil undrained elastic modulus  $E_u$  as:  $k_0 \approx 2.5E_u$  (from finite element study by Aubeny et al., 2005).

The partial separation stage between Points 2 and 3 is defined in the form of a cubic relationship as:

$$P = \frac{P_2}{2} + \frac{P_2}{4} \left[ 3 \left( \frac{y - y_0}{y_m} \right) - \left( \frac{y - y_0}{y_m} \right)^3 \right] \quad (\text{Eq.3.12})$$

$$y_0 = (y_2 + y_3) / 2 \quad (\text{Eq.3.13})$$

$$y_m = (y_2 - y_3) / 2 \quad (\text{Eq.3.14})$$

Figure.3.6 shows the relationship between the lower boundaries which consist of hyperbolic unloading boundary curve and cubic unloading boundary curve.

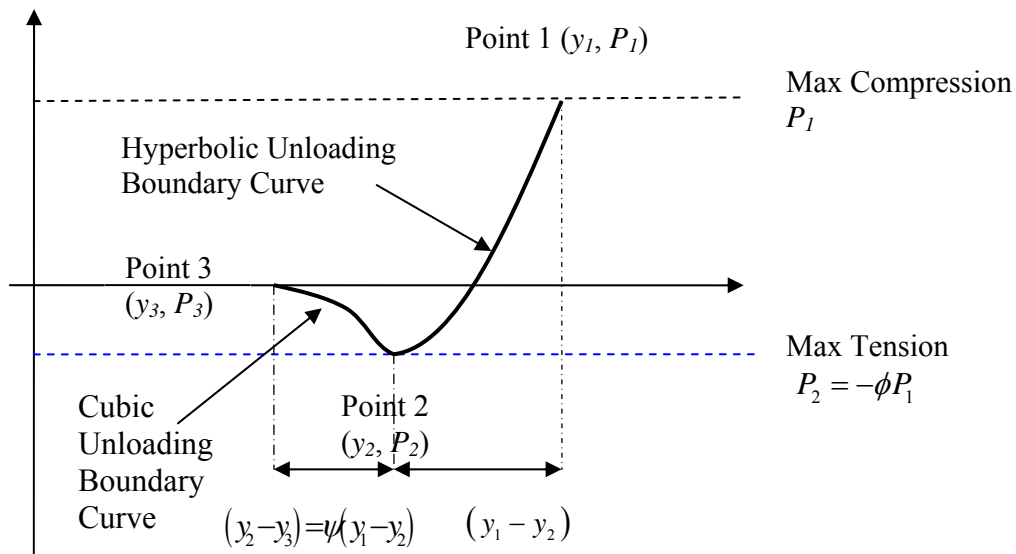


Figure 3.6 Lower Boundary Curve

When the riser pipe experiences downward deflections after full separation from the seafloor soil, it re-contacts the seafloor gradually and the soil springs recovers compression forces until the riser eventually returns to the initial self-weight penetration position which is described through Point 3 to Point 1. This re-contact reloading stage defines an upper boundary of the reloading response. For reloading from any points in

the range between Point 2 and Point 3, when the separation is only partial, the path still follows a cubic relationship, similar to Eq.3.12:

$$P = \frac{P_1}{2} + \frac{P_1}{4} \left[ 3 \left( \frac{y - y_0}{y_m} \right) - \left( \frac{y - y_0}{y_m} \right)^3 \right] \quad (\text{Eq.3.15})$$

$$y_0 = (y_1 + y_3) / 2 \quad (\text{Eq.3.16})$$

$$y_m = (y_1 - y_3) / 2 \quad (\text{Eq.3.17})$$

Figure.3.7 shows an example boundary curves with pipe and soil parameters as: diameter  $d=0.5$  ft; self-weight per unit length  $w=16.61$  lb/ft; soil strength  $S_{u0}=5$  psf,  $S_g=0$ ; the trench width  $w/d=1$ ;  $\phi=0.203$ ;  $\psi=0.661$ ;  $\omega=0.433$ .

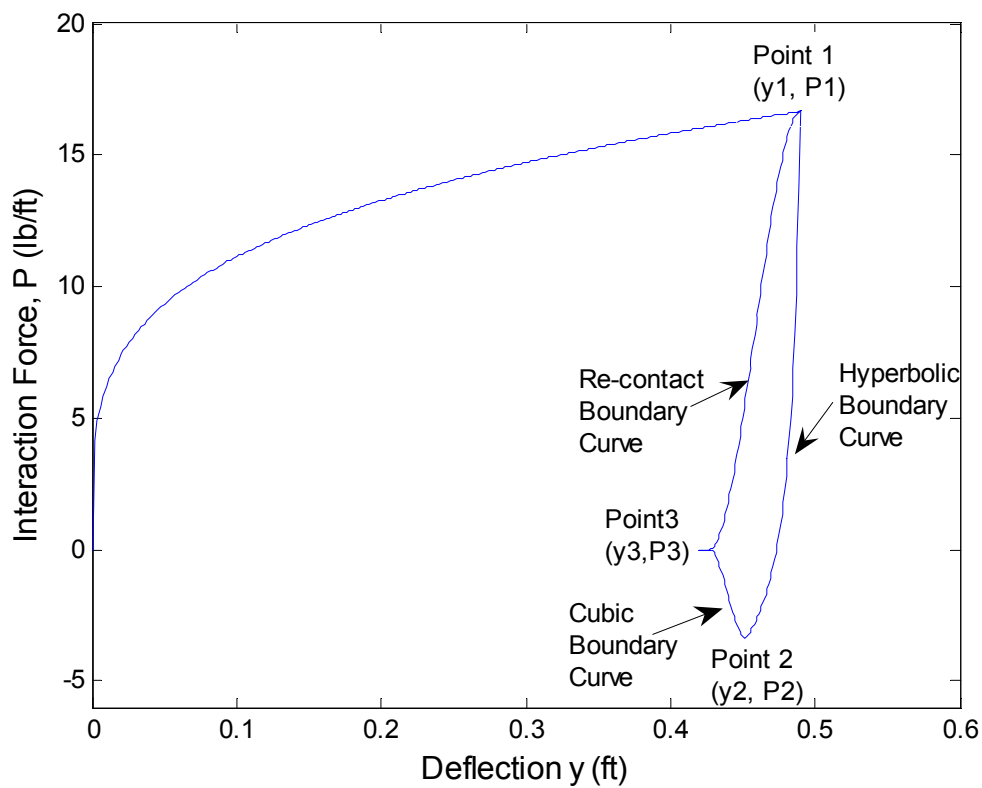


Figure 3.7 Example of Boundary Loop

### 3.2.3 Model of Reversal Curves within Bounding Loop

Reversal loops can occur from any point within the boundary curves. As the loading paths are very complex, several different model equations are developed to describe the unloading/reloading response in different conditions.

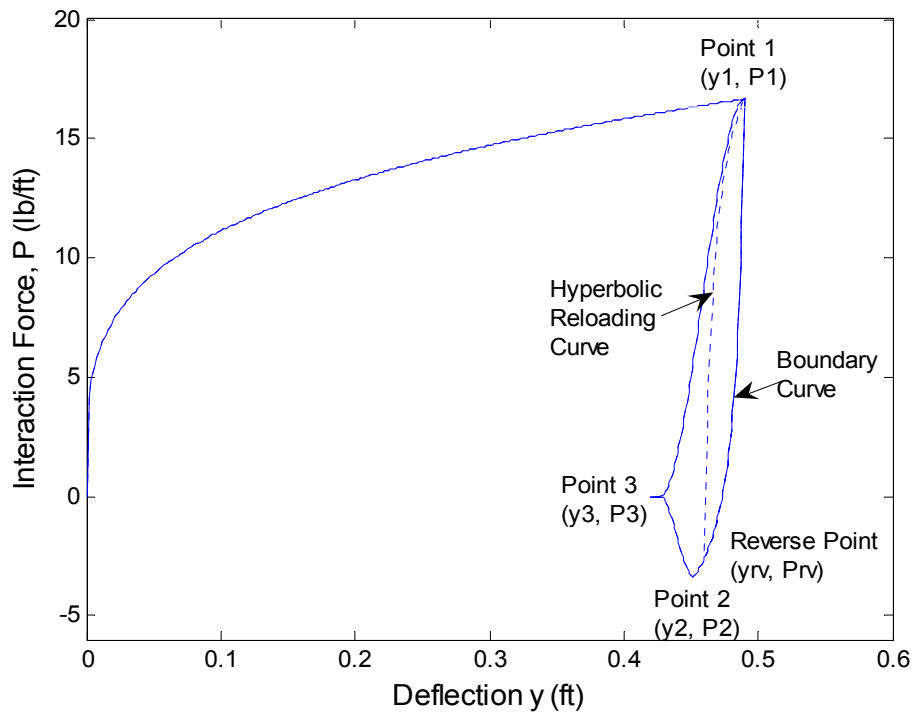


Figure 3.8 Example of Reversal Curve from Hyperbolic Unloading Boundary

Reversals from elastic rebound segment from Point 1 to Point 2 (reloading) and re-contact reloading segment between Point 3 and Point 1 (unloading) on the bounding loop, with an arbitrary reversal point  $(y_{rB}, P_{rB})$ , follow a hyperbolic path from the reversal point:

$$P = P_{rB} + \frac{y - y_{rB}}{\frac{1}{k_0} + \chi \frac{y - y_{rB}}{(1 + \omega)P1}} \quad (\text{Eq.3.18})$$

where  $\chi$  is the displacement loading direction parameter, as for unloading curves  $\chi = -1$  and conversely for loading loops  $\chi = 1$ .

Figure.3.8 shows an example reloading reversal curve starting from elastic rebound segment between Point 1 and Point 2. Figure 3.9 shows an example unloading reversal curve which starts from re-contact reloading segment between Point 3 and Point 1. Both of these two reversal curves are in hyperbolic shape.

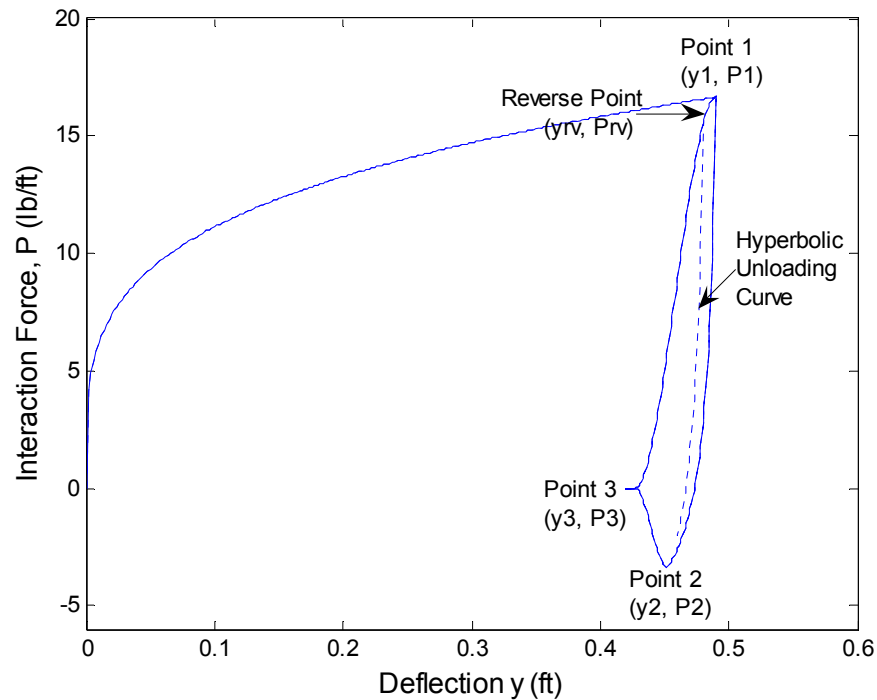


Figure 3.9 Example of Reversal Curve from Cubic Reloading Boundary

Function for reversal loops at any arbitrary reversal point  $(y_r, P_r)$ , which does not lay on the boundary curves, is:

$$P = P_r + \frac{y - y_r}{\frac{1}{k_0} + \chi \frac{y - y_r}{(1 + \omega)P1}} \quad (\text{Eq.3.19})$$

Figure.3.10 shows an example of reversal curves inside of the bounding loop. These reversal curves are all in hyperbolic shape as they just reverse from 1-2 and 3-1 boundary curves.

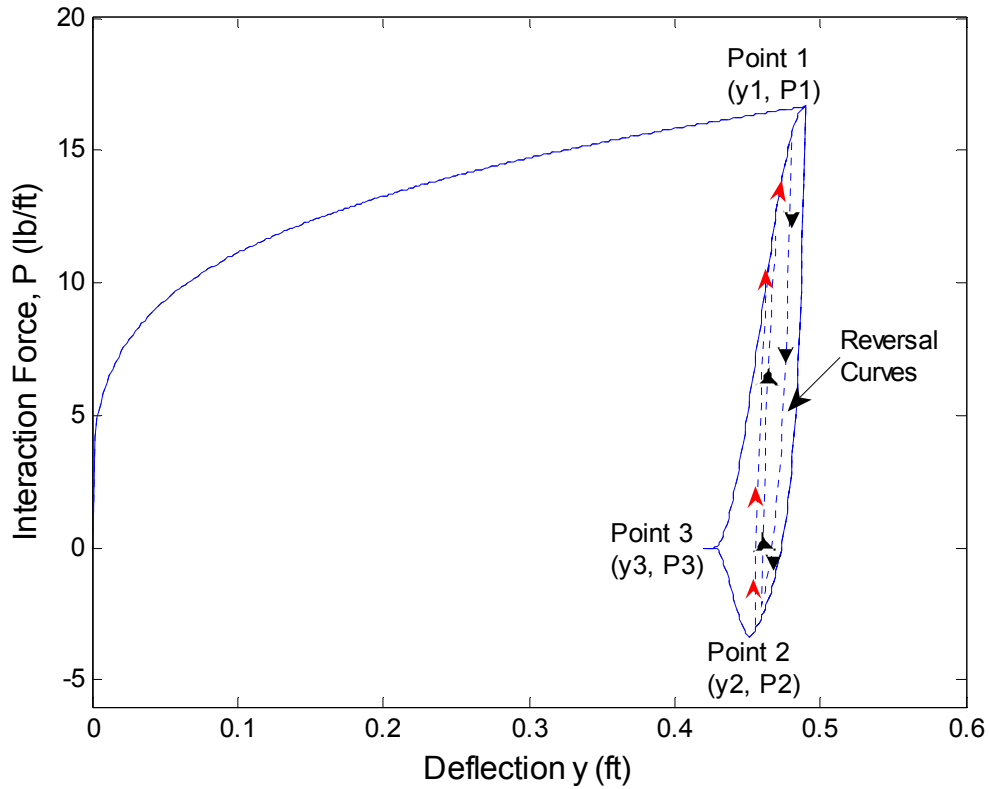


Figure 3.10 Reversal Curves inside Boundary Loops

Reversal loop from the partial separation region between Point 2 and Point 3 on the bounding loop follows a cubic relationship:

$$P = \frac{P_1 + P_{rB}}{2} + \frac{P_1 - P_{rB}}{4} \left[ 3 \left( \frac{y - y_0}{y_m} \right) - \left( \frac{y - y_0}{y_m} \right)^3 \right] \quad (\text{Eq.3.20})$$

$$y_0 = (y_1 + y_{rB}) / 2 \quad (\text{Eq.3.21})$$

$$y_m = (y_1 - y_{rB})/2 \quad (\text{Eq.3.22})$$

Figure.3.11 shows the reversal curve starting from the boundary curve for partial separation in the region between Point 2 and Point 3.

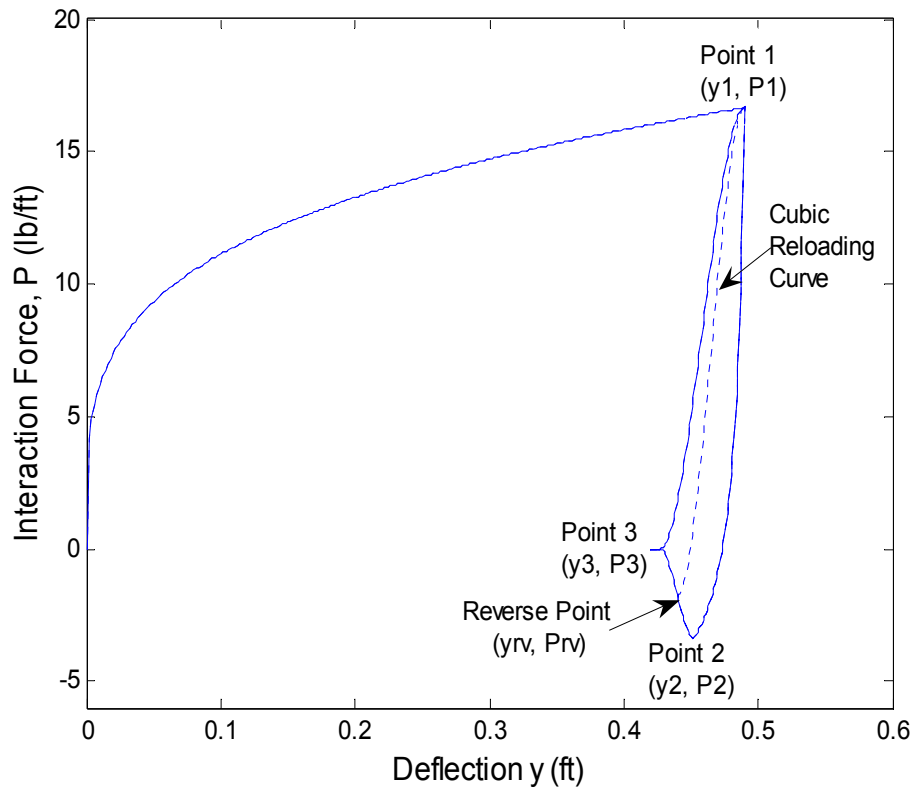


Figure.3.11 Cubic Reversal Curve from Cubic Unloading Boundary

### 3.3 NON-DEGRADATING $P$ - $y$ MODEL PROGRAMMING

A MATLAB programming code, applying with this non-degradation model, was developed to simulate complex  $P$ - $y$  behaviors of seafloor-riser interaction. The aim of this code is to be capable to process large amount of input data of a fixed point along the riser and then output the response curves for this point. Notice that the load input file data are in form of displacement rather than force.



The code first reads the physical parameters of the riser and seafloor soil in order to form the backbone curve and the boundary loop. In the next step, the code would read displacement history data of a fixed point from input files and then calculate the interaction forces of the soil spring at various positions. Finally, the  $P$ - $y$  response curve for this point is developed and the stiffness of the seafloor could be characterized by this curve. The programming code must include the following steps:

- 1) Read property parameters of riser and seafloor soil from the parameter input file which includes four riser pipe properties - the elastic modulus of the riser  $E$ , diameter  $d$ , thickness  $t$ , weight per unit area of the steel riser  $\rho$ ; two soil properties – soil strength at mudline  $S_{u0}$  and strength gradient  $S_g$ ; and two backbone curve coefficients -  $a$  and  $b$ . Calculate pipe moment of inertia  $I$ , and weight per unit length  $W$  using the input riser properties.
- 2) Develop the backbone curve to describe the initial penetration due to riser self-embedment.
- 3) Read model parameters from the parameter input file, which includes four bounding loop parameters -  $k_0$ ,  $\omega$ ,  $\phi$ , and  $\psi$ . Calculate and determine the three critical fixed points and define the bounding loop.
- 4) Read displacement history data for a fix riser point from the load input file.
- 5) Calculate spring force  $P$  for each deflection according to appropriate  $P$ - $y$  relationship defined in the non-degradating  $P$ - $y$  model.
- 6) Plot the  $P$ - $y$  response curve of this riser point.

A flow chart (Figure.3.12) is formulated to describe the work processes of this code.

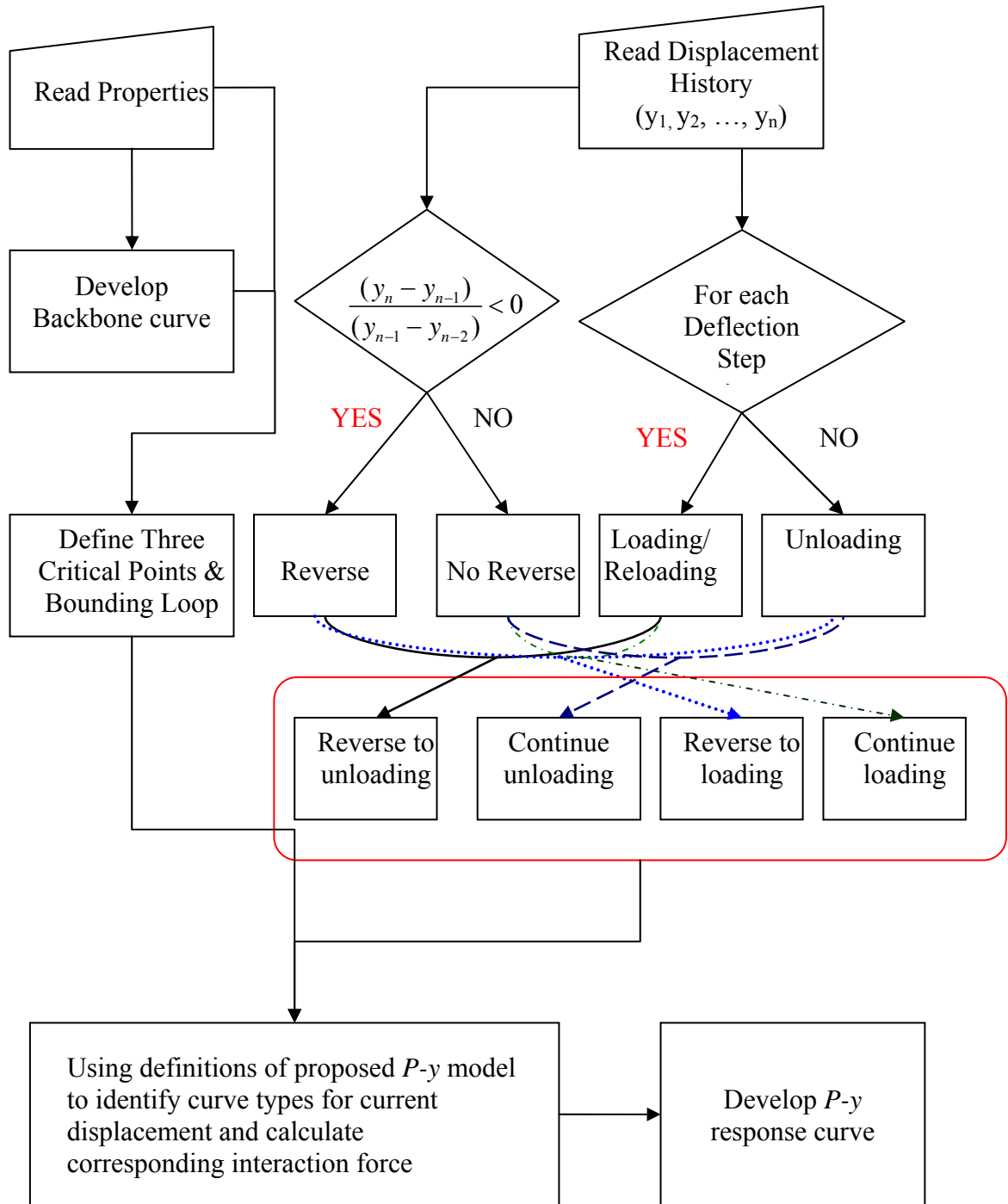


Figure.3.12 Flow Chart of Non-Degrading *P*-*y* Curve Code

### 3.4 PARAMETRIC STUDY AND VERIFICATION

In the non-degradating  $P$ - $y$  model, the critical parameters which characterize the  $P$ - $y$  interaction curve include two soil strength parameters ( $S_{u0}, S_g$ ), three trench parameters ( $w, d$ , roughness) which, in term, require other two backbone parameters ( $a, b$ ), and four bounding loop parameters ( $k_0, \omega, \phi$ , and  $\psi$ ). The three riser pipe properties ( $E, I, W$ ) are well defined for a given pipe material.

#### 3.4.1 Parametric Study on Soil Strength and Trench Formulation

The backbone curve is influenced by the two soil strength parameters ( $S_{u0}, S_g$ ), three trench parameters ( $w, h$ , and roughness), which influence two backbone parameters ( $a, b$ ) very much. The effects of these parameters will studied in the following steps.

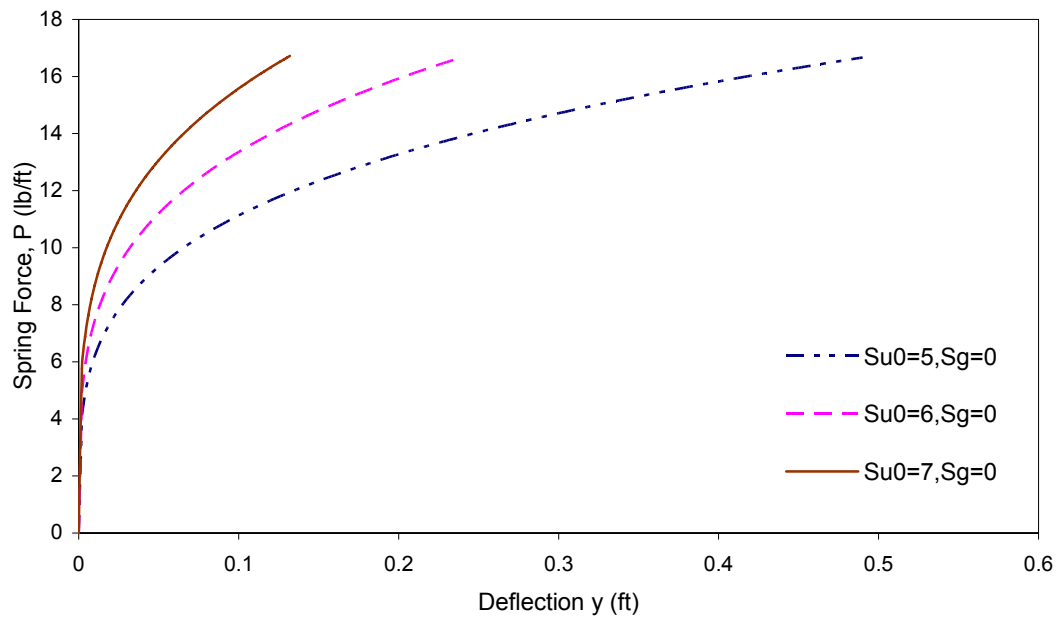


Figure.3.13 Effects of  $S_{u0}$

Figure.3.13 and Figure.3.14 illustrate the influence of two soil strength parameters at  $w/d = 1$ . The comparison between cases:  $S_{u0} = 5$  psf,  $S_g = 0$ ;  $S_{u0} = 6$  psf,  $S_g = 0$  and  $S_{u0} = 7$  psf,  $S_g = 0$  is shown in Figure.3.13 and the difference between cases:  $S_{u0} = 5$  psf,  $S_g = 0$ ;  $S_{u0} = 5$  psf,  $S_g = 1$  psf and  $S_{u0} = 5$  psf,  $S_g = 2$  psf is shown in Figure.3.14.

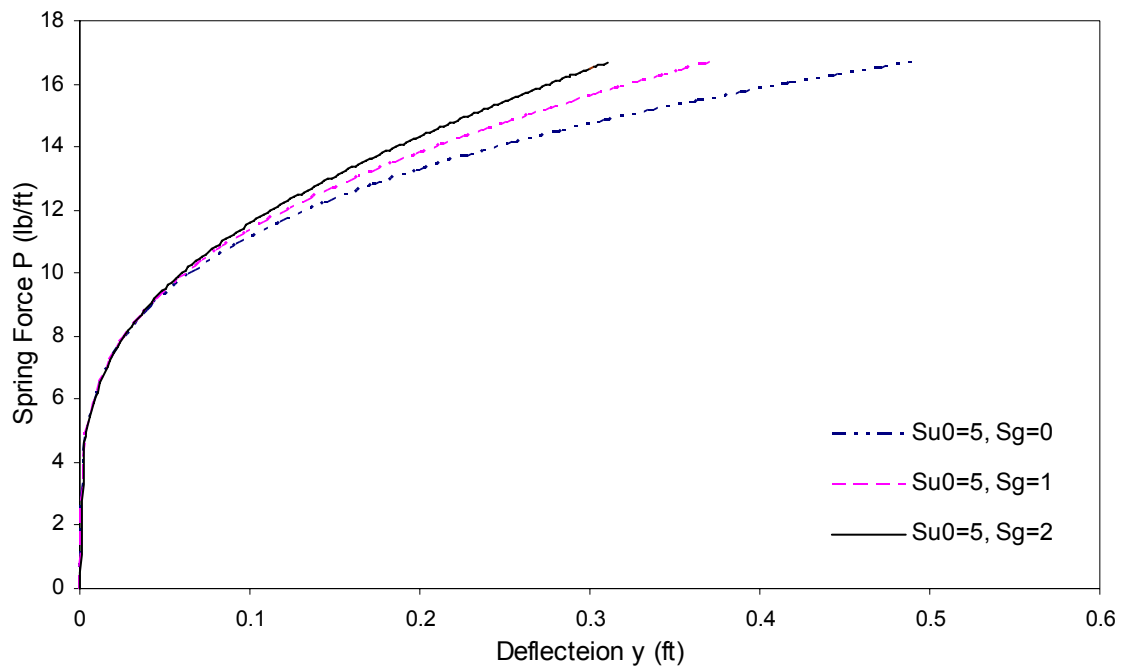


Figure.3.14 Effects of  $S_g$

Figure.3.13 and Figure.3.14 show that the stiffness of soil spring increases as the soil becomes stronger. Figure.3.15 compares the influence of these two soil strength parameters and it seems that  $S_{u0}$  has more influence on the initial soil stiffness than  $S_g$  does.

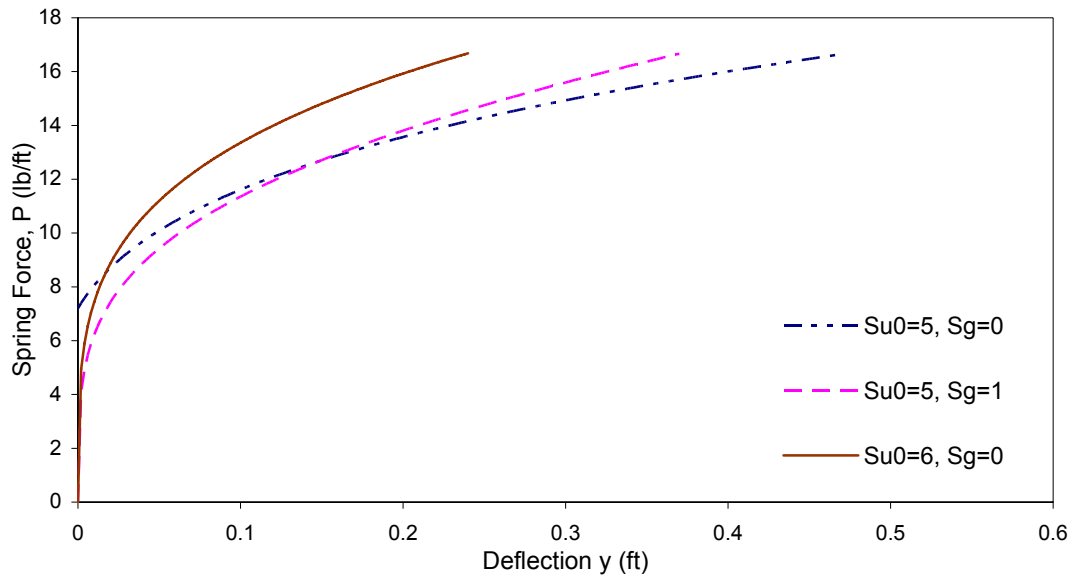


Figure.3.15 Comparison of the Influence of  $S_{u0}$  and  $S_g$

Figure.3.16 and Figure.3.17 illustrate the influence of two trench parameters: trench width,  $w/d$ , and pipe-soil surface roughness, with the same soil strength  $S_{u0} = 5$  psf,  $S_g = 0$  and parameters of riser pipe. The comparison between cases:  $w/d = 1$  (for  $h/d < 0.5$ ,  $a=6.73$ ,  $b=0.29$ ; for  $h/d > 0.5$ ,  $a=6.15$ ,  $b=0.15$ ),  $w/d = 1.5$  (for  $h/d < 0.5$ ,  $a=6.13$ ,  $b=0.22$ ; for  $h/d > 0.5$ ,  $a=5.96$ ,  $b=0.105$ ) and  $w/d = 2$  (for  $h/d < 0.5$ ,  $a=5.9$ ,  $b=0.06$ ; for  $h/d > 0.5$ ,  $a=5.6$ ,  $b=0.05$ ) for rough surface is shown in Figure.3.16 and the difference between cases: smooth and rough surface at  $w/d = 1$  is shown in Figure.3.17.

Figure.3.16 shows the soil stiffness decreases and the trench width increase when the penetration depth  $h/d > 0.5$  and for penetration depth  $h/d < 0.5$  there is not obvious influence with the trench width increases.

Figure.3.17 describes the influence of roughness on the surface of the soil-riser pipe,

and it is clear that rough soil-pipe surface has bigger stiffness than smooth condition.

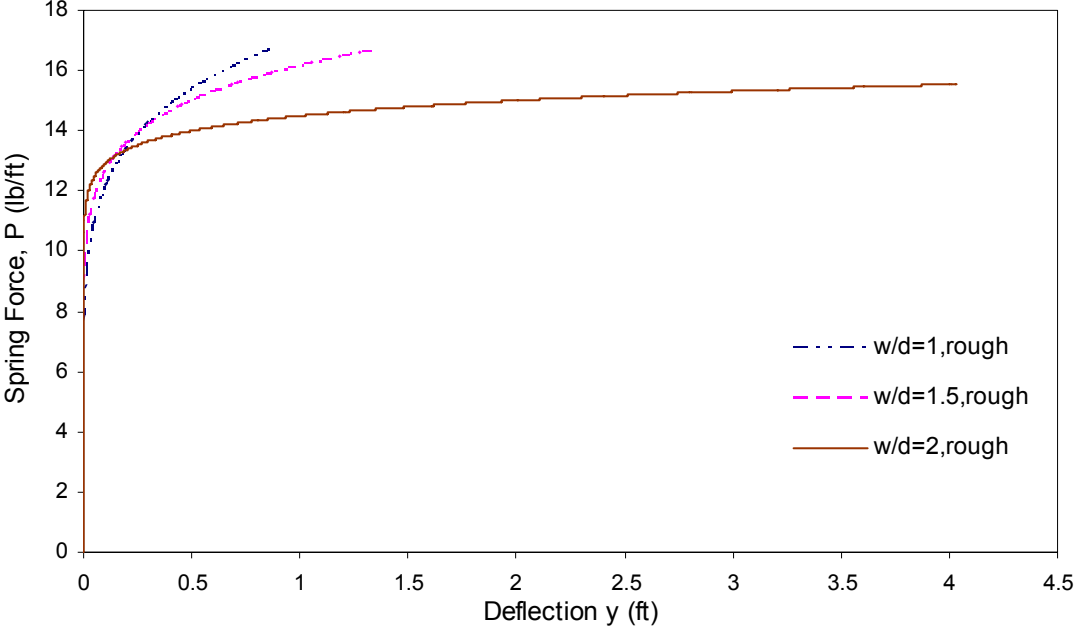


Figure.3.16 Effects of Trench Width

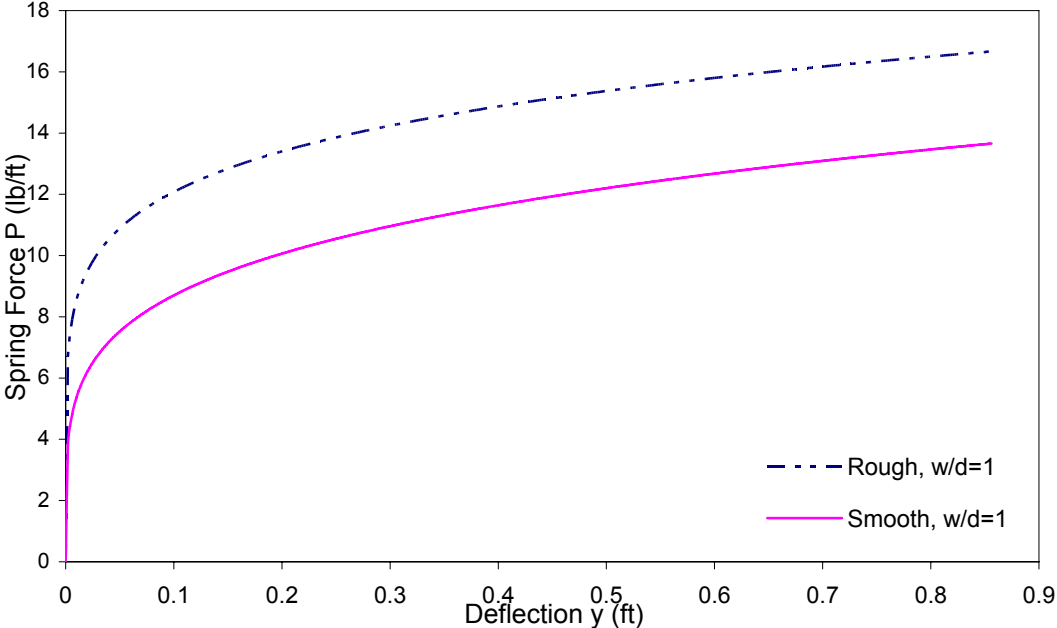


Figure.3.17 Effects of Roughness

### 3.4.2 Parametric Study on Bounding Loop Parameters

The bounding loop parameters consist of hyperbolic curve parameters  $k_0$  and  $\omega$ , the tension limit parameter  $\phi$  and the soil-riser separation parameter  $\psi$ .

Figure.3.18 shows the effect of initial stiffness  $k_0$  as its value varies at 500, 600 and 700 and Figure 3.19 shows the influence of asymptote factor  $\omega$  when it equals to 0.4, 0.5, and 0.6 respectively. As shown in Figure.3.18 and Figure.3.19,  $k_0$  and  $\omega$  have similar influence tendency that as  $k_0$  and  $\omega$  increases, the separation of the soil-riser occurs at larger deflection as well as the stiffness in bounding loop increases. As described in Eq.3.11,  $y_2$  would increase if  $k_0$  or  $\omega$  increase and conversely  $y_2$  would decrease if  $k_0$  or  $\omega$  decreased.

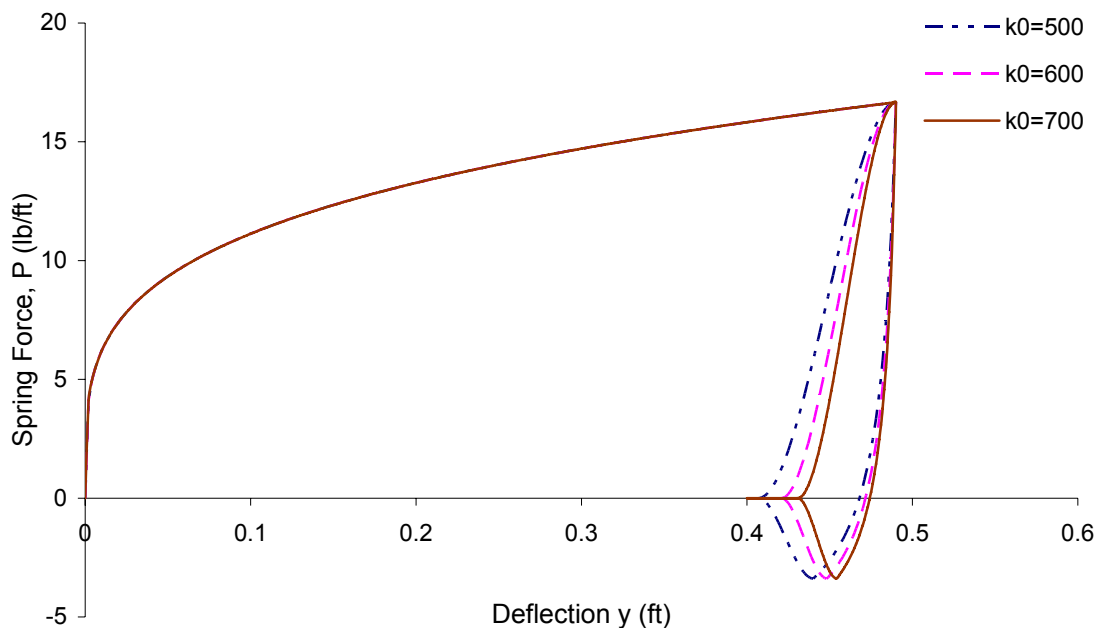


Figure.3.18 Effects of  $k_0$

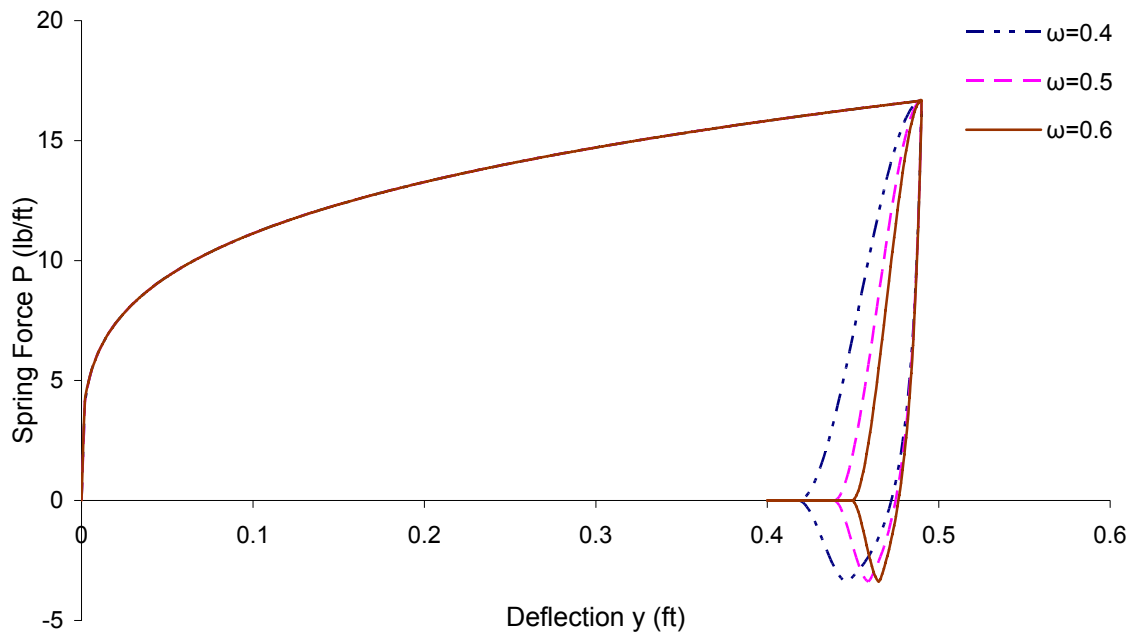
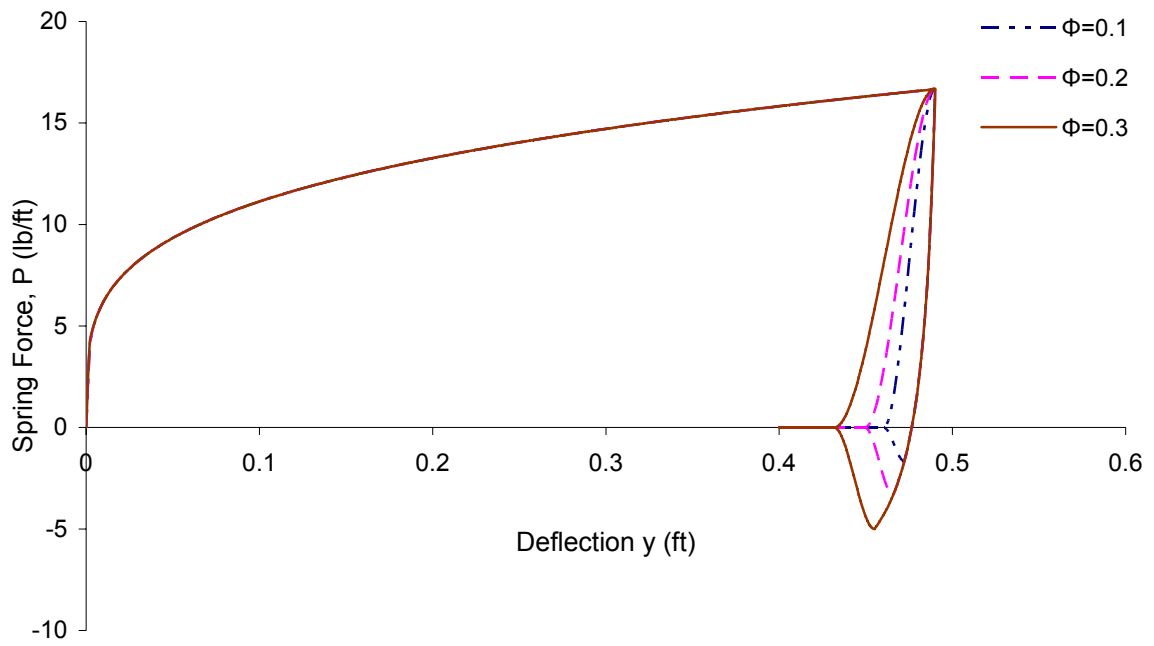
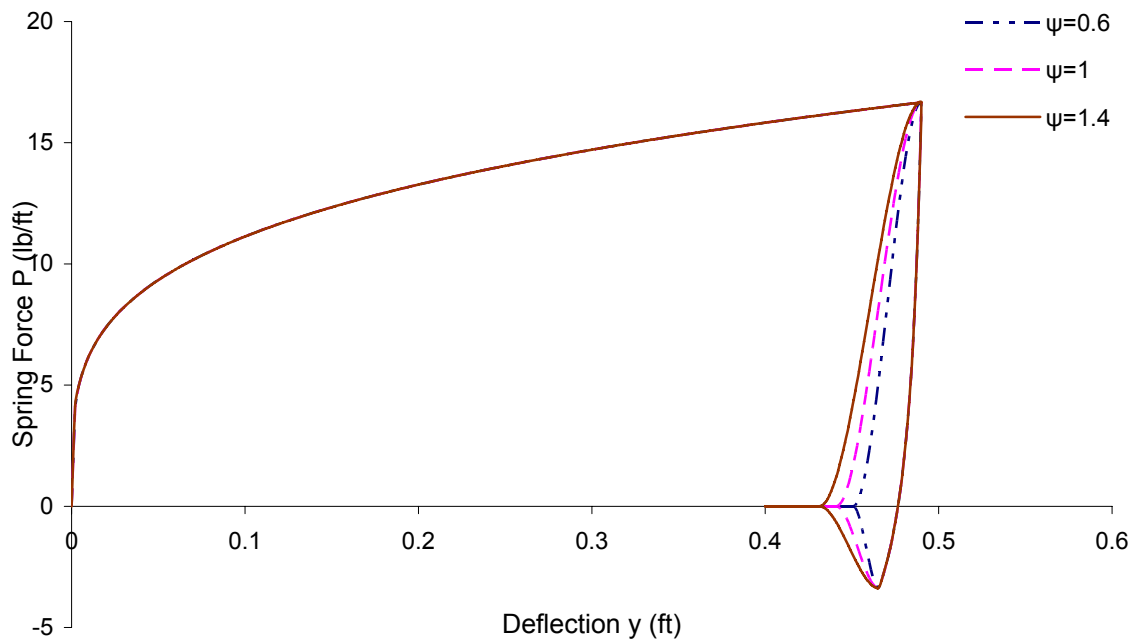


Figure.3.19 Effects of  $\omega$

The effects of tension limit parameter  $\phi$  and the soil-riser separation controlled parameter  $\psi$  are illustrated in Figure.3.20 and Figure.3.21 respectively. In Figure 3.20, the value of  $\phi$  varies from 0.1, 0.2 to 0.3 and in Figure3.21 the value of  $\psi$  equals to 0.6, 0.7 and 0.8.

It is clearly shown that as  $\phi$  increases, the maximum tension increases and  $y_2$  and  $y_3$  decrease which cause the decrease of the cubic boundary stiffness. The hyperbolic boundary is not affected. Figure.3.21 shows that for  $y_3$  decreasing as  $\psi$  increases, which causes the stiffness to decrease in the cubic function boundaries. There is no influence for the hyperbolic boundary.



Figure.3.20 Effects of  $\phi$ Figure.3.21 Effects of  $\psi$

### 3.4.3 Validation of the Model

Dunlap et al. (1990) conducted a series of laboratory tests to simulate pipeline-sediment interaction under cyclic load conditions. Figure.3.21 shows an example of such a test interpretation using the basin test data. The test includes initial plastic pipe penetration to Point 1, followed by unloading to full separation between soil and pipe.

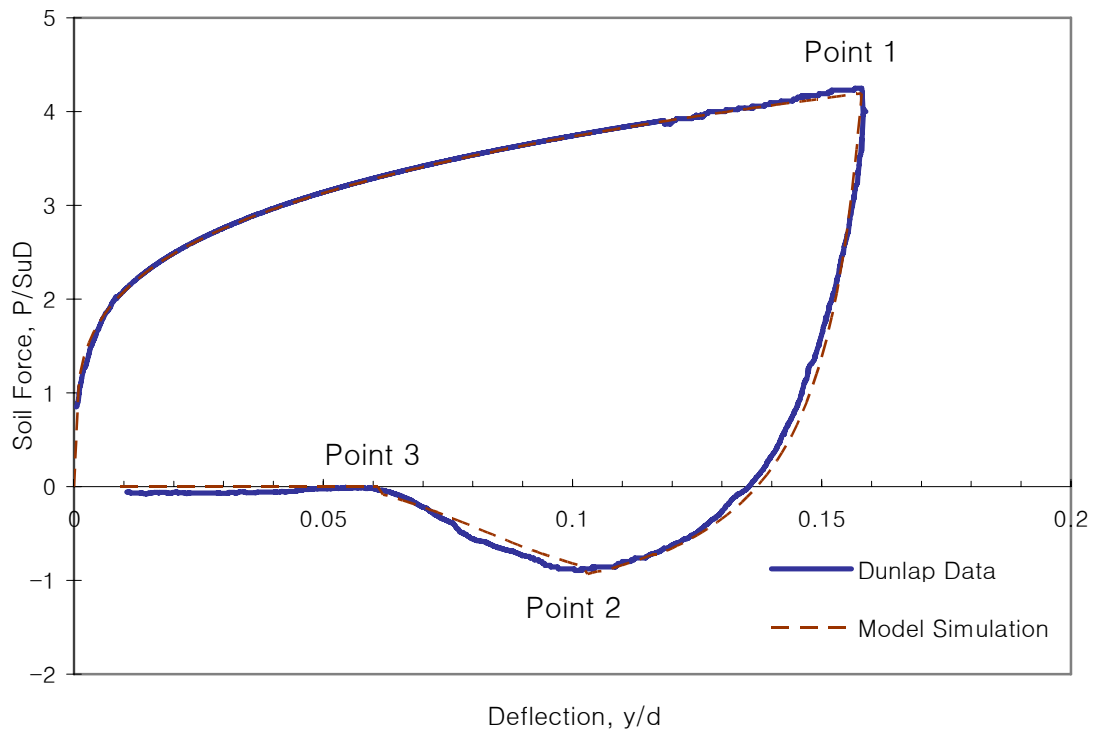


Figure.3.22 Comparison of Model Simulation with Measured Data

A simulation of the proposed  $P$ - $y$  model is carried out with the same soil and riser pipe properties as Dunlap's tests (Table 3.1). In this simulation, the model parameters use the value recommended by Aubeny et al. (2006), which are listed in Table 3.2. The simulation result is shown as a dashed line in Figure.3.21, which matches the laboratory data very well. The comparison of model simulation to laboratory data indicates that the proposed  $P$ - $y$  model is capable of accurately describing the actual  $P$ - $y$  relationship of seafloor-riser. Here, it is noted that

due to lack of data for re-contact and re-loading path after full separation of soil and riser, the accuracy of the cubic model for this stage (Path 3-1) can not be verified thus additional test data are needed.

Table 3.1 Soil and Riser Properties

| Property | Description                            | Value |
|----------|--|-------|
| $d$      | Riser Diameter (ft)                    | 0.5   |
| $t$      | Riser Thickness (in)                   | 0.2   |
| $W$      | Riser's Unit Weight per Length (lb/ft) | 12.2  |
| $S_{u0}$ | Soil Strength at mudline               | 21    |
| $S_g$    | Soil gradient                          | 0     |

Table 3.2 Model Parameters (Aubeny et al., 2006)

| Parameter      | Description                | Value |
|----------------|----------------------------|-------|
| $a$            | Backbone Curve Coefficient | 6.70  |
| $b$            | Backbone Curve Coefficient | 0.254 |
| $k_0 / S_{u0}$ | Unload Initial Stiffness   | 660   |
| $\omega$       | Unload Large Deflection    | 0.433 |
| $\phi$         | Unload Large Tension Limit | 0.203 |
| $\psi$         | Soil-Riser Separation      | 0.661 |

## CHAPTER IV

### DEGRADATING $P$ - $y$ MODEL FOR SEAFLOOR-RISER INTERACTION

#### 4.1 INTRODUCTION

Cyclic loads degrade stiffness due to fatigue. Cyclic degradation is generally thought to affect the capacities of structural systems to resist failure under cyclic loading condition. After the forces exerted on structural members subjected to cyclic loading reach the maximum strength of those members, the members tend to lose strength and stiffness with the increase in plastic displacement that occurs in loading cycles.

From the results of several of triaxial shear tests on undisturbed and remolded specimens of soft soils, Idriss et al. (1978) concluded that as the number of load cycles increases, the stiffness of cohesive soils is degraded, resulting in progressive reduction in the modulus. Figure.4.1 shows the degradation effects for secant Young's modulus  $E$  of soft soils. The amount and rate of degradation depend on soil type and state, stress level,

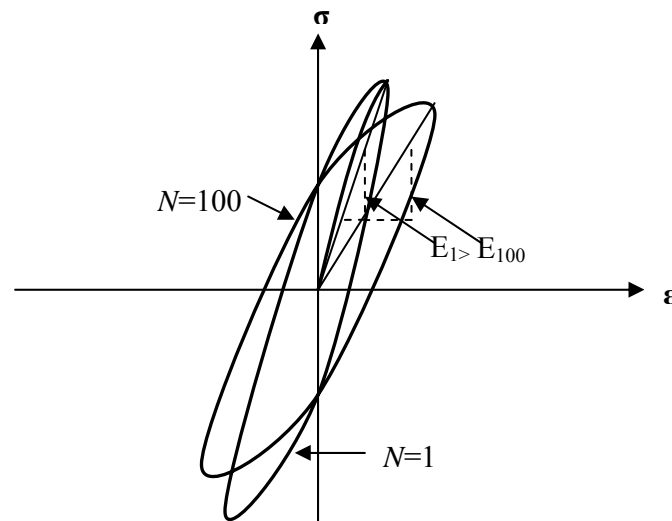


Figure 4.1 Cyclic Modulus Degradation Curves

cyclic stress amplitude and number of applied cycles of stress.

Seafloor stiffness degradation due to cyclic loading has a significant impact on the performance of steel catenary risers in the touchdown zone, and especially on the riser's resistance to fatigue. In order to capture this effect on the riser's response, soil degradation must be included in the modeling efforts.

The seafloor stiffness degradation mechanism includes the cyclic damage and stiffness reduction produced in uplift movements and separations as well as re-penetration process (Fontaine et al., 2004). In the unloading and reloading processes, the riser pipe uplift and downward movements cause the seafloor soil to be remolded with stiffness and strength reduced under the cyclic loading. Also, if separation occurs in the unloading stage, the soil has been loaded to a failure state which cause significant cyclic damage. And the reloading process that occurs after separation also significantly reduced soil stiffness. Clukey et al. (2005) concluded that as the pipe moves back toward the soil, the water underneath the pipe is pushed downward. The jetting action by the water can lead to soil-water mixing and trench erosion which can also reduce the strength and stiffness of the soil.

To better simulate the realistic seafloor-riser response, the cyclic degradation effects should be accurately modeled and illustrated in the seafloor-riser load-deflection ( $P$ - $y$ ) model. And to be in accord with previous  $P$ - $y$  model, the stiffness parameter  $k$  in force-displacement relationship is adopted to describe the cyclic degradation effects instead of the undrained Young's modulus  $E$  in stress-strain curve which is commonly used in previous research. (e.g., Rajashree et al., 1996; Romo et al., 1999).

In the following study, cyclic degradation effects are incorporated into the  $P$ - $y$  model for seafloor-riser response following observations and laboratory tests. The degradation model proposes three degradation control parameters, which consider the effects of the number of cycles and cyclic unloading-reloading paths. Accumulated deflections serve as a measure of energy dissipation. The  $P$ - $y$  model can simulate all loading cases, including initial penetration and uplift, as well as re-penetration under complex soil-riser contact conditions considering cyclic degradation effects. Comparison of model simulations with published experimental results illustrates the proposed model could realistically and accurately simulate actual behavior of seafloor-riser system.

#### **4.2 DEGRADATING $P$ - $y$ MODEL**

The seafloor stiffness degradation mechanism includes the cyclic damage and stiffness reduction during uplift movement and seafloor-riser separation as well as re-penetration process. During unloading and reloading, the riser pipe uplift or downward movements cause the seafloor soil to be remolded, with stiffness and strength reduced under the cyclic loading. And, if the separation occurs in the unloading stage, the soil has been loaded to failure which causes significant strength damage. In addition, model tests indicate that reloading occurs after separation also significantly reduced soil stiffness. As the riser moves back toward the soil, the water underneath the pipe is pushed downward. The jetting action by the water can lead to soil-water mixing and trench erosion which can also reduce the strength and stiffness of the soil.

Based on previous load-deflection framework, the refined  $P$ - $y$  model presented in this paper incorporates seafloor stiffness degradation effects to better simulate the

seafloor-riser's  $P$ - $y$  behavior in complex cyclic loading conditions. The degrading  $P$ - $y$  model should include the following components: 1) Initial penetration into the seafloor due to riser's self-weight (Path 0-1<sup>1</sup>). 2) Bounding loops comprised with boundaries of elastic rebound with full seafloor-riser contact (Path 1<sup>n</sup>-2<sup>n</sup>), up-lift with partial separation (Path 2<sup>n</sup>-3<sup>n</sup>) and re-contact reloading with stiffness degradation (Path 3<sup>n</sup>-1<sup>n+1</sup>). 3) Reversal loops from or within the bounding loop (dash lines). 4) Fully separation stage in uplift and downward movement (Path 3<sup>n</sup>-4<sup>n</sup>). Fig.4.2 shows the general form of the degrading  $P$ - $y$  model.

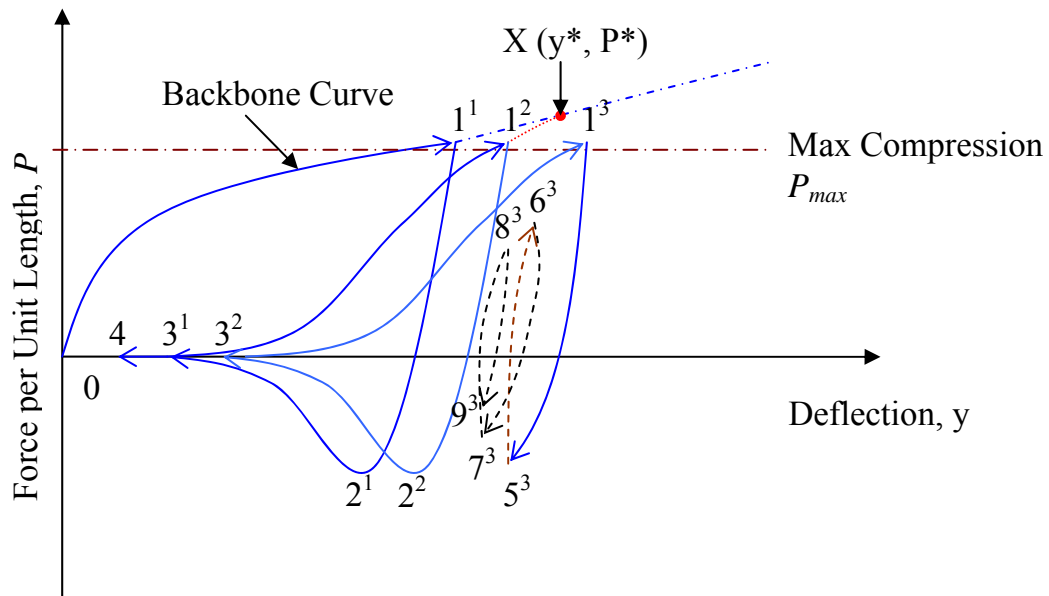


Figure.4.2 Typical Degrading  $P$ - $y$  Curves

In the case of cyclic degradation analysis, riser's accumulated deflection,  $\lambda_n$ , serves as the energy dissipation factor. It is defined as:

$$\lambda_n = \sum_{i=1}^n |\Delta y_i| \quad (\text{Eq.4.1})$$

where  $\Delta y_i$  is the deflection within one loading cycle and  $n$  is the number of loading cycles.

#### 4.2.1 Backbone Curve of Degrading Model

The backbone curve has the same form as the non-degrading model as shown in Fig.4.3.

$$P = a\left(\frac{y}{d}\right)^b (S_{u0} + S_g y) d \quad (\text{Eq.4.2})$$

where  $a$  and  $b$  are the curve coefficient which varies with trench conditions and pipe roughness;  $d$  is the diameter of the riser pipe;  $S_{u0}$  is the shear strength at the mudline and  $S_g$  is strength gradient and  $y$  is the trench depth (riser deflection).

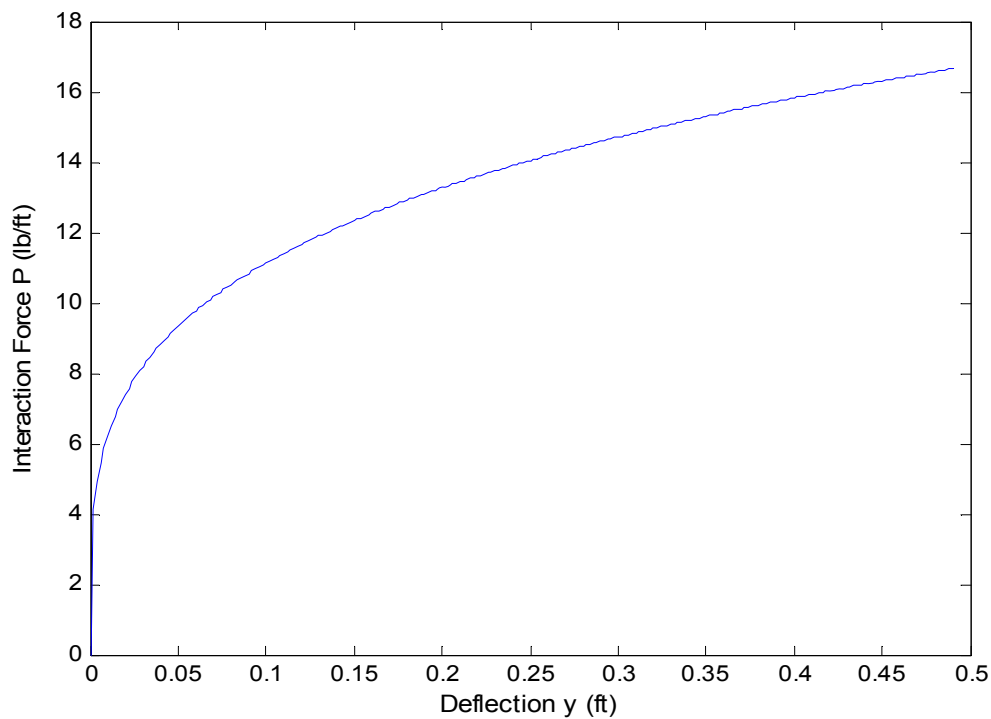


Figure.4.3 Backbone Curve of Degrading Model



And the maximum compression load of seafloor-riser interaction,  $P_{max}$ , is equal to the self-weight of the riser.

#### 4.2.2 Bounding Loops of Degrading Model

For each load cycle, under extremely large deflection conditions, the bounding loop could be described in terms of four points. In the  $n^{th}$  loading cycle, the degradation control point  $X (y^*, P^*)$ , is the end of the reloading curve (Path  $3^n - 1^{n+1}$ ) when it emerges into the backbone curve (Path  $0 - 1^{n+1}$ ). For all reloading paths, the reloading  $P$ - $y$  curve would go back to this control point from the reversal point (Fig.4.4). This control point is defined as a function of energy dissipation factor ( $\lambda_n$ ), as shown in Eq.4.3:

$$y^* = y_1^1 + \alpha \lambda_n^{0.5} \quad (\text{Eq.4.3})$$

where  $y_1^1$  refers to the riser deflection due to self-embedment;  $\alpha$  serves as the first degradation control factor which controls the degradation effects for cubic reloading curve.

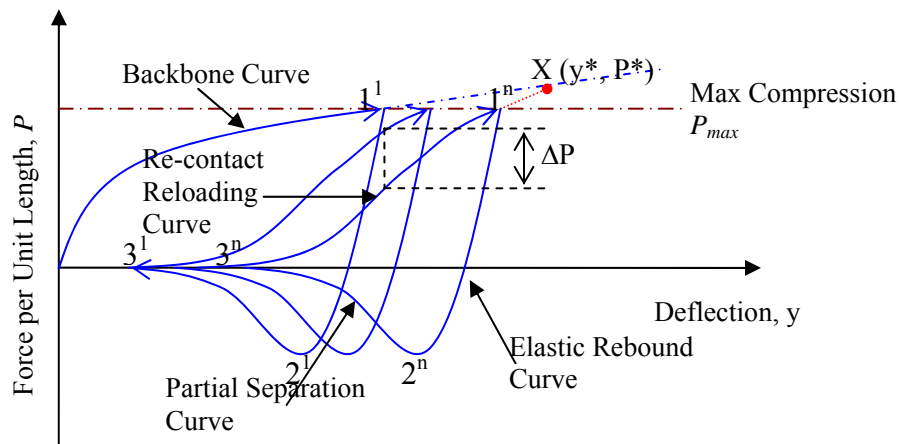


Figure.4.4 Illustration of Bounding Loops of Degrading  $P$ - $y$  Model under Extremely Large Condition

As point X ( $y^*$ ,  $P^*$ ) is on the backbone curve, the value of the seafloor-riser interaction force could be determined by:

$$P^* = a\left(\frac{y^*}{d}\right)^b (S_{u0} + S_g y^*) d \quad (\text{Eq.4.4})$$

According to Eq.4.3, the control point X ( $y^*$ ,  $P^*$ ) would be updated as new accumulated deflection generated when the next loading cycle started.

The bounding loops of this degradation model are formed by three series of characteristic points. In the  $n^{\text{th}}$  loading cycle, point  $1^n$  is defined as the point of maximum compression of the soil spring at the reloading bound curve; thus  $P_1^n = P_{\max}$ ; point  $2^n$  is defined as the point of maximum tension of the soil spring reached and point  $3^n$  is the point at which the riser pipe totally separated from the seafloor. These three points have the same relationship as the non-degradation model defines:

$$P_2^n = -\phi P_1^n \quad (\text{Eq.4.5})$$

$$(y_2^n - y_3^n) = \psi (y_1^n - y_2^n) \quad (\text{Eq.4.6})$$

$$P_3^n = 0 \quad (\text{Eq.4.7})$$

where  $\phi$  is defined as suction limit parameter;  $\psi$  is defined as soil-riser separation parameter and it is used to determine the deflection of the riser when full separation occurred; and  $\omega$  is the parameter which controls the asymptote of the hyperbolic curve. These three model parameters are determined directly from laboratory model test.

The elastic rebound curve (Path  $1^n - 2^n$ ) is defined in a hyperbolic relationship (Figure.4.4):

$$P = P_{\max} + \frac{y - y_1^n}{\frac{1}{k_0} + \chi \frac{y - y_1^n}{(1 + \omega)P_{\max}}} \quad (\text{Eq.4.8})$$

Where  $\chi$  is the displacement loading direction parameter, as for unloading curves  $\chi = -1$  and conversely for loading loops  $\chi = 1$ . Here  $\chi = -1$  as the riser is in unloading stage.

The partial separation curve (Path  $2^n - 3^n$ ) is defined in form of cubic relationship (Figure.4.4):

$$P = \frac{P_2^n + P_3^n}{2} + \frac{P_2^n - P_3^n}{4} \left[ 3 \left( \frac{y - y_0}{y_m} \right) - \left( \frac{y - y_0}{y_m} \right)^3 \right] \quad (\text{Eq.4.9})$$

$$y_0 = (y_2^n + y_3^n) / 2 \quad (\text{Eq.4.10})$$

$$y_m = (y_2^n - y_3^n) / 2 \quad (\text{Eq.4.11})$$

The re-contact reloading curve along Path  $3^n - 1^{n+1}$  is also in form of cubic relationship (Figure.4.4):

$$P = \frac{P^* + P_3^n}{2} + \frac{P^* - P_3^n}{4} \left[ 3 \left( \frac{y - y_0}{y_m} \right) - \left( \frac{y - y_0}{y_m} \right)^3 \right] \quad (\text{Eq.4.12})$$

$$y_0 = (y^* + y_3^n) / 2 \quad (\text{Eq.4.13})$$

$$y_m = (y^* - y_3^n) / 2 \quad (\text{Eq.4.14})$$

An example of bounding loops (Figure.4.5) clearly describes the  $P$ - $y$  behavior under extremely large deflection. Notice that the effect of degradation parameters is directly illustrated in the re-contact reloading stage and then affects the whole loading cycles. In

this model, the maximum spring force could not exceed the value of  $P_{\max}$ , so the limitation to the model application is that the reloading forces could not exceed the spring force at self-embedment.

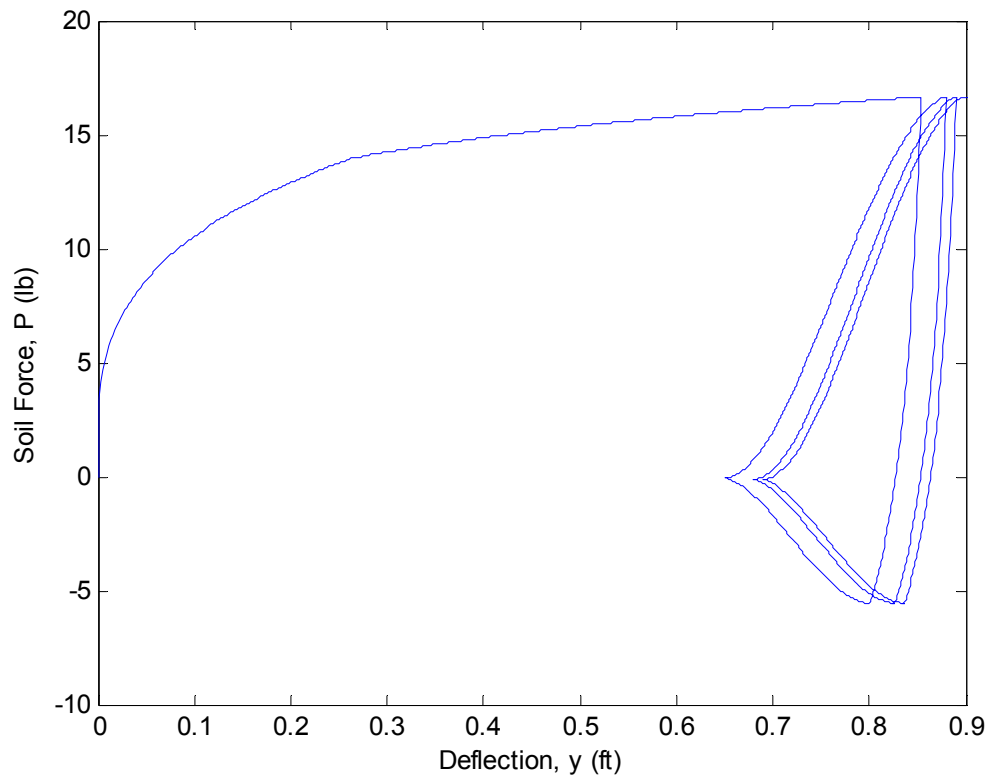


Figure.4.5 Example Bounding Loop for Degrading Model

### 4.2.3 Degradation Reversal Cycles from or within the Bounding Loop

There are 3 types of curve models for the reversal loops starting from the bounding loop.

Reversal loops (reloading loop) from elastic rebound curve along Path 1<sup>n</sup> - 2<sup>n</sup>, with an arbitrary reversal point  $(y_{rB}, P_{rB})$  are defined in form of degradation hyperbolic relationships (Figure.4.6):

$$P = P_{rB} + \frac{y - y_{rB}}{\frac{1}{k_0} + \chi \frac{y - y_{rB}}{(1 + \omega)P^* \xi}} \quad (\text{Eq.4.15})$$

$$\xi = \frac{y^* - y_{rB}}{P^* \left( \frac{y^* - y_{rB}}{P^* - P_{rB}} - \frac{1}{k_0} \right)} \quad (\text{Eq.4.16})$$

where  $\xi$  is the second degradation control factor. It defines the degradation effects for hyperbolic reloading curves;  $\chi = 1$  for reloading stage.

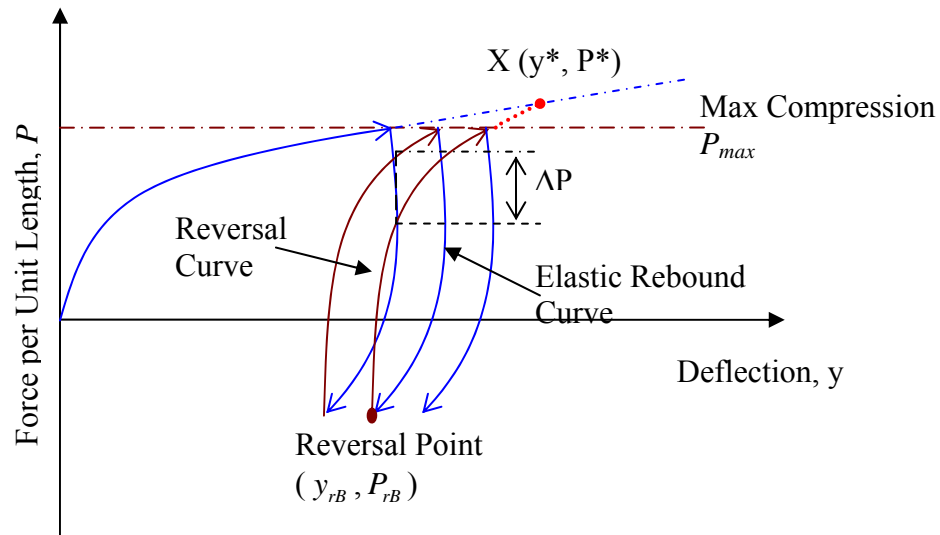


Figure.4.6 Illustration of Hyperbolic Reversal Curves from Elastic Rebound Bounding Curve

Reversal loops from partial separation bounding curve along Path 2<sup>n</sup> - 3<sup>n</sup> follow a cubic relationship (Figure.4.7):

$$P = \frac{P^* + P_{rB}}{2} + \frac{P^* - P_{rB}}{4} \left[ 3 \left( \frac{y - y_0}{y_m} \right) - \left( \frac{y - y_0}{y_m} \right)^3 \right] \quad (\text{Eq.4.17})$$

$$y_0 = (y^* + y_{rB}) / 2 \quad (\text{Eq.4.18})$$

$$y_m = (y^* - y_{rB})/2 \quad (\text{Eq.4.19})$$

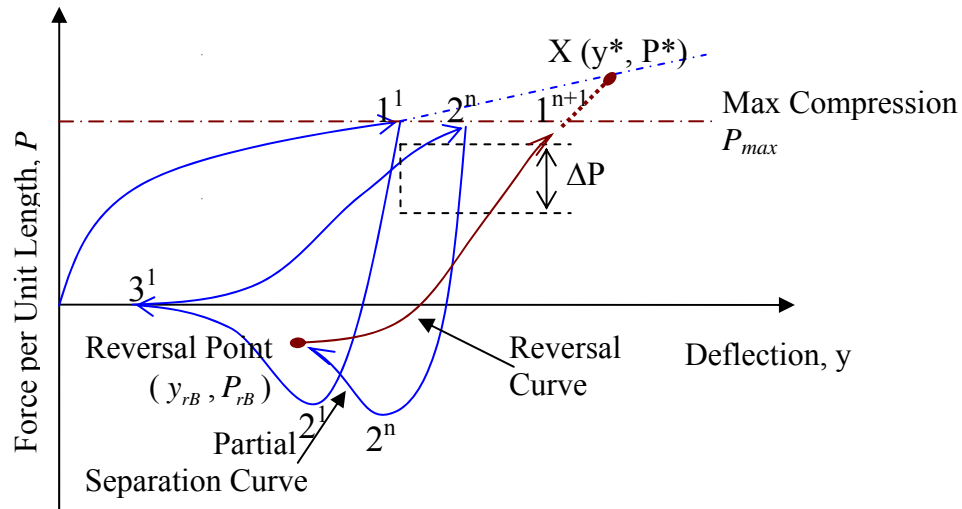


Figure.4.7 Illustration of Cubic Reversal Curve

Reversal loops from re-contact reloading curve along the re-contact and reloading bounding loop (Path  $3^n - 1^{n+1}$ ), with an arbitrary reversal point  $(y_{rB}, P_{rB})$  follow the general hyperbolic relationship (Figure.4.8):

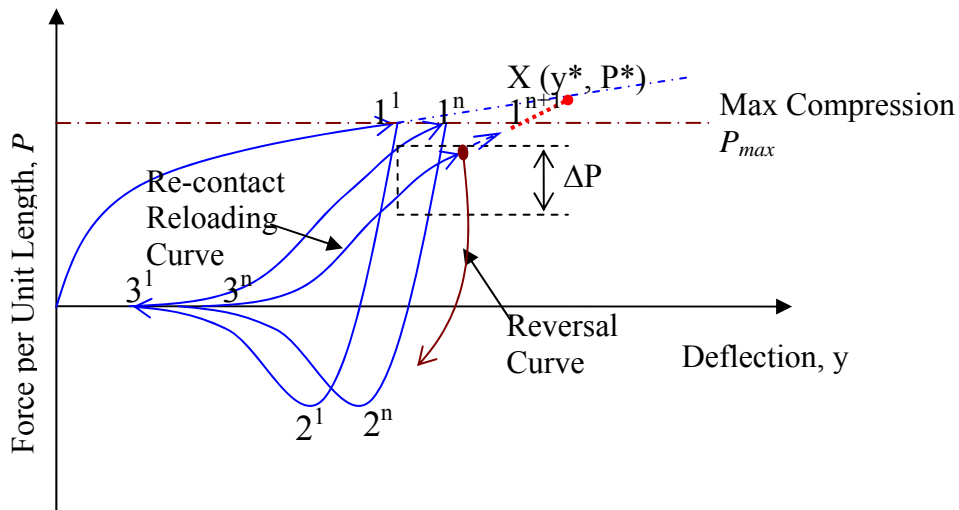


Figure.4.8 Illustration of Hyperbolic Reversal Curves from Re-contact Reloading Bounding Curve

$$P = P_{rB} + \frac{y - y_{rB}}{\frac{1}{k_0} + \chi \frac{y - y_{rB}}{(1 + \omega)P_1^n}} \quad (\text{Eq.4.20})$$

Here  $\chi = -1$  for unloading stage.

Two model curves are used to describe the reversal loops within the bounding loop. The reloading cycles within the bounding loops, with an arbitrary reversal point  $(y_r, P_r)$ , are described by degradation hyperbolic equations (Figure.4.9):

$$P = P_r + \frac{y - y_r}{\frac{1}{k_0} + \chi \frac{y - y_r}{(1 + \omega)P^* \xi}} \quad (\text{Eq.4.21})$$

$$\xi = \frac{y^* - y_r}{P^* \left( \frac{y^* - y_r}{P^* - P_r} - \frac{1}{k_0} \right)} \quad (\text{Eq.4.22})$$

where  $\xi$  is the second degradation control factor and it is determined by Eq.4.22;

$\chi = 1$  for reloading stage.

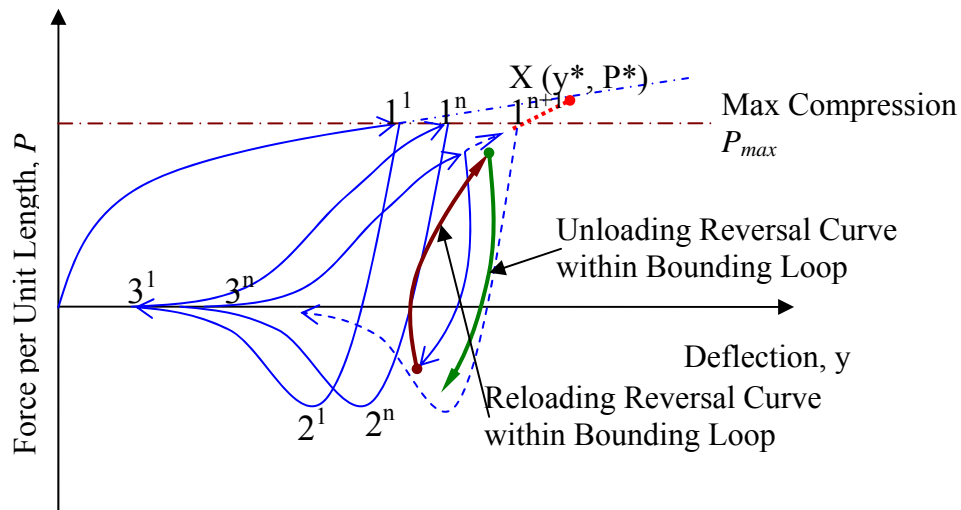


Figure.4.9 Illustration of Reversal Curves within Bounding Curve

For the unloading cycles within the bounding loops, with an arbitrary reversal point  $(y_r, P_r)$ , general hyperbolic equation is used for description (Figure.4.9):

$$P = P_r + \frac{y - y_r}{\frac{1}{k_0} + \chi \frac{y - y_r}{(1 + \omega)P_1^n}} \quad (\text{Eq.4.23})$$

Here  $\chi = 1$  for reloading stage.

### 4.3 DEGRADATING $P$ - $y$ MODEL PROGRAMMING

A MATLAB programming code is developed to implement this degradation model to simulate the real  $P$ - $y$  behavior of seafloor-riser interaction considering seafloor stiffness degradation effect. The aim of this code is to incorporate degradation parameters into the non-degradating code to be capable to accurately simulate the cyclic degradation effect. It is noted that the load input file data are also in form of displacement rather than force.

The code first reads the physical parameters of the riser and seafloor soil in order to form the backbone curve and the boundary loop. In the next step, the code would read displacement history data of an arbitrary point from input files and then choose suitable curve model for current load path. Then the code would implement fitted degradation model to calculate soil spring force. Finally, the  $P$ - $y$  response curve considering cyclic degradation effects is developed and the stiffness of the seafloor could be characterized. The source code and input files for this degradating program are shown in Appendix C&D. The programming code must include the following steps:

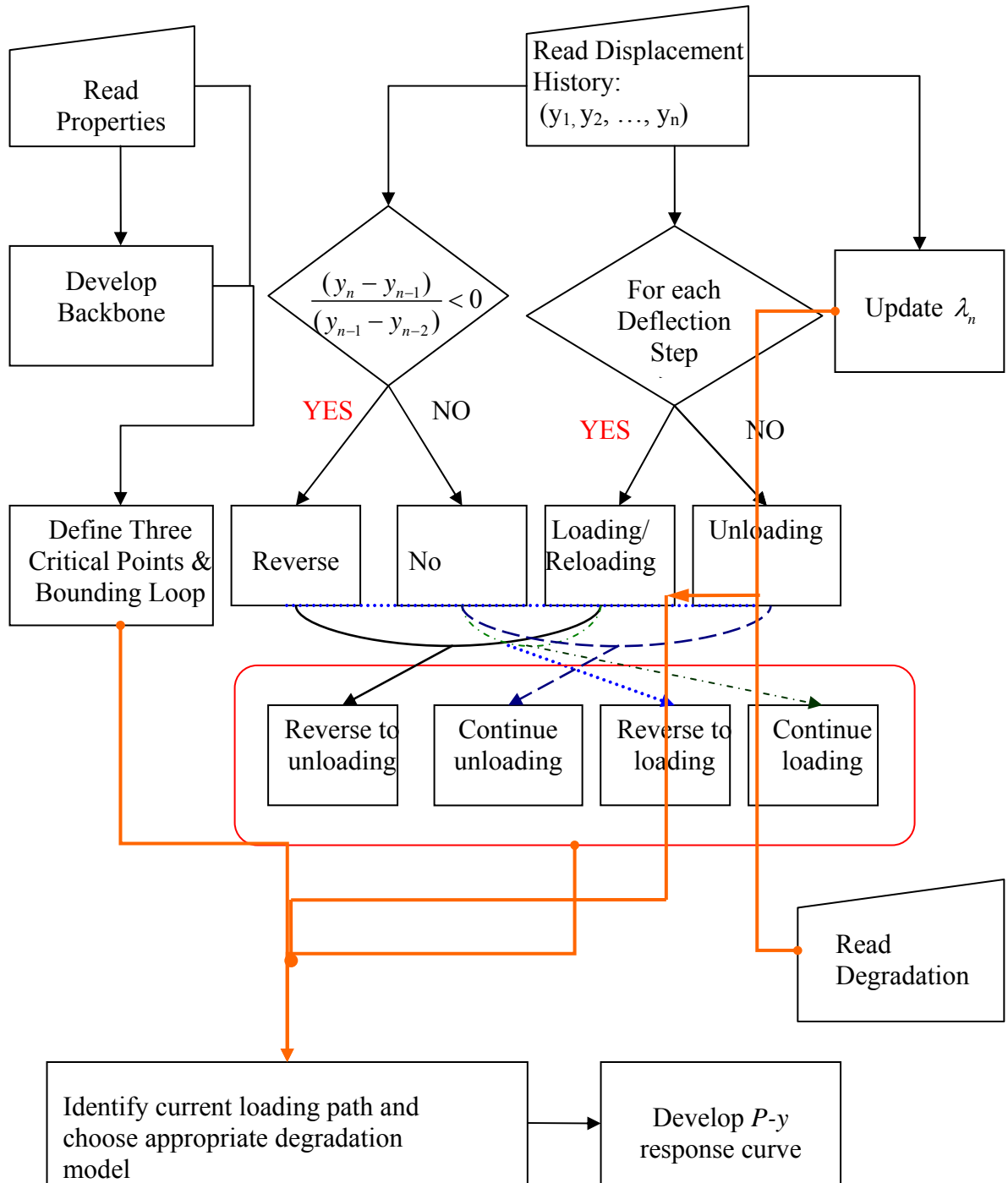
- 1) Read property parameters of riser and seafloor soil from the parameter input



file which includes four riser pipe properties - the elastic modulus of the riser  $E$ , diameter  $d$ , thickness  $t$ , weight per unit area of the steel riser  $\rho$ ; two soil properties – soil strength at mudline  $S_{u0}$  and strength gradient  $S_g$ ; and two backbone curve coefficients -  $a$  and  $b$ . Calculate pipe moment of inertia  $I$ , and weight per unit length  $W$  using the input riser properties.

- 2) Develop the backbone curve to describe the initial penetration due to riser self-embedment.
- 3) Read model parameters from the parameter input file, which includes four bounding loop parameters -  $k_0$ ,  $\omega$ ,  $\phi$ , and  $\psi$ . Calculate and determine the three critical fixed points and define the bounding loop.
- 4) Read degradation parameters -  $\alpha$  and  $\xi$  from degradation parameter input file.
- 5) Read load data for a fixed riser point from the load input file. There are two types of load files for this code. One is in form of deflection history data for small load cycles and the other is in form of cyclic loading cycles with a same peak force for long duration of cyclic loading.
- 6) Update riser's accumulated deflection,  $\lambda_n$  at each displacement step.
- 7) Identify current loading path and choose appropriate degrading model.
- 8) Calculate spring force  $P$  for each displacement with proper degrading  $P$ - $y$  model already determined.
- 9) Plot the  $P$ - $y$  response curve of this riser point.

A flow chart (Figure.4.10) is formulated to describe the work processes of this code.

Figure.4.10 Flow Chart of Degrading  $P$ - $y$  Curve Code

## 4.4 PARAMETRIC STUDY AND VERIFICATION

### 4.4.1 Parametric Study on Degrading Effect

In the degrading  $P$ - $y$  model, there are total three parameters employed to simulate the seafloor stiffness degradation effects. These three parameters include one energy dissipation factor,  $\lambda_n$ ; two degrading model factor- cubic reloading degrading model factor,  $\alpha$  and hyperbolic reloading degrading model factor,  $\xi$ .

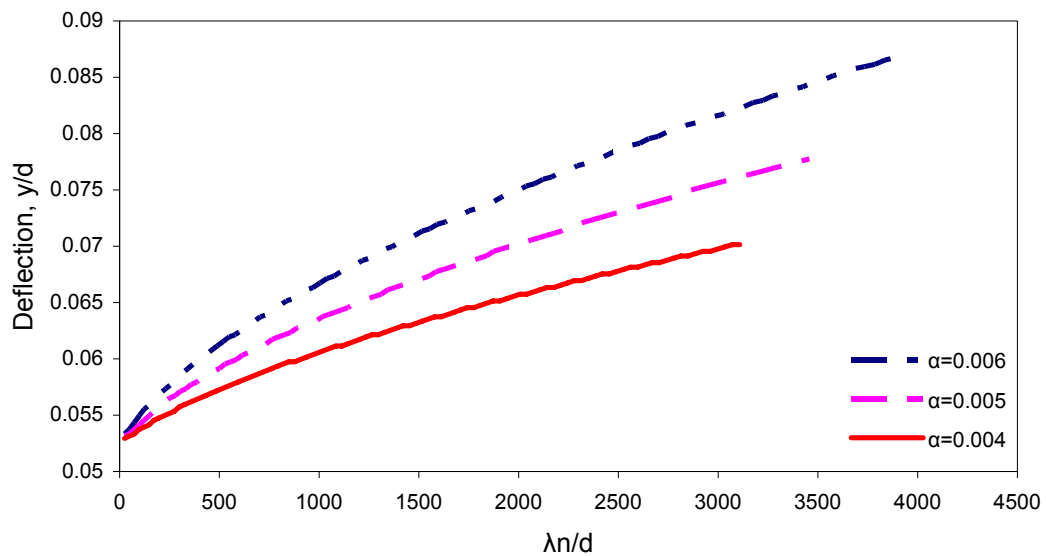


Figure.4.11 Effects of  $\lambda_n$  and  $\alpha$  on Riser Deflection

The energy dissipation factor,  $\lambda_n$ , is defined as the riser's accumulated deflection under cyclic loading. It directly affects the position of the control point (Eq.4.3& Eq.4.4). Figure.4.11 illustrates the influence of  $\lambda_n$  on riser deflections under cyclic loading. The deflection ratio of the riser after the  $n^{\text{th}}$  loading cycle,  $y_1^n/d$ , varies approximately logarithmically with  $\lambda_n/d$  for  $\alpha=0.004$ , 0.005 and 0.006. The relationship between

$\lambda_n$  and  $y_1^n$  differs from the exponential function between  $\lambda_n$  and  $y^*$  (Eq.4.3). This is because in large deflection cycles,  $y^*$  and  $y_1^n$  are in cubic relationship.

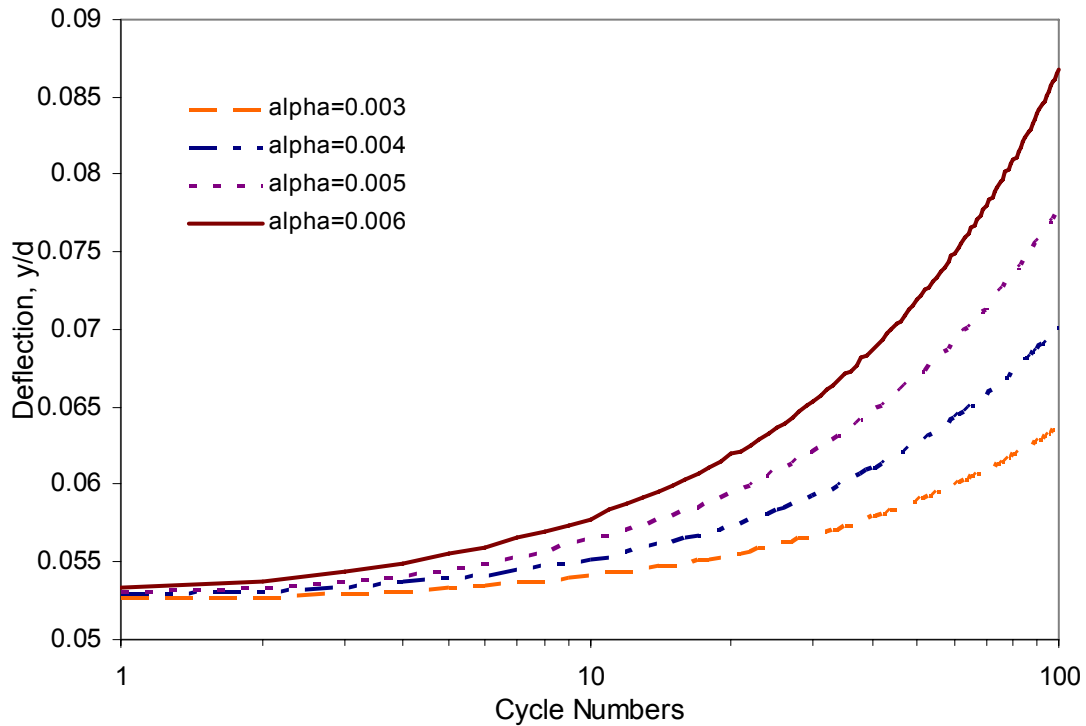


Figure.4.12 Effects of Cycle Number  $n$  and  $\alpha$  on Riser Deflection

Figure.4.12 shows the variation of deflection ratio  $y_1^n / d$  as a function of number of loading cycles for  $\alpha = 0.003, 0.004, 0.005$  and  $0.006$  respectively. After 100 cyclic cycles, the deflection ratio,  $y_1^{100} / d = 0.05774, 0.06094, 0.06434$  and  $0.06834$  for different  $\alpha$  values. Figure.4.13 shows the relationship between  $y_1^n / d$  and  $\alpha$  after 100 loading cycles, which indicates that the riser's deflection increases approximately linearly with the cubic degradation control factor,  $\alpha$ .

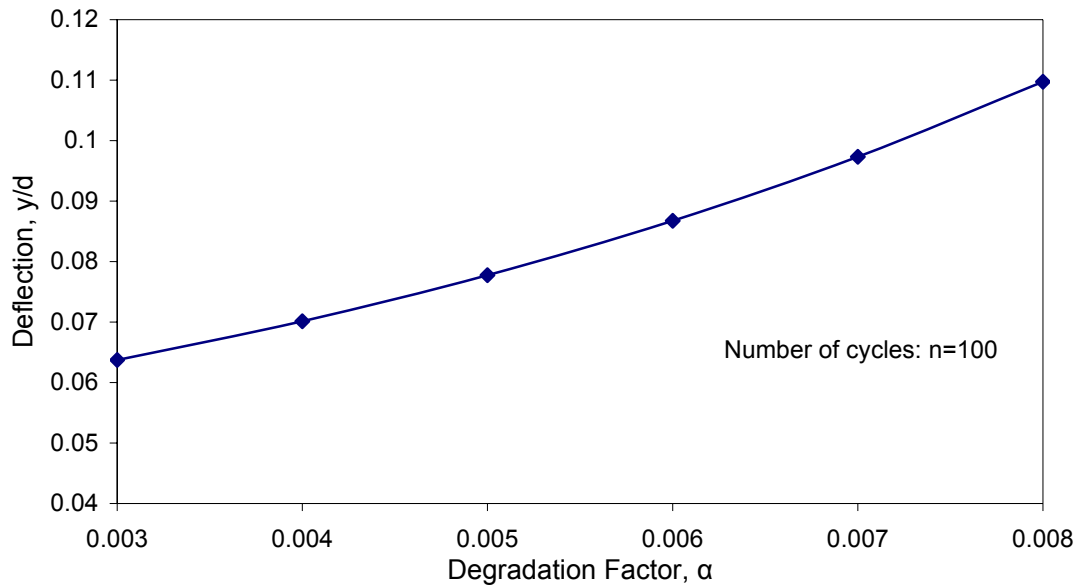


Figure.4.13 Effects of  $\alpha$  on Riser Deflection

From Figure.4.11~Figure.4.13, it indicates that the deflection under cyclic loading with a same peak force load would increase as the value of degradation factor  $\alpha$  increase. The value of  $\alpha$  should be determined by laboratory cyclic loading tests. Through the regression analysis of cyclic displacement controlled model test data (Dunlap et al., 1990) the value of cubic degradation model factor can be interpreted as  $\alpha = 0.000977$ . The hyperbolic control factor  $\xi$  could be directly derived from Eq.4.16 and Eq.4.22.

#### 4.4.2 Validation of the Model

Dunlap et al. (1990) conducted a series of cyclic loading tests on a pipe. Figure.4.14 shows a test interpretation from cyclic basin tests with confining force  $P_{\max} = 16.7$  lb after 100 loading cycles. The degradation model code was applied to simulate the  $P$ - $y$

behavior under the same soil, riser and loading conditions. The code used  $\alpha=0.000977$  for the cubic degrading model factor and the same parameters described in Table.3.1 and Table.3.2. The simulation curve within 100 loading cycles is shown in Figure.4.15.

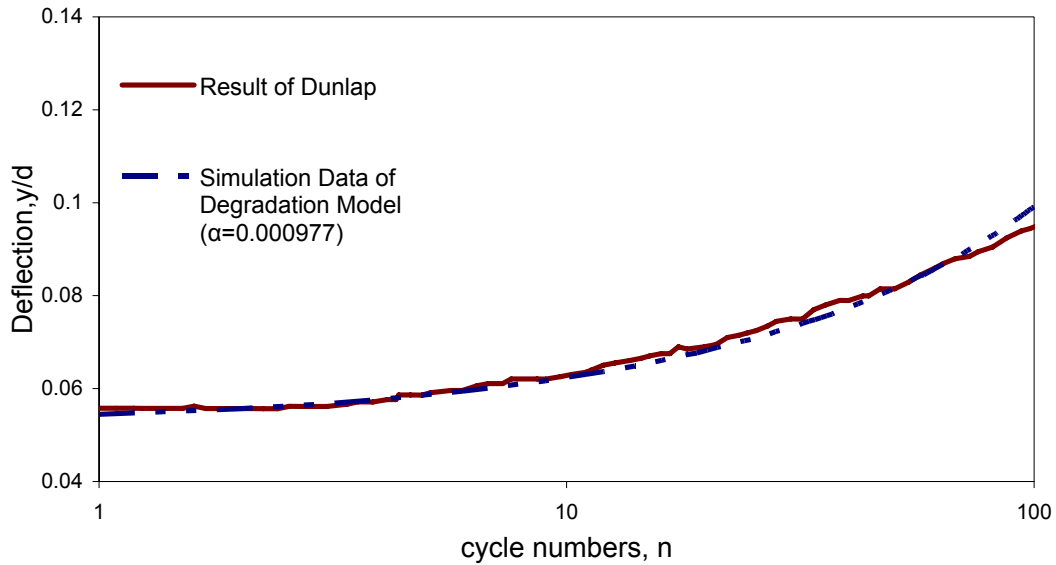


Figure.4.14 Comparison of the Degrading Model with Experiment

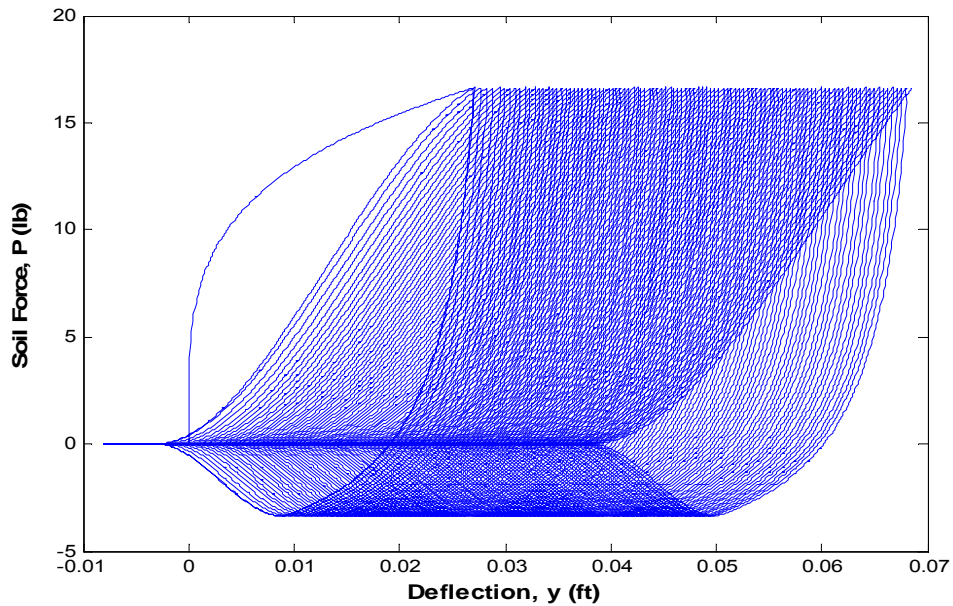


Figure.4.15 Degrading  $P$ - $y$  curve for  $P_{\max} = 16.7$  lb and  $n=100$

The curve of riser deflection  $y_1$  versus loading cycles  $n$  derived from model simulation (dash line in Figure.4.14) was plotted to compare with laboratory measurement (Dunlap et al., 1990). The good accordance (Figure.4.14) of these two curves indicates that the proposed degradation model could accurately describe the realistic  $P$ - $y$  behavior considering soil stiffness degradation effect. It should be noted that the hyperbolic reloading model still need to be validated with additional laboratory measurements. Notice that the degradation effects of this model just directly act on the reloading curves, and for unloading curves there no degradation parameters directly act on them.

## CHAPTER V

### SUMMARY, CONCLUSIONS AND RECOMMENDATION

#### 5.1 Summary and Conclusions

This thesis presents two load-deflection ( $P$ - $y$ ) models (non-degradating model and degradating model) to describe  $P$ - $y$  behavior of seafloor-riser interaction and characterize the soil stiffness for simulation of seafloor-riser interaction. Both of these two models are formulated in terms of a backbone curve describing self-embedment of the riser, bounding curves describing  $P$ - $y$  behavior under extremely large deflections, and a series of rules for describing  $P$ - $y$  behavior within the bounding loop. The Matlab codes implement these two models can be used to simulate the  $P$ - $y$  behavior of any riser element in the tough down zone.

The non-degradating  $P$ - $y$  model considers the soil-riser system in terms of an elastic pipe supported on non-linear soil spring. This model is capable of simulating the riser behavior under very complex loading conditions, including unloading (uplift) and re-loading (downwards) cycles under conditions of partial and full separation of soils and riser.

The first component of this model is a backbone curve following power law function to describe the plastic penetration due to self-embedment. This power law function is validated through comparison to laboratory measurement (Dunlap et al., 1990).

Bounding loop is defined to describe to behavior for conditions of extremely large loading and unloading deflections. The bounding loop is made up by four components:



elastic rebound from the backbone curve to soil tension limit (Path 1-2), partial separation stage (Path 2-3), full separation between soil and pipe (Path 3-4) and soil-riser re-contact and reloading stage (Path 3-1). Comparison of model simulations to data measurements supports the accuracy of the cases of Path 1-2, Path 2-3 and Path 3-4. Additional laboratory measurements are required to confirm the adequacy for Path 3-1.

Reversal loops from and within the bounding loop are also well defined in the model (Eq.3.15~Eq.3.19). However, these reversal functions have not been validated through comparison to laboratory test data.

In the non-degradating model, there include a series of model parameters which include three riser properties (elastic modulus  $E$ , diameter  $d$ , unit weight per length  $W$ ) two trench geometry parameter (width  $w$  and depth  $d_{trench}$ ) and one trench roughness parameter, two backbone curve model parameters ( $a$  and  $b$ ) and four bounding loop model parameters ( $k_0$ ,  $\omega$ ,  $\phi$ , and  $\psi$ ). The effect of these parameters were investigated and discussed. The value of these curve parameters are determined by regression analysis of laboratory measurements (e.g. Dunlap et al., 1990).

Based on the framework of non-degradation model, a degradating  $P$ - $y$  model was presented in this thesis through incorporating cyclic seafloor stiffness degradation effect into the non-degradation model. In the degradating model, a virtual degradation control point X ( $y^*$ ,  $P^*$ ) was introduced to describe the degradation effects. For all reloading conditions, the response  $P$ - $y$  curve will definitely go back to this control point from the loading reversal point. This control point is defined as function (Eq.4.1&Eq.4.2) of two

degradation parameters (energy dissipation factor  $\lambda_n$  and cubic degradation control factor  $\alpha$ ).

The degrading model is also made up by three components. The first one is the backbone curve, same as non-degrading model. The bounding loops define the  $P$ - $y$  behavior of extremely loading deflections. The elastic rebound curve and partial separation stage are in the same formation as the non-degradation model. However, for the re-contact and re-loading curve, degradation effects are taken into calculation (Eq.4.12~Eq.4.14).

For reversal loop from and within bounding loops, the reloading curves are in form of hyperbolic (controlled by all three degradation parameters- $\lambda_n$ ,  $\alpha$  and  $\xi$  as shown in Eq.4.15) or cubic (controlled by  $\lambda_n$ ,  $\alpha$  as shown in Eq.4.21) degrading type and the unloading curves are in form of hyperbolic unloading equation as non-degrading model does.

Besides the same model parameters as in non-degrading model, there are three degradation parameters in this model-  $\lambda_n$ ,  $\alpha$  and  $\xi$ . The effects of  $\lambda_n$  and  $\alpha$  on degradation are discussed and the value of  $\alpha$  is determined from laboratory cyclic tests. The cubic degrading model has been validated through comparison with laboratory measurements. As lack of data for hyperbolic degrading model, the adequacy of this type needs to be verified for  $P$ - $y$  simulation.

## 5.2 Recommendations for Future Research

The author would recommend the following work for future research:

- 1) For non-degradating model, review or carry out basin tests for conditions of re-contact re-loading and loading reversals from and within bound loop to verify the adequacy of re-contact bounding curve and reversal loops within the bounding loop.
- 2) For degradating model, obtain sufficient laboratory measurements data for hyperbolic reloading model to confirm the accuracy of the hyperbolic reloading model.
- 3) Based on current degradating model, develop advanced models which could directly describe the degradation effects through both unloading and reloading paths, rather than only reloading cases in current model.
- 4) Incorporate riser's lateral deflection into current work because of the lateral movements also have significant influence on seafloor-riser interaction response.

## REFERENCES

- Aubeny, C., Biscontin, G., & Zhang, J. (2006). "Seafloor Interaction with Steel Catenary Risers", *Final Project Report for Offshore Technology Research Center*, College Station, TX.
- Aubeny, C. and Shi, H. (2006). "Interpretation of impact penetration measurements in soft clays." *J. Geotech. Geoenviron. Eng.*, 132(6), 770–777.
- Aubeny, C., Shi, H., and Murff, J. (2005). "Collapse load for cylinder embedded in trench in cohesive soil." *Int. J. Geomechanics*, 5(4), 320–325.
- Bridge, C., Howells, H., Toy, N., Parke, G., and Woods, R. (2003). "Full-scale model tests of a steel catenary riser." *Fluid Structure Interaction II*, S. Chakraborti, C. Brebbia, D. Almorza, and Gonzalez-Palma, eds., Southampton, UK. WIT Press, 107–116.
- Bridge, C., Laver, K., Clukey, E., and Evans, T. (2004). "Steel catenary riser touchdown point vertical interaction model." *Offshore Technology Conf.*, OTC 16628, Houston.
- Bridge, C. and Willis, N. (2002). "Steel catenary risers - results and conclusions from large scale simulations of seafloor interactions." *Inter Deep Offshore Technology Conf.*, Houston, TX, 501-513.
- Clukey, E., Houstermans, L., and Dyvik, R. (2005). "Model tests to simulate riser-soil interaction effects in touchdown point region." *Inter. Symp. on Frontiers in Offshore Geotechnics*, Perth, Australia. 651–658.

Dunlap, W., Bhoanala, R., Morris, D.(1990). “Burial of vertically loaded offshore pipelines”, *22nd Annual Offshore Technology Conf.*, Houston, TX. 263-270.

Fontaine, E., Nauroy, J.F., Foray, P., Roux, A., and Gueveneux, H. (2004). “Pipe-soil interaction in soft kaolinite: vertical stiffness and damping”, *Proc. 14<sup>th</sup> Int. Offshore and Polar Engineering Conf.*, Toulon, France, 517-524.

Hale, J., Morris, D., Yen, T., and Dunlap, W. (1992). “Modeling pipeline behavior on clay soils during storms.” *24th Offshore Technology Conf., number OTC 7019*, Houston, TX. 339–349.

Idriss, I.M., Dobry, R., and Singh, R.D. (1978). “Nonlinear Behavior of Soft Clays during Cyclic Loading.” *J. Geotech. Eng.*, 102(12), 1427-1447.

Mekha, B. (2001). “New frontiers in the design of steel catenary risers for floating production systems.” *Proc. 20<sup>th</sup> Int. Offshore Mechanics and Arctic Engineering Conf.*, Rio de Janeiro, Brazil, 547-554.

Morris, D., Webb, R., and Dunlap, W. (1988). “Self-burial of laterally loaded offshore pipelines.” *20th Annual Offshore Technology Conf.*, number OTC 5855, Houston, TX. 421–428.

Pesce, C.P., Aranha, J.A.P., Martins, C.A., Ricardo, O.G.S., and Silva, S. (1998). “Dynamic curvature in catenary risers at the touch down point region: An experimental study and the analytical boundary-layer solution.” *Int. J. Offshore and Polar Engineering.*, 8(4), 303-310.

Rajashree, S.S. and Sundaravalivelu.R. (1996). “Degradation model for one-way cyclic lateral load on piles in soft clay.” *Computers and Geotechnics.*, 19(4), 289-300.

Romo, M.P. and Ovando-shelley, E. (1999). "P-y curve for piles under seismic lateral loads." *Geotechnical and Geological Engineering.*, 16(4), 251-272.

Thethi, R. and Moros, T. (2001). "Soil interaction effects on simple catenary riser response." *Deepwater Pipeline & Riser Technology Conf.*, Houston, TX.

Willis, N. and West, P. (2001). "Interaction between deepwater catenary risers and a soft seabed: large scale sea trials." *Offshore Technology Conf.*, Houston, TX. OTC 13113.

**APPENDIX A****MATLAB CODE: PROGRAM FOR NON-DEGRADATION P-y MODEL**

```

=====
%
%
%Full cases: Non-degradation P-y loop for seafloor stiffness
%
%
%=====
clc

clear all

%===== Input Variables =====%

%-----Read Soil&Riser Data-----%

    input=fopen('soilriserproperties.txt','r'); %input soil properties
    Su0=fscanf(input,'%g',1); %soil strength at mudline
    Sg=fscanf(input,'%g',1); %soil strength gradient
    Er=fscanf(input,'%g',1); %Eu/Su
    t=fscanf(input,'%g',inf); %define wall thickness of pipe
    d=fscanf(input,'%g',inf); %define diameter of pipe
    rhosteel=fscanf(input,'%g',inf); %unit weight of steel
    fclose(input);

    xa=(pi/4)*(d^2-(d-2*t)^2); %cross section area of pipe
    w=rhosteel*xa; %pipe weight per unit length

%-----Read Model Parameters-----%

    input=fopen('modelparameters.txt','r');
    a1=fscanf(input,'%g',1); %power law coefficient for h/d<0.5
    b1=fscanf(input,'%g',1); %power law exponent for h/d<0.5
    a2=fscanf(input,'%g',1); %power law coefficient for h/d>0.5
    b2=fscanf(input,'%g',1); %power law exponent for h/d>0.5
    k_normal=fscanf(input,'%g',1); %(\Delta P/\Delta y)/Eu
    phi=fscanf(input,'%g',1); %yield parameter for tension

```



```

psi=fscanf(input, '%g', 1);    %deformation at which P=0 after rupture
omiga=fscanf(input, '%g', 1);    %full separation parameter
fclose(input);

%===== Define boundary =====%
%first loading under self-weight: Path 0-1 powerlaw
y(1)=0;
P(1)=0;
err2=-1;
ib=1;
while (err2<=0)
    y(ib+1)=y(ib)+.002;
    if y(ib+1)/d<0.52
        a=a1;
        b=b1;
    else
        a=a2;
        b=b2;
    end
    P(ib+1)=a*(y(ib+1)/d)^b*(Su0+Sg*y(ib+1))*d;
    err2=P(ib+1)-w;
    ib=ib+1;
end
yy1=y(ib)-.002;
PP1=a*(yy1/d)^b*(Su0+Sg*yy1)*d;
y1=yy1;
P1=PP1;
Prup=-phi*P1;

```

```

Y=y1;
y_1=y1;
alpha=0.016;
beta=0.0016;
k0=k_normal*Er*(Su0+Sg*yy1);
%===== Read loading history =====%
input=fopen('yhistory.txt','r');           %input loading history
yhist=fscanf(input,'%g',inf);
fclose(input);
ylength2=size(yhist);
yy=[y(1:ib-1) yhist'];
%===== Loop for unloading & reloading =====%
ul0=-1;
yold=y1;
Pold=P1;
ib=ib-1;
Prev=P1;
yrev=y1;
for i=1:ylength2
    ynew=y(ib+1);
    ul=(ynew-yold)/abs(ynew-yold);
    [P2 y2 y3]=f(y1,P1,k0,phi,psi,omega);
    if ynew<=y3 || i==1
        yrc=y3;
        Prc=0;
    end
end

```

```

if ul~=ul0
    Prev=Pold;
    yrev=yold;
    ul0=ul;
end

dy=ynew-yrev;
if ul== -1
    if ynew>y2
        Pnew=Prev+(dy/((1/k0)+ul*dy/((1+omiga)*P1)));
        if Pnew<=bound1(ynew,y1,P1,k0,omiga)
            Pnew=bound1(ynew,y1,P1,k0,omiga);
        end
    elseif ynew>y3
        Pnew=Prev+(dy/((1/k0)+ul*dy/((1+omiga)*P1)));

        if Pnew<=bound2(ynew,y2,y3,P2)
            Pnew=bound2(ynew,y2,y3,P2);
        end

    else
        Pnew=0;
    end

elseif ul==1
    %reload loop
    if ynew>y1
        %power law loading

```

```

Pnew=a*(ynew/d)^b*(Su0+Sg*ynew)*d;
P1=Pnew;
y1=ynew;
Prup=-phi*P1;
[P2,y2,y3]=f(y1,P1,k0,phi,psi,omiga);      %new P2,y2,P3,y3
elseif ynew>y3
    if yrev<=y1&&yrev>=y2                    %hyperbolic reloading
        Pnew=Prev+(dy/((1/k0)+ul*dy/((1+omiga)*P1)));
    else                                     %cubic reloading&hyperbolic reloading
        Pnew=Prev+(dy/((1/k0)+ul*dy/((1+omiga)*P1)));
        if Prev==bound2(yrev,y2,y3,P2)
            yrc=yrev;
            Prc=Prev;
            Pnew=bound3(ynew,y1,yrc,Prc,P1);
        end
    end
    if Pnew>=bound3(ynew,y1,yrc,Prc,P1)
        Pnew=bound3(ynew,y1,yrc,Prc,P1);
    end
end

else
    Pnew=0;
end

else
    disp('err11')
end
end

```

```
y(ib+1)=ynew;
P(ib+1)=Pnew;
yold=ynew;
Pold=Pnew;
ib=ib+1;
end

output=[y;P];
fid = fopen('output.txt', 'wt');           %write out calculation
results into file
fprintf(fid, 'y P\n');
fprintf(fid, '%g %g\n ', output);
fclose(fid)

plot (y,P,'b-', 'LineWidth',1)           %Plot P-y curve
axis auto
title('P-y curve','fontsize',12,'fontweight','bold')
ylabel('P (lb)','fontsize',12,'fontweight','bold')
xlabel('y (ft)','fontsize',12,'fontweight','bold')
grid on
hold off
```

**APPENDIX B****INPUT FILES FOR NON-DEGRADATION P-y MODEL PROGRAMMING**

Soil and riser properties input file "soil& riser  
properties.txt"

```

5          #soil strength at mudline (psf)#
0          #soil strength gradient (psf)#
100       #ratio of Young's modulus to soil strength, Eu/Su #
0.0226    #thickness of riser pipe (ft)#
0.5       #diameter of riser pipe (ft)#
490.75    #density of steel (pcf)#

```

Model Parameters input file "modelparameters.txt"

```

6.70      #a value for h/d>0.5#
0.254     #b value for h/d>0.5#
6.25      #a value for h/d<0.5#
0.231     #b value for h/d<0.5#
6.6       #  $k_0/Er/Su$  #
0.203     # value of  $\phi$  #
0.661     # value of  $\psi$  #
0.433     # value of  $\omega$  #

```

Loading input file "yhistory.txt"

```

0.452     # riser deflection #
0.453     .
0.454     .
0.455     .
0.456     .
0.457
0.458

```

0.459  
0.46  
0.461  
0.462  
0.463  
0.464  
0.465  
0.466  
0.467  
0.468  
0.469  
0.47  
0.471  
0.472  
0.473  
0.474  
0.475  
0.476  
0.477  
0.478  
0.479  
0.48  
0.481  
0.482  
0.483  
0.484  
0.485  
0.486  
0.487  
0.488

.

.



0.489

.

0.49

# riser deflection #

**APPENDIX C****MATLAB CODE: PROGRAM FOR DEGRADATION P-y MODEL**



```

k_normal=fscanf(input, '%g', 1);           %[(DeltaP/Deltay)/Eu]
phi=fscanf(input, '%g', 1);               %yield parameter for tension
psi=fscanf(input, '%g', 1);               %deformation at which P=0 after rupture
omega=fscanf(input, '%g', 1);             %full separation parameter
fclose(input);

%-----Read Degradation Parameter-----%
input=fopen('degradationpramater.txt', 'r');
apha=fscanf(input, '%g', inf);           %cubic degradation control parameter
fclose(input);

%===== Define boundary =====%
%first loading under self-weight: Path 0-1 powerlaw
%=====

y(1)=0;
P(1)=0;
err2=-1;
ib=1;
while (err2<=0)
    y(ib+1)=y(ib)+.002;
    if y(ib+1)/d<0.52
        a=a1;
        b=b1;
    else
        a=a2;
        b=b2;
    end
end

```

```

P(ib+1)=a*(y(ib+1)/d)^b*(Su0+Sg*y(ib+1))*d;

err2=P(ib+1)-w;

ib=ib+1;

end

k0=k_normal*Er* (Su0+Sg*yy1);

yy1=y(ib)-.0001;

PP1=a*(yy1/d)^b*(Su0+Sg*yy1)*d;

y1=yy1;

P1=PP1;

Prup=-phi*P1;

Y=y1;

y_1=y1;

%===== Read loading history =====%

input=fopen('yhistory.txt','r'); %input loading history

filetype=fscanf(input,'%g',1);

if filetype==1 %displacemnet history type

yhist=fscanf(input,'%g',inf);

fclose(input);

ylength2=size(yhist);

yy=[y(1:ib-1) yhist'];

%===== Loop for unloading&reloading =====%

ul0=-1;

yold=y1;

Pold=P1;

ib=ib-1;

Prev=P1;

```

```

yrev=y1;
for i=1:length2
    ynew=yy(ib+1);
    ul=(ynew-yold)/abs(ynew-yold);
    [P2 y2 y3]=f(y1,P1,k0,phi,psi,omiga);
    if ynew<=y3 || i==1
        yrc=y3;
        Prc=0;
    end
    if ul~=ul0
        Pprev=Pold;
        yrev=yold;
        ul0=ul;
    end
    %=====define degradation control parameters=====
    dy=ynew-yrev;
    Y=Y+abs(dy);
    y_1=yy1+eta*Y^0.5;
    P_1=a*(y_1/d)^b*(Su0+Sg*y_1)*d;
    %=====
    if ul== -1
        if ynew>y2
            Pnew=Pprev+(dy/((1/k0)+ul*dy/((1+omiga)*P1)));
            if Pnew<=bound1(ynew,y_1,P_1,k0,omiga)
                Pnew=bound1(ynew,y_1,P_1,k0,omiga);
            end
        elseif ynew>y3

```

```

Pnew=Prev+(dy/((1/k0)+ul*dy/((1+omiga)*P1)));

if Pnew<=bound2(ynew,y2,y3,P2)
    Pnew=bound2(ynew,y2,y3,P2);
end

else
    Pnew=0;
end

elseif ul==1 %reload loop
if ynew>y3
    xi=(y_1-yrev)/((P_1*(1+omiga))*((y_1-yrev)/(P_1-Prev)-1/k0));
    if yrev<=y1&& yrev>=y2 %hyperbolic reloading
        Pnew=Prev+(1/((1/(k0*dy))+ul/((1+omiga)*P_1*xi)));
        if Pnew>=PP1
            Pnew=PP1;
            P1=PP1;
            y1=ynew;
            [P2,y2,y3]=f(y1,P1,k0,phi,psi,omiga);
        end
    else %cubic reloading&hyperbolic reloading
        Pnew=Prev+(dy/((1/k0)+ul*dy/((1+omiga)*P_1*xi)));
        if Prev==bound2(yrev,y2,y3,P2)
            yrc=yrev;
            Prc=Prev;
            Pnew=bound3(ynew,y_1,yrc,Prc,P_1);
        end
    end
    if Pnew>=PP1

```

```

        Pnew=PP1;

        y1=ynew;

        [P2,y2,y3]=f(y1,P1,k0,phi,psi,omiga);

    end

end

if Pnew>=bound3(ynew,y_1,ycr,Prc,P_1)

    Pnew=bound3(ynew,y_1,ycr,Prc,P_1);

end

else

    Pnew=0;

end

if ynew>=y_1

    Pnew=a*(ynew/d)^b*(Su0+Sg*ynew)*d-(P_1-PP1);

    P1=Pnew;

    P_1=2*Pnew-P_1;

end

else

    disp('err11')

end

y(ib+1)=ynew;

P(ib+1)=Pnew;

yold=ynew;

Pold=Pnew;

ib=ib+1;

end

```



```

elseif filetype==2          % the loading file is in form of cycle numbers
    NumCycle=fscanf(input, '%g', 1);
    fclose(input);
    [P2 y2 y3]=f(y1,P1,k0,phi,psi,omiga); % define whole loading cycle
if y3<0
    yend=-0.3*yy1;
    step=0.0001;
else
    yend=0.8*yy1;
    step=0.0001;
end
%=====
%===== Loop for unloading &reloading =====
%=====
for N=1:NumCycle
    yhist=[y1-step:-step:yend,yend+step:step:10*y1];
    [ylength1,ylength2]=size(yhist);
    ul0=-1;
    yold=y1;
    Pold=P1;
    Prev=P1;
    yrev=y1;
for i=1:ylength2
    ynew=yhist(i);
    ul=(ynew-yold)/abs(ynew-yold);
    [P2 y2 y3]=f(y1,P1,k0,phi,psi,omiga);
    if ynew<=y3 || i==1

```

```

    yrc=y3;
    Prc=0;
end
if ul~=ul0
    Pprev=Pold;
    yrev=yold;
    ul0=ul;
end
dy=ynew-yrev;
Y=Y+abs(dy);
y_1=yyl+eta*Y^0.5;
P_1=a*(y_1/d)^b*(Su0+Sg*y_1)*d;

if ul==--1                                     %unloading loop
    if ynew>y2
        Pnew=Prev+(dy/((1/k0)+ul*dy/((1+omiga)*P1)));
        if Pnew<=bound1(ynew,y1,P1,k0,omiga)
            Pnew=bound1(ynew,y1,P1,k0,omiga);
        end
    elseif ynew>y3
        Pnew=Prev+(dy/((1/k0)+ul*dy/((1+omiga)*P1)));
        if Pnew<=bound2(ynew,y2,y3,P2)
            Pnew=bound2(ynew,y2,y3,P2);
        end
    else
        Pnew=0;
    end
end

```

```

elseif ul==1 %reloading loop
    if ynew>y3
        if yrev<y3
            yrc=y3;
            Prc=0;
            Pnew=bound3(ynew,y_1,yrc,Prc,P_1);
            if Pnew>PP1
                Pnew=PP1;
                y1=ynew;
                [P2,y2,y3]=f(y1,P1,k0,phi,psi,omiga);
                break;
            end
        end
        if Pnew>=bound3(ynew,y_1,yrc,Prc,P_1)
            Pnew=bound3(ynew,y_1,yrc,Prc,P_1);
        end
    else
        Pnew=0;
    end
else
    disp('err11')
end
yn(i)=ynew;
PN(i)=Pnew;
yold=ynew;
Pold=Pnew;

```

```

end

y=[y,yn];

P=[P,PN];

y_peak(1,N)=y1;

y_Peak=y_peak'/d;

Yn(N,1)=Y'/d;

end

end

output=[y;P];

fid = fopen('output.txt', 'wt');    %write calculation results into file
fprintf(fid, 'y P\n');
fprintf(fid, '%g %g\n ', output);
fclose(fid)

plot (y,P,'b-','LineWidth',1)           %Plot P-y curve
axis auto
title('P-y curve','fontsize',12,'fontweight','bold')
ylabel('P (lb)','fontsize',8,'fontweight','bold')
xlabel('y (ft)','fontsize',8,'fontweight','bold')
hold off

```

**APPENDIX D****INPUT FILES FOR NON-DEGRADATION P-y MODEL PROGRAMMING**

Soil and riser properties input file "soil& riser  
properties.txt"

```
5          #soil strength at mudline (psf)#
0          #soil strength gradient (psf)#
100       #ratio of Young's modulus to soil strength, Eu/Su #
0.0226    #thickness of riser pipe (ft)#
0.5       #diameter of riser pipe (ft)#
490.75    #density of steel (pcf)#
```

Model parameters input file "modelparameters.txt"

```
6.70      #a value for h/d>0.5#
0.254     #b value for h/d>0.5#
6.25     #a value for h/d<0.5#
0.231     #b value for h/d<0.5#
6.6       #  $k_0/Er/Su$  #
0.203     # value of  $\phi$  #
0.661     # value of  $\psi$  #
0.433     # value of  $\omega$  #
```

Degradation parameters input file "degradationpramater.txt"

```
0.00097   # value of  $\alpha$  #
```

Loading input file type 1: "yhistory.txt"

```
1          # type number #
0.452     # riser deflection #
```

0.453 .  
0.454 .  
0.455 .  
0.456 .  
0.457  
0.458  
0.459  
0.46  
0.461  
0.462  
0.463  
0.464  
0.465  
0.466  
0.467  
0.468  
0.469  
0.47  
0.471  
0.472  
0.473  
0.474  
0.475  
0.476  
0.477  
0.478  
0.479  
0.48  
0.481  
0.482

```
0.483
0.484
0.485
0.486
0.487      .
0.488      .
0.489      .
0.49       # riser deflection #
```

```
Loading input file type 2: "cyclenumber.txt"
```

```
100       # number of cyclic loading #
```



### VITA

Yaguang Jiao was born on June 22, 1983 in Dezhou, China. He received his Bachelor of Engineering degree in civil engineering from Jilin University in July 2005. In the fall of 2005, he enrolled in the Zachry Department of Civil Engineering at Texas A&M University for M.S. degree. He received his M.S. degree in May 2007.

His permanent address is:

53-2, Dongfanghong Street

Dezhou, Shandong Province, 253013

P.R.China